

# **INVESTIGATION ON DUAL FUEL LTC ENGINE FOR OPTIMISATION OF NO<sub>x</sub> AND SOOT PARTICULATE MATTER EMISSION**

**Ph.D. Thesis**

By  
**JYOTIRMOY BARMAN**



**DISCIPLINE OF MECHANICAL ENGINEERING  
INDIAN INSTITUTE OF TECHNOLOGY INDORE  
SEPTEMBER 2022**



# **INVESTIGATION ON DUAL FUEL LTC ENGINE FOR OPTIMISATION OF NO<sub>x</sub> AND SOOT PARTICULATE MATTER EMISSION**

**A THESIS**

*Submitted in partial fulfillment of the  
requirements for the award of the degree  
of*  
**DOCTOR OF PHILOSOPHY**

*by*  
**JYOTIRMOY BARMAN**



**DISCIPLINE OF MECHANICAL ENGINEERING  
INDIAN INSTITUTE OF TECHNOLOGY INDORE  
SEPTEMBER 2022**





# INDIAN INSTITUTE OF TECHNOLOGY INDORE

I hereby certify that the work which is being presented in the thesis entitled **INVESTIGATION ON DUAL FUEL LTC ENGINE FOR OPTIMISATION OF NO<sub>x</sub> AND SOOT PARTICULATE MATTER EMISSION** in the partial fulfillment of the requirements for the award of the degree of **DOCTOR OF PHILOSOPHY** and submitted in the **DISCIPLINE OF MECHANICAL ENGINEERING, Indian Institute of Technology Indore**, is an authentic record of my own work carried out during the time period from June 2016 to Sep 2022 under the supervision of Dr. Devendra Deshmukh.

The matter presented in this thesis has not been submitted by me for the award of any other degree of this or any other institute.

(JYOTIRMOY BARMAN)

---

This is to certify that the above statement made by the candidate is correct to the best of my/our knowledge.

(DR. DEVENDRA DESHMUKH)

(P. KUMAR)

---

JYOTIRMOY BARMAN has successfully given his/her Ph.D. Oral Examination held on **September 2022**.

(DR. DEVENDRA DESHMUKH)

(P. KUMAR)

---



**Dedicated to  
dear  
Kabir & Kiaan**



## ACKNOWLEDGEMENTS

Firstly, I would like to express my sincere gratitude to my advisor Dr. Devendra Deshmukh for the continuous support of my Ph.D. study and related research, for his patience, motivation, and immense knowledge. His guidance helped me all the time during the research and writing of this thesis. I could not have imagined having a better advisor and mentor for my Ph.D. study.

Besides my advisor, I would like to thank Mr.P Kumar as co supervisor of Ph.D. work and rest of my thesis committee: Dr. Amod C. Umarikar, Dr. I. A. Palani, and for their insightful comments and encouragement, but also for the hard question which incited me to widen my research from various perspectives.

A special thanks to my family. Words cannot express how grateful I am to Mr. Hardik Lakhani, my mother, father and In-laws family who always motivated me to complete my thesis work. Your prayer for me was what sustained me thus far. I would also like to thank all my friends who supported me in writing and incited me to strive towards my goal. At the end I would like express appreciation to my beloved wife Mrs. Lipika who spent sleepless nights with and was always my support in the moments through this journey. I wish to express my deepest gratitude to my sons and family in general, who have encouraged me every day in my undertakings.

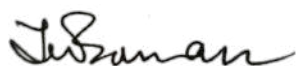


Jyotirmoy Barman



## **DEDICATION**

I declare that the research contained in this thesis, unless otherwise formally indicated within the text, is the original work of the author. The thesis has not been previously submitted to this or any other university for a degree and does not incorporate any material already submitted for a degree.



Signed

Dated: 20.02.2023

## **DISCLAIMER**

As the contents of this thesis are my own work, they reflect my views and not necessarily those of the collaborators.

## **COPYRIGHT**

Attention is drawn to the fact that copyright of this thesis rests with its author. The present copy of the thesis has been supplied on condition that anyone who consults it is understood to recognise that its copyright rests with its author. No quotation from the thesis and no information derived from it may be published without the prior written consent of the author.

This thesis may be available for consultation within the Indian Institute of Technology, Indore and may be photocopied or lent to other libraries for the purposes of consultation.

## ABSTRACT

The compression ignition (CI) engine is preferred for automotive applications owing to its higher thermal efficiency, however, suffers from high  $\text{NO}_x$  and soot emissions. Low temperature combustion with dual fuel has a potential to reduce  $\text{NO}_x$  and soot emissions simultaneously in the CI engine. The present study was conducted to understand the effect of fuel reactivity on engine performance and emission in a CI engine with dual fuel. The novelty of the research is in its study of emission and performance behavior with dual fuel (Low and high reactive fuel) and to assess the best strategy to control  $\text{NO}_x$  and PM with a low-temperature combustion approach. Engine performance tests were done with and without EGR using the dual fuel to understand its behavior in emission and BSFC, soot formation in terms of particulate matter, particulate number, and composition. An optimal combination of EGR rate and injection timing in dual-fuel combustion behavior is the most effective method to reduce combustion temperature significantly, leading to a significant drop of  $\text{NO}_x$  and soot emission. The fuel composition D30G7 showed fuel consumption improvement by 1.9% in comparison with diesel fuel combustion with simultaneous reduction of  $\text{NO}_x$  and soot emissions. Hydrocarbon and carbon monoxide emissions increased more than 10- 15 times with an increase in gasoline content which can be reduced with oxidation catalyst. An increase in the gasoline content leads to soot particle formation mode shift from accumulation to nuclei mode. The particle diameter and particle concentration decrease with increasing gasoline content due to the homogeneous mixture. The average particle size decreases with an increase in the injection pressure, while particle diameter increases with an increase in engine load. The sulfur content is found to increase soot emission due to high soluble content. Diesel oxidation catalyst and its PGM content is critical to meet emission with dual fuel combustion. Particulate mass can be reduced to 99% without DPF with dual-fuel (D15G85) and DOC with PGM loading of  $20 \text{ g/cft}^3$ . Particulate mass and Particulate Number show a linear correlation for engine out and DOC out condition emission with diesel and dual fuel. The study shows LTC combustion with dual fuel can potentially eliminate costly after-treatments like Selective Catalytic Reduction (SCR) and Diesel Particulate Filter (DPF) from the exhaust layout to meet emission norms for a diesel engine.

# TABLE OF CONTENTS

LIST OF FIGURES.....	vii
LIST OF TABLES.....	ix
NOMENCLATURE.....	x

# CONTENTS

<b>1: INTRODUCTION.....</b>	<b>1</b>
1.1. Background and Motivation.....	1
1.2. Scope and Objective of This Work .....	2
1.3. Organization of This Work .....	3
<b>2: LITERATURE SURVEY .....</b>	<b>4</b>
2.1. Homogeneous Charge Compression Ignition (HCCI).....	5
2.2. Reactivity Controlled Compression Ignition (RCCI).....	10
2.3. Partially Premixed Compression Ignition (PPCI).....	11
2.4. Low Temperature Combustion .....	18
2.4.1 Steps of LTC .....	18
2.4.2 Benefits of LTC.....	19
2.4.3 Challenges with LTC.....	19
2.5. Fuel Reactivity .....	19
2.5.1 Diesel Fuel .....	20
2.5.2 Gasoline Fuel .....	21
2.6. PM Formation Mechanism .....	22
2.6.1 Particulate Emission Formation in High Reactive Fuel .....	23
2.6.2 Soot Formation in Diesel Combustion .....	24
2.6.3 Analysis of Diesel Engine Particle Size Distribution.....	26
2.6.4 Particulate Emission Formation in LTC.....	28
2.7. Objective of the Study.....	29

<b>3: CFD SIMULATION OF AIR FUEL MIXTURE FORMATION .....</b>	<b>31</b>
3.1 Background .....	31
3.2 Methodology used in Simulation Work.....	32
3.2.1 Geometry .....	32
3.2.2. Meshing .....	33
3.2.3. Solution.....	33
3.3 Simulation Results.....	34
3.4 Summary .....	37
<b>4: EXPERIMENTAL SET UP AND METHODOLOGY.....</b>	<b>38</b>
4.1 Engine Specification in Test Bed .....	38
4.2 Engie Test Bed Layout .....	42
4.3 Engine Test Bed Equipment .....	42
4.3.1 Engine Dynamometer.....	44
4.3.2. Oil and Coolant System.....	44
4.3.3 Air Handling System.....	45
4.3.3.1 Air Temperature .....	45
4.3.3.2 Air Pressure.....	46
4.3.3.3 Air Humidity.....	46
4.3.3.4 Air and Fuel Measurement Method.....	46
4.3.3.5 Air Cooling and Ventilation .....	47

4.3.4 Fuel System .....	47
4.3.5 Emission System .....	49
4.3.6 Controller and Data Acquisition System.....	52
4.3.7 Summary .....	55
<b>5: ENGINE PERFORMANANCE WITH DUAL FUEL .....</b>	<b>56</b>
5.1 Effect of Dual Fuel Combustion in NO <sub>x</sub> and Soot Emission .....	56
5.2 Impact of EGR on Dual Fuel Combustion.....	58
5.3 Impact of HC and CO on Dual Fuel Combustion .....	59
5.4 Effect of Gasoline on Brake Specific Fuel Consumption .....	60
5.5 Effect of NO <sub>x</sub> and Brake Specific Fuel Consumption with dual fuel.....	60
5.6 Effect of EGR in Emissions with dual fuel.....	61
5.7 Effect on Cylinder Pressure with dual fuel.....	63
5.8 Effect of Injection Timing on BSFC with dual fuel.....	64
5.9 Summary .....	65
<b>6: PARTICULATE MASS AND NUMBER CHARACTERIZATION .....</b>	<b>66</b>
6.1 Particulate size distribution with different gasoline ratio .....	66
6.2 Effect of fuel, injection pressure, and engine load on particulate size.....	67
6.3 Effect of EGR on particulate size distribution.....	68
6.4 Effect of sulphur content on particulate size distribution .....	69
6.5 Composition of PM and PN with filter paper measurement in dual fuel .....	70
6.6 Effect of composition with Dual Fuel on Particulate Mass Emission .....	74
6.7 Effect of composition with Dual Fuel on Particulate Size Distribution .....	75
6.8 SOF and IOF distribution from Engine and DOC Out with Dual Fuel .....	76

6.9 Correlation of Particulate Mass and Particle Number with Dual Fuel.....	77
6.10 Summary .....	79
<b>7: CONCLUSION AND WAY FORWARD .....</b>	<b>82</b>
<b>BIBLIOGRAPHY .....</b>	<b>86</b>
<b>APPENDIX .....</b>	<b>102</b>
<b>LIST OF PUBLICATION .....</b>	<b>103</b>

## LIST OF FIGURES

2.1 Composition of particulate matter in diesel engine exhaust emission.....	24
2.2 Particulate matter formation of diesel engine .....	25
2.3 Soot Formation Process .....	26
2.4 Particulate size distribution .....	28
2.5 Reactions at low and high temperatures in fuel reaction .....	29
3.1 Intake Manifold with single point manifold injection .....	32
3.2 Gasoline Entry across all different Intake Port Area in Intake Manifold .....	33
3.3 Uniformity Index in Port 1 and 2 with single injection in Intake Manifold .....	35
3.4 Uniformity Index in Port 1 and 2 with single injection in Intake Manifold .....	36
3.5 Uniformity Index in Port 1 and 2 with multiple injection in Intake Port.....	36
3.6 Uniformity Index in Port 3 and 4 with multiple injection in Intake Port.....	37
4.1 Engine Test Bed.....	40
4.2 Engine Test and Measurement Layout.....	43
4.3 Test Cell Layout.....	48
4.4 Emission Analyzer Equipment Layout .....	49
5.1 Effect of Gasoline Ratio on NO <sub>x</sub> and Soot Emission with Dual Fuel.....	57
5.2 NO <sub>x</sub> and Soot reduction with different EGR Flow Rate in Dual Fuel.....	58
5.3 HC and CO emissions with increasing gasoline percentage (EGR 20%).....	59
5.4 NO <sub>x</sub> and BSFC comparison with different compositions of dual-fuel.....	60
5.5 Comparison of NO <sub>x</sub> and BSFC for different load points (1520rpm).....	61
5.6 Comparison of Emission Parameters (with and without EGR).....	62
5.7 Impact of Gasoline percentage on cylinder pressure at different load point).....	64
5.8 Impact of Impact of Injection Timing on Dual-fuel Combustion .....	65
6.1. Particulate size distribution for different gasoline ratio.....	67
6.2. Particulate size distribution for different gasoline ratio.....	68
6.3 Effect of EGR on particulate size distribution.....	69

6.4 Effect of sulphur content in diesel on particulate size distribution .....	70
6.5 Filter paper composition with D100, D50G50 and D15G85 Fuel.....	72
6.6 Particulate Mass with different dual fuel ratio and DOC configuration.....	74
6.7 Particulate Size distribution with different dual fuel ratio and DOC.....	75
6.8 SOF and IOF ratio from Engine and DOC Out with Dual Fuel and Diesel.....	77
6.9 Correlation of Particulate Mass and Particle Number with Dual Fuel Ratio.....	78

## LIST OF TABLES

2.1. Comparison of Different Types of Combustion Technique .....	12
4.1 Engine Specification .....	39
4.2 Diesel Injector Specification.....	39
4.3 Gasoline Injector Specification.....	40
4.4 Technical Specification of Diesel Oxidation Catalyst .....	41
4.5 Technical Specification of Diesel Particulate Filter .....	42
4.6 Instrumentation and Accuracy of Test Bed Measurement Units.....	48
4.7 Emission Analyzer Operating Principle and Accuracy.....	51
4.8 Uncertainty Percentage in Test Lab Equipment .....	51
4.9 Technical specification of BSVI Diesel Fuel.....	53
4.10 Technical specification of BSVI Gasoline Fuel.....	54
6.1 Filter paper sample with dual fuel (with and without EGR).....	71
6.2 Particulate Mass and Particle Number test data with dual fuel.....	78

## NOMENCLATURE

CI- Compression Ignition

HC- Hydrocarbon

CO - Carbon Monoxide

PM - Particulate Matter

NO<sub>x</sub> - Oxides of Nitrogen

EGR- Exhaust Gas Recirculation

BSFC-Brake Specific Fuel Consumption

BMEP – Brake Mean Effective Pressure

LRF- Low Reactive Fuel

HRF – High Reactive Fuel

LTC - Low temperature combustion

PCCI - Partially premixed compression ignition

HCCI - Homogenous Charge Compression Ignition

RCCI - Reactivity Controlled Compression Ignition

HRR – Heat release Rate

PN - Particulate Number

PM -Particulate Mass

AFR – Air Fuel Ratio

FSN – Filter Smoke Number

BTDC – Before Top Dead Centre

Nm – Newton Meter

SI- Spark ignition

CI- Compression Ignition

PCP- Peak Combustion Pressure

MPRR- Maximum Pressure Rise Rate

EGR- Exhaust Gas Recirculation

CO<sub>2</sub> - Carbon Dioxide

ECU – Electronic Control Unit

EATS – Exhaust After Treatment System

NABL - National Accreditation Board for Testing and Calibration Laboratories

IOCL – Indian Oil Corporation Limited

BSVI – Bharat Stage Emission Norms (BSVI)

PN - Particulate Number

Nm – Newton Meter

nm- Nanometer

mm- millimeter

D100- Diesel Fuel Only

D50G50 – Diesel 50% and Gasoline 50%

D25G75 – Diesel 25% and Gasoline 75%

D15G85 – Diesel 15% and Gasoline 85%

D35G65 – Diesel 35% and Gasoline 65%

D23G77 – Diesel 23% and Gasoline 77%

DOC – Diesel Oxidation Catalyst

DPF – Diesel Particulate Filter

SCR – Selective Catalyst Reduction

BSVI – Bharat Stage VI Emission

PGM – Precious Group Material

SOF – Soluble Organic Fraction

IOF – Insoluble Organic Fraction

# CHAPTER 1

## INTRODUCTION

### 1.1 Background and Motivation

#### Energy Crisis and Environmental Issues

The ability to travel is crucial for enabling people to advance as well as connect with one another. The creation of novel automotive technologies has become essential to meet the growing need for transport systems that are safe, dependable, inexpensive, efficient, and environmentally friendly. However, automotive industry is facing a big challenge due to rapidly diminishing petroleum supplies. The exploration of alternative energy sources, such as renewable fuels like biofuels, solar energy, and hydrogen, has thus been the focus of research efforts. The two biggest problems faced by ICEs (internal combustion engines) is energy efficient and air pollution. The efficiency needs to be raised to conserve fossil fuels. Strict emission norms, scarcity of fossil fuels, and greenhouse gas mitigation rules have made it essential to enhance the thermal efficiency of diesel combustion engines. Though the CI engine is preferred for automotive applications owing to its higher thermal efficiency, it suffers from high  $\text{NO}_x$  and soot emissions. HCCI and PCCI technologies have the potential to reduce  $\text{NO}_x$  and soot emissions simultaneously in the CI engine. Predominantly, HCCI and PCCI are managed using either gasoline or diesel fuel because of the prevailing fuel infrastructure across different parts of the world and engine design. Owing to the volatility of gasoline (Low Reactivity Fuel), its evaporation rate is high, and thus, with the help of port-fuel injection, a premixed charge is prepared before inducting it into the combustion chamber. However, combustion in low load conditions is difficult due to the poor auto-ignition properties of gasoline. Conversely, the superior auto-ignition properties of diesel fuel (High Reactivity Fuel) result in challenges to control the combustion phase when there is an increase in engine load and speed. Both low reactivity and high reactivity fuel have certain benefits and drawbacks for premixed combustion with their pure forms. Low-temperature combustion (LTC) strategies such as HCCI and PCCI are not implemented in advanced engines due to problems in managing HRR (heat release rate) and combustion phasing control mechanisms.

In conventional diesel combustion, the typical path of the fuel passes through different zones for soot formation,  $\text{NO}_x$  formation, and soot oxidation zone. Soot and  $\text{NO}_x$  formation zones are avoided when combustion of the lean homogeneous mixture is achieved. Mixing controlled LTC conditions are achieved with high rates of EGR to keep the combustion process away from the soot and  $\text{NO}_x$  formation zone. Despite their significant emission benefits, some practical complexities are caused by the concept of HCCI combustion, which must be resolved before its application in CI engines. The most important barriers are obtaining proper combustion phasing, controlling variation in the cycle-to-cycle combustion process, and performance at high load conditions. To alleviate these problems, some of the techniques used are control of intake oxygen concentration using EGR, modification of the compression ratio, the use of different injection methods, and the control of intake air temperature. The aim is to reduce the high chemical response of HRF (diesel fuel) by altering the properties of fuel and slowing down auto-ignition. Reactivity Controlled Combustion Ignition (RCCI) combustion, also known as dual-fuel PCCI, has come into existence as a combustion method in which the reactivity of the fuel mainly controls combustion. Dual-fuel combustion is a modification from the PCCI method, since reactivity of the fuel differs across cylinders, along with the mixing of fuel and air before combustion. To maximize the combustion, phasing, and duration, RCCI technology uses in-cylinder fuel mixing with at least two fuels with different reactivity and multiple injections, to manage in-cylinder fuel reactivity and emission. This process creates a well-mixed charge in low-temperature combustion; low reactivity fuel, air, and exhaust recirculated gases are introduced into the cylinder. The high-reactivity fuel is injected into the combustion chamber before premixed fuel is ignited, which can be done with single or multiple injections. The control of HRF and LRF with optimum mixing of air and fuel is the key to control and improve efficiency of CI engine.

## **1.2 Scope and Objectives of Thesis Work**

Using a compression engine with dual fuel is the most promising technology to control emission and for fuel economy, to meet the upcoming legislative norms. This experimental study is required to understand the effect of fuel reactivity on engine performance and emission in a CI engine.

The effect of injection timing, gasoline ratio, and EGR rate on emission on dual fuel must be investigated in intake manifold. Experimental study was done to understand the characteristics of particulate mass and particulate size distribution in engine emission with Low Reactivity Fuel and High Reactivity dual fuel.

**The objectives of experimental study are:**

- To study the emission and performance behaviour with dual fuel (Low and high reactive fuel) in CI engine to assess the best strategy to control NO<sub>x</sub> and PM
- To investigate particulate matter emissions and particulate matter composition
- To study effect of fuel composition, fuel injection pressure, EGR content, sulphur content and engine load on particulate size
- To study correlation of particulate mass and particle number with dual fuel ratio

**1.3 Organization of the Thesis Work**

The thesis is organized as follows: In Chapter 2, literature on various dual fuel combustion considered for HCCI, RCCI, PCCI and Low Temperature Combustion is presented. The advance LTC concepts, operation and fuel chemistry is also discussed to obtain the near zero emissions. 3D Computational Fluid Dynamics (CFD) simulations are discussed in Chapter 3 to examine the variation of the gasoline/air combination at each cylinder's inlet port. Chapter 4 presents details of experimental setup used to study dual fuel combustion behaviour with low reactivity and high reactivity fuel.

A detailed discussion on dual fuel combustion NO<sub>x</sub> and soot characteristic with different experimental trials are conducted to study combustion behaviour of LTC is presented in Chapter 5. Chapter 6 provides experimental study to comprehend particle mass and particle size distribution with various dual fuel mixes. Finally, the conclusions and scope for future work is summarized in Chapter 7.

## **CHAPTER 2**

### **LITERATURE SURVEY**

Internal combustion engines (ICEs) continue to power light- and heavy-duty transportation vehicles despite the introduction of new energy conversion devices. Innovative ICE technologies are used to operate engines at high thermal efficiency and low emission levels to handle the current issues of depleting fossil fuel supplies and harmful combustion-generated pollutants. Compression ignition (CI) engines are most efficient power-producing devices but has the drawback of high  $\text{NO}_x$ –soot emissions [1].  $\text{NO}_x$  and soot (particulate mass) are big challenges in the use of diesel engines, leading to the use of costly after-treatment devices to meet stringent emission regulations [2]. Low temperature combustion (LTC) technology has the potential of reducing simultaneously both  $\text{NO}_x$  and particulate mass. A literature review is conducted to understand the dual fuel engine performance and emission, soot composition behaviour with a different dual fuel ratio, and correlation between the particle number (PN) and mass.

Fundamental research on efficient and cleaner combustion technologies (homogeneous charge compression ignition (HCCI), reactivity-controlled compression ignition (RCCI), etc.) using various forms of alternative fuel is going on for more than two decades. By altering the compression ratio and inlet temperature, these techniques are expected to use practically any fuel. These technologies are categorized as part of the low-temperature combustion (LTC) method, which produces great efficiency and low emissions by using extremely lean fuel/air (generally) or by highly diluted mixing. [3]. Numerous researchers have shown that the LTC, HCCI, and premixed charge combustion ignition (PCCI) ideas are efficient means of decreasing  $\text{NO}_x$  and soot at the same time [4]. The majority of HCCI and PCCI research works have utilized either gasoline or diesel fuel due to the presence of the current fuel infrastructure. However, each fuel has distinct benefits and drawbacks for premixed combustion in their unblended forms [5]. RCCI provides greater control on combustion and significant improvement in thermal efficiency, approaching 60%, compared with HCCI and PCCI [6]. Soot and  $\text{NO}_x$  formation zones are avoided when combustion of the lean homogeneous mixture is achieved. Mixing-controlled LTC conditions are achieved

with high rates of EGR to keep the combustion process away from the soot and  $\text{NO}_x$  formation zone. Despite significant emission benefits of LTC, its practical implementation in CI engine is limited due to practical difficulties. The most important barriers are obtaining proper combustion phasing, controlling variation in the cycle-to-cycle combustion process, and performance at high load conditions. The literature review on LTC is divided into the following sections:

1. HCCI, PCCI, and RCCI combustion
2. LTC
3. Fuel reactivity and fuel characteristics
4. Particulate emission formation in dual fuel
5. Particle matter formation mechanism

The conventional diesel engine combustion is characterized by both high temperature and heterogeneous mixture zones that lead to  $\text{NO}_x$  and soot formation. The region with rich fuel–air mixture is prone to soot formation while the high temperature region with lean fuel–air mixture promotes  $\text{NO}_x$  formation. Reducing the combustion temperature along with the lean fuel–air mixture locally will avoid  $\text{NO}_x$  and soot formation.

## **2.1 Homogeneous Charge Compression Ignition (HCCI)**

In the past 20 years, HCCI has received considerable attention. A homogeneous charge compression engine is produced via port injection or early fuel injection inside the cylinder, and it ignites when the cylinder reaches a certain temperature and pressure. In 1979, Noguchi et al. [1] used a spectroscopic technique to explore the HCCI combustion process. The HCCI combustion mechanism is unique compared with typical gasoline engines, where all radicals are almost always visible at the same moment. In comparison with conventional diesel and gasoline engines, HCCI can produce low  $\text{NO}_x$  and soot emissions and is very efficient, but its operating range is limited and managing the auto-ignition timing is challenging. Hence, certain novel approaches are utilised, including active stratification of charge and temperature, modifications to the fuel characteristics, and alternative injection techniques.

Air and gasoline are combined before induction into the cylinder, and auto-ignition of the charge at multiple points in the cylinder is achieved by compressing charge under conditions of very high temperatures and pressures. The HCCI engine requires dilution of the intake charge in normal operation to control the rate of rise in pressure during combustion. As a result, the combustion temperature drops, which is good for reducing NO<sub>x</sub> and soot emission. However, the premixing and low combustion temperature result in high CO and HC emissions. A range of fuels can be utilised with HCCI by carefully regulating the compression ratio and intake charge temperature. The usage of HCCI has been constrained to that of an ideal combustion research tool due to difficulties in controlling the combustion rate. The HCCI approach is not yet matured for commercial implementation. The auto-ignition properties of fuel for extending the operating range in HCCI were defined by Yao et al. [2], Dec [3], Musculus et al. [4], and Komninos and Rakopoulos [5]. Richter et al. [6] studied the fuel–air mixture in an HCCI engine using planar laser-induced fluorescence (PLIF). The fuel–air charge was homogenized to varying degrees using two different premixing methods, namely, a typical port injection and a 20-litre preheated mixing tank. Different fuel preparation methods had an impact on the homogeneity of the fuel–air mixture and the spatial variability of the combustion process. They reported that despite the great degree of homogeneity as observed in the PLIF data, local inhomogeneous fluctuations were observed in the measurements of Raman scattering, due to cycle-to-cycle variability. Musculus [7] studied in-cylinder spray and mixing processes under LTC conditions and reported 4 bar as the indicated mean effective pressure at low loads. To test both naturally aspirated at low boost pressure of 1.34 bar cases, the start of injection (SOI) was set to 22°CA ATDC. Fuel vapor fluorescence was employed to assess the vapour jet, whereas Mie scattering was used to represent liquid fuel penetration. The maximum liquid fuel penetration for the normally aspirated condition was between 45 and 50 mm, while for the low-boost condition it was between 40 and 45 mm. However, under standard diesel operating conditions, the usual liquid fuel penetration was around 25 mm [8, 9]. The ambient gas density and temperature were lower for early-injection settings than for near top dead centre (TDC) injection in a typical diesel engine. The extended penetration caused the fuel to impinge on the piston bowl.

The in-cylinder mixture distribution in an optically visible direct-injection HCCI engine was studied by Kashdan et al. [10]. A maximum injection pressure of 1100 bar was used with a high-pressure common-rail injection system. The qualitative distribution of the mixture (liquid and vapour phase) inside the piston bowl was compared using planar laser-induced exciplex fluorescence imaging. The liquid fuel normally emerges 2°CA after the commencement of injection (SOI) and strikes the piston face at around 33°CA ATDC. Fuel stratification and a fuel-rich area were seen in the centre of the piston bowl at about 30°CA ATDC because of fuel impingement. The delay in injection timings accelerated the stratification trend. In a high-speed direct inject diesel engine, Fang et al. [11, 12] studied the liquid spray evolution process using Mie scattering. For both the standard wide angle injector and the narrow angle injector, the injection time was adjusted from 40° to 80°CA ATDC while maintaining the IMEP in order to generate the homogeneous charge. The narrow angle injector was reported to reduce the amount of fuel that was left on the liner; however, it was found to cause fuel-wall impingement on the bowl wall and ensuing pool fires. Liu et al. [13] also noted wall impingement for early injection cases.

Steeper and de Zilwa [14] studied the HCCI concept with two gasoline direct injection injectors for the stratified charge under low-load condition. The first injector had eight holes with a 70° spray angle, while the second was a swirl injector with a 53° spray angle. For both injectors, the distribution of the equivalence ratio was identical, but the eight-hole injector produced more and smaller fuel packets than the swirl injector. Spray penetration was examined by Liu et al. [15] under various ambient temperature circumstances (700–1000 K), including both LTC and conventional diesel combustion. The high ambient temperature due to the combustion flames downstream showed lower liquid penetration lengths. Lower ambient temperatures had less impact on the length of liquid penetration; n-butanol spray slightly changed the length of liquid penetration when compared with soybean biodiesel. It could be because n-butanol spray flames have a longer soot lift-off time.

Prior to ignition, early direct injection helps to provide a more uniform air–fuel mixture; however, fuel impingement on the piston head or cylinder lining might result in oil dilution and wall-wetting [16–18]. The discussion lead to the conclusion that the direct injection technique offers more benefits than port injection for HCCI auto-ignition control and for

expanding the operational range [19–21]. The recommended methods for enhancing the mixing include the use of narrow angle injectors [22–25], two- or multistage injection [26], and high injection pressures [27]. Researchers also studied the combustion mechanism in engines to understand and improve the combustion with HCCI, PCCI, and RCCI concepts. Most spectral analysis research works have focused on ordinary gasoline engines or diesel engines that use low soot fuels such as dimethyl ether (DME) [28]. However, it was reported that HCCI, PCCI, and LTC only produced small amounts of soot emissions [29–32]. It was recently found that these new combustion modes are suitable for chemiluminescence images and spectral analysis [33–36]. The effects of various operational parameters, such as intake temperatures, fuel delivery techniques, and engine loads, on the chemiluminescence spectra in the HCCI engine, were described by Augusta et al. [37]. Adjusting the engine operating parameters resulted in varied auto-ignition timings, but it had no impact on the reaction pathways of HCCI combustion after initiation of combustion. Liu et al. [13] and Murase et al. [38] reported similar findings.

The combustion and auto-ignition behaviour of HCCI was studied by Mancaruso and Vaglieco [39] with a high-pressure injection of the diesel engine. The chemiluminescence pictures and spectra demonstrated the homogeneous distribution of HCO and OH in the visible region. It was hypothesised that OH radicals could have contributed to the soot reduction in the cylinder because a significant amount of OH radicals were observed. No luminosity between low temperature heat release (LTHR) and high temperature heat release (HTHR) was recorded. Using a high-speed intensified camera, Dec et al. [40] reported that HCCI combustion is a gradual process from the hot zone to the cold zone before intake under the condition that air and fuel are fully premixed. The inhomogeneities were believed to be mostly a product of naturally occurring thermal stratification brought on by heat transfer during compression and turbulence transport inside the cylinder. This result showed that the HCCI combustion was not homogenous. Hultqvist et al. [41] have also reported that thermal stratification is also a part of the HCCI combustion process. The HCCI operating range can be further extended, to control combustion phasing by strengthening the charge or thermal stratification using methods such as different multiple injection strategies, EGR

configuration (external or internal), combustion bowl geometry, and modulated intake temperatures [42].

Larger temperature stratification can increase the operating range to greater loads, resulting in a slower rate of heat release. The HCCI combustion processes may be impacted by turbulence or temperature stratification brought on by changes in the piston shape. This was studied in many papers related to charge and temperature stratification in HCCI combustion. A greater temperature stratification was created by the 125 °C intake temperature, which was higher, and the 55 °C coolant temperature, which was lower [43–45]. Aleiferis et al. [46] produced charge and temperature stratification by varying the injection timings, heating the inlet air, and trapping residual gas (internal EGR) in HCCI combustion. A slower auto-ignition front movement speed was demonstrated by the cylinder's increased temperature inhomogeneities.

Under HCCI operating circumstances, Berntsson and Denbratt [47] looked at the impact of charge stratification on combustion and emissions. HCCI under homogenous circumstances required 4°CA, while the stratified condition required 8°CA, as evidenced from the appearance of auto-ignition to reactions occurring across the combustion chamber. The combustion images revealed that the local modification of the equivalency ratio could limit the rate of heat release and so further expand the HCCI operating range. The images also revealed that the combustion duration was extended. Dual-fuel injection combined with port and in-cylinder injection is studied in depth to achieve high efficiency and clean combustion [48–55]. In a dual-fuel system, a homogenous mixture may be produced by employing high volatility fuels for port injection, and in-cylinder injection can be used to produce a variety of stratifications in the cylinder by adjusting injection timings. Additionally, two fuels that have opposing auto-ignition characteristics can be combined to form different fuel reactivities in the cylinder. This can control auto-ignition and extend the operating window for high efficiency and clean combustion. Although charge stratification and reactivity stratification were studied [56], there are presently few optical diagnostics available for dual-fuel injection mixture formation.

## 2.2 Reactivity-Controlled Compression Ignition (RCCI)

RCCI combines two fuels with varied reactivities (auto-ignition resistance) in different amounts. The two fuels considered include one with low auto-ignition resistance directly injected and another fuel with high auto-ignition resistance premixed with air in the intake manifold. RCCI uses dilution and the LTC method as opposed to the dual-fuel approach. Experiments with RCCI report high efficiency paired with HCCI-like emission characteristics.

The effects of charge inhomogeneity on the RCCI combustion process were examined by Kumano et al. [57]. In an optical engine with DME as a test fuel, the homogeneous charge was provided with a device installed upstream of the intake manifold. It was evident that at inhomogeneous mixtures, the combustion time increased, leading to a moderate heat release and a slower maximum pressure rise rate. The maximum heat release rates and pressure increase rates can be reduced by charge or thermal stratification. This may result in an extension of the operating range. The effective methods for charge stratification include two-stage direct injection in the cylinder or port injection combined with direct injection [58–62]. Altering the intake and coolant temperatures is a simple way to address temperature or thermal stratification, but it is challenging to implement this strategy in a real engine. Hence, internal EGR is a better way to create temperature inequalities inside the cylinder [63, 64]. However, this could also have an impact on combustion due to temperature changes, chemical action, and dilution. Additionally, a certain piston geometry may produce turbulence with a varied intensity, which would lead to temperature inhomogeneity. Thus, thermal and charge stratification are efficient ways to control RCCI combustion [65–67].

The late-injection diesel fuel RCCI combustion process was studied by Kashdan et al. [68] at 45% EGR dilution. Similar to homogeneous circumstances, formaldehyde was quickly consumed at the beginning of the high-temperature reactions, and subsequent reactions were triggered by the presence of OH-LIF. The strong PAH fluorescence served as evidence that soot precursors were also present as the late injection produced certain localized high-equivalence ratio regions. RCCI combustion with port injection or early injection can be seen in low emissions of  $\text{NO}_x$  and soot due to the relatively homogeneous charge. However,  $\text{NO}_x$  and soot emissions may increase if fuel stratification is created through late direct injection.

Hence, research on the processes of  $\text{NO}_x$  and soot generation in RCCI combustion is required. RCCI combustion is also reported to produce significant amounts of unburned hydrocarbon (UHC) and CO emissions. More research has been done on formaldehyde-LIF measurements than on HCCI's CO distributions [69–75]. The chemical kinetics can adequately explain the evolution of UHC and CO. For EGR-diluted engines, fuel-lean zones developed during the ignition delays are probably a significant source of UHC and CO emissions under LTC conditions. The UHC and CO emission need to be researched in detail [76–80].

Direct injection is more advantageous than port injection for RCCI auto-ignition control and for extending the operating range. The application of early injection is constrained by the potential of gasoline to impinge on the piston head or cylinder liner and cause wall-wetting. Wall impingement further hinders the formation of a more uniform air–fuel mixture prior to ignition. Dual-fuel injection allows for flexible stratification of charge and fuel reactivity, even if an additional fuel tank is required.

### **2.3 Partially Premixed Compression Ignition (PPCI)**

Both RCCI and HCCI's guiding principles can be found in PPCI as a concept. Direct injection event and auto-ignition combustion are separated in PPCI. Entirely premixed or fully heterogeneous situations can be prevented by infusing the fuel during the compression process, along with air dilution, significant residual gas concentrations, and a fuel. This results in great efficiency and low emissions of soot,  $\text{NO}_x$ , HC, and CO. With liquid fuels, PPC demonstrates significant fuel flexibility by adjusting the injection method to the fuel's auto-ignition characteristics. Low auto-ignition resistance of the fuel makes it harder to accomplish sufficient premixing, which could result in increased soot emissions. PPCI is a novel combustion mode that has been developed. These strategies of combustion modes are controlled and governed by the kinetics of chemical reactions, and the combustion produces more UHC and CO than  $\text{NO}_x$  and soot. Some novel terms, including stratification charge compression ignition (SCCI) [81–84] and PPCI [85–90], are used to identify these combustion modes. High EGR dilution LTC has been the subject of extensive research [90–92] in diesel engines over the past decade. PPCI combustion with two-stage injection was

studied by Kook and Bae [93] in diesel engines. The temperature of the initial injection ( $10 \text{ mm}^3$ ) was adjusted to  $200^\circ\text{CA}$  ATDC to create a uniform and complete mixing of diesel and air. As an ignition stimulant and to regulate the auto-ignition process, the second injection ( $1.5 \text{ mm}^3$ ) was adjusted to  $15^\circ\text{CA}$  ATDC. The injection pressure was kept at 120 MPa. The PCCI combustion was compared with conventional diesel combustion with the whole fuel ( $11.5 \text{ mm}^3$ ) being injected into the cylinder at  $15^\circ\text{CA}$  ATDC. However, for the PCCI, the brilliant flames only appeared in the heterogeneous combustion zones of the second injection, and the dispersion was likewise quite constrained. The authors concluded that for homogeneous combustion flames, the first injection timing needs to be pushed earlier than  $100^\circ\text{CA}$  ATDC. A comparison among different combustion strategies is presented in Table 1.

**Table 2.1 – Comparison of Different Types of Combustion Techniques**

Type	SI	CI	HCCI	PCCI	RCCI
Ignition Type	Spark Ignition	Compression-Ignition			
Fuel Type	Octane	Cetane	Blend of high and low reactive fuels (liquid and gas fuel)		Blend of high octane and high cetane fuel
Control Mechanism	Speed of flame propagation	Duration of fuel evaporation, mixing, and ignition	Chemical kinetics	Chemical kinetics and fuel injection timing	Chemical kinetics and fuel reactivity control
Emission Behaviour	HC, CO, $\text{NO}_x$ , and $\text{CO}_2$	High PM and $\text{NO}_x$ lower than $\text{CO}_2$	High HC, CO, and low $\text{NO}_x$ , PM, and $\text{CO}_2$	High HC, CO, and low $\text{NO}_x$ , PM, and $\text{CO}_2$	Very high HC and CO and ultra-low $\text{NO}_x$ , PM, and $\text{CO}_2$

## **2.4 Low Temperature Combustion (LTC)**

The potential of LTC is to reduce combustion temperature and soot formation using dual fuel. Lean homogeneous air–fuel mixture combined with lower combustion temperature is a key factor for achieving LTC. The homogeneous mixture is achieved through various ways such as early injection, premixed charge, extending the ignition delay, and EGR. This gives rise to various concepts for combustion improvement. The LTC techniques are used with CI and run without a throttle at compression ratios akin to those used in diesel engines to maintain excellent thermal efficiency. RCCI, homogenous charge compression ignition, premixed charge compression ignition, and partially premixed combustion are all examples of low-temperature combustion techniques. Early fuel injections are used to give enough time for air–fuel mixing prior to combustion [94, 95].

By diminishing the CN in the fuel mixture by adding fuel with low-cetane and high-octane values, the ignition delay can be extended. Studies are now being carried out to discover strategies to prolong the delay. Longer ignition delay gives more time for air and fuel to mix before combustion begins. This diminished the fuel-rich zone and prevents soot production while maintaining an excellent fuel economy. Premixed LTC operation can offer advantages in fuel economy over traditional fuel mixing or diffusion-controlled techniques by properly controlling combustion phasing.

Lower  $\text{NO}_x$  is dependent on a longer ignition delay and a slower combustion rate in PCCI, HCCI, and RCCI combustion modes [97–100]. The lack of a combustion phasing control mechanism and challenges in controlling the heat release rate make some low-temperature combustion techniques difficult to implement for use in automobiles [101–103]. The RCCI combustion idea was developed to address these issues. RCCI is a dual-fuel partially premixed combustion concept that uses direct injection of a high-reactivity fuel (such as diesel and biodiesel) and port fuel injection of a low-reactivity fuel (such as gasoline, natural gas, and alcohol fuels) with blending inside the combustion chamber to prolong combustion and control phasing. The relative ratios of the two fuels regulate combustion phasing, while the spatial stratification between the two fuels regulates combustion duration [104, 105].

High EGR dilution low-temperature combustion (LTC) has been extensively studied during the last ten years [106–108]. Since the start of the injection in LTC is close to TDC, the auto-ignition time can be loosely controlled by the injection timing. Late injection timing also prevents fuel from impinging on the piston head or cylinder lining [109, 110]. However, because of the incomplete mixing of diesel and air caused by the late injection, there is a locally rich zone in the mixture that resembles diesel conventional combustion. The relatively low combustion temperature brought on by the high levels of EGR, though, can steer clear of the soot generation area.

In their research work on an optical diesel engine, Akihama et al. [111] were the first to report that high EGR dilution can minimise soot generation. Luminosity of soot initially grew as EGR rates increased, but as EGR rates increased further, the brightness of the soot reduced, and no luminosity was seen under high EGR dilution. In addition, because of high EGR dilution and associated low combustion temperature,  $\text{NO}_x$  emissions could potentially be close to negligible. The injection parameter, which includes injection pressure, timing, and multiple injections, affects the temperature during the ignition delay period, the peak flame temperature, and premixing improvement. High boost levels are required to maintain the engine power density and thermal efficiency with a high rate of EGR percentage. As a result, the regulation and optimization of the EGR rate, injection characteristics, and high boost form the basis of the LTC study [112-115].

Upatnieks et al. [116] used in-cylinder flame luminosity images to determine the flame lift-off lengths. They reported that soot incandescence was not visible even for a locally fuel-rich mixture, whereas the same stoichiometric combustion produce soot incandescence without EGR dilution. The low flame temperature caused a blue flame to simultaneously be visible for the LTC condition. The flame lift-off was higher under LTC circumstances than during regular diesel combustion. Musculus et al. investigated the LTC using a variety of laser diagnostics [117]. Using various fuels, including diesel, soybean biodiesel, n-butanol, ethanol, and blended fuels [118-120] examined the natural luminosity during both normal diesel combustion and LTC. They discovered that natural flame luminosities decreased when ambient temperatures and oxygen concentrations decreased. Furthermore, at low oxygen concentrations of 10.5 percent, the dispersion or area of the flame was clearly enlarged, and

a lot of flames were visible close to the chamber walls. The distinction between high and low ambient temperatures is that soot emissions rose even while the natural luminosity dropped with the decline in oxygen concentrations at 1000 K ambient temperature.

Different soot emissions were produced because of altered soot formation and oxidation rates in combustion process [121]. Based on the analyses of the natural luminosity of LTC, it was concluded that the bigger dispersion of the combustion flame was closer to the cylinder wall, indicating higher flame lift-off than traditional diesel combustion. The natural luminosity decreased monotonically as oxygen concentrations decreased, although soot emissions increased initially before declining after reaching their highest value. Singh et al. [122] and Huestis et al. [123] used two-colour pyrometry to study soot oxidation and production processes under LTC condition. Multiple injection strategies (early, late, and double) were investigated in detail to understand its behaviour. Nitrogen gas was employed to create reduced oxygen concentration. The authors reported that LTC had lower soot thermometry and luminosity photographs than in typical high temperature combustion. Under LTC conditions, soot temperatures determined by two-colour pyrometry were not far from adiabatic flame temperatures. The peak soot volume was almost 1.5 times greater for late and double injection than for early injection. Since there was sufficient time for diesel fuel to permeate and combine with the surrounding air under LTC conditions, soot combustion primarily took place close to the edge of the bowl. However, under high temperature combustion circumstances, soot formed in the fuel jet further upstream.

Other many conducted research [124] on low-temperature combustion's soot luminosity and soot laser-induced incandescence at the injection timing of 22°CA ATDC. Soot generation could only be observed in areas devoid of OH radicles, indicating that soot and OH don't coexist in the same areas [125, 126]. Furthermore, with traditional diesel combustion, soot continued to build up in the head vortex zones. Thus, compared with standard diesel combustion conditions, it can be said that the upstream soot production can be avoided for new LTC modes. Additionally, even if aiming for a relatively longer premixed LTC process, the decrease in soot production in the head vortex zones remains a significant problem.

Under both standard diesel combustion and LTC circumstances, Liu et al. [127] quantitatively studied the soot concentration with copper vapour laser by using the forward-illumination light-extinction technique. To better understand soot evolution, soot models have been updated [128]. They discovered that at 18% oxygen, soot formation and oxidation rates rose simultaneously in comparison with those at 21% oxygen concentration. However, the higher soot formation rate led to a higher soot mass during the combustion phase. At 15% oxygen concentration, both soot creation and oxidation rates were simultaneously decreased. Nevertheless, the amount of soot produced during combustion increased further, which is thought to be a result of the suppressed oxidation rates of the soot. As oxygen levels continued to drop, soot generation was severely repressed, which in turn lowered soot emissions. At 1000 K, the soot mass rose as oxygen concentrations decreased, which could be explained by an increase in high-equivalence ratio locations and an increase in the synthesis of acetylene and soot precursors at lower ambient oxygen concentrations. However, at 800 K ambient temperature, the soot mass decreased as oxygen concentrations increased, which was the result of reduced high-equivalence ratio regions, as well as lower acetylene and soot precursor generation. Considering the ambient oxygen dilution in conventional and low-temperature fires, the authors concluded that the soot production transition from 1000 K to 800 K should be the primary factor for varied soot emissions.

Zhang et al. [129] used two-colour pyrometry and soot luminosity to conduct similar research about oxygen concentrations and ambient temperatures. Contrary to traditional diesel combustion, which produces soot just downstream of the liquid spray and throughout the jet cross section, LTC soot generation happens significantly further downstream of the liquid spray and only at the head of the jet, in the head vortex, or close to the edge of the bowl. The locations along the chamber walls and further downstream of the liquid spray still have the highest concentrations of soot, according to experimental studies. Therefore, it may be argued that very low oxygen concentrations lead to certain soot distributions.

Although HCCI and LTC can produce very low levels of  $\text{NO}_x$  and soot emissions, they frequently produce higher levels of CO and UHC emissions. Under LTC circumstances, many researchers [130-133] investigated the overmixing and UHC emissions from a heavy-duty optical diesel engine. The LIF of a fuel tracer in an optical engine and planar laser-

Rayleigh scattering in a constant volume combustion chamber were used to calculate the equivalency ratio of mixtures close to the injector under no-combustion conditions. The optical diagnostic images showed that the transitory ramp-down of injector caused a low-momentum spray penetration at the conclusion of injection, resulting in the formation of a fuel-lean mixture in the upstream region of the spray jet.

The distribution of UHC and CO on a light-duty diesel optical engine in LTC circumstances with early and late injection was studied by Ekoto et al. [134–135] and Petersen et al. [136]. Most of the fuel collected in the inner bowl during high temperature heat release (HTHR), according to the LIF measurements on the equivalence ratio, leads to UHC and CO emission. A significant amount of this fuel was also transferred into the squish volume by the action of reverse squish flows. Then fuel oxidation in the squish zones was suppressed by the lean mixes and substantial heat transfer losses to the wall. Because of this, squish regions were able to capture the primary distributions of UHC and CO.

In LTC circumstances, the soot production only occurs at the beginning of the jet, in the head vortex, or close to the edge of the bowl, considerably further downstream from the liquid spray [137]. Furthermore, the soot distributions are concentrated in the areas further downstream of the liquid spray and close to the chamber walls even when the combustion temperature is not low. Therefore, it can be argued that quite low oxygen concentrations are what lead to soot-specific distributions in LTC circumstances. In HCCI combustion processes, there are also significant amounts of UHC and CO emissions, and some studies concentrate on formaldehyde-LIF measurements to depict the distribution of UHC in the late cycle. Although HCCI is governed by chemical kinetics and the evolution of UHC and CO can be adequately explained by chemical reaction mechanisms, there are a few research works on CO distributions in HCCI. Chemical kinetics and a combined process including diesel fuel and air are both used to manage it under LTC settings in addition to chemical kinetics alone. For EGR-diluted LTC diesel engines, fuel-lean zones that are developed during the time of ignition delays are probably a significant source of UHC and CO emissions under LTC conditions.

The major challenge with LTC is to control hydrocarbon and carbon monoxide emission in the dual-fuel mode, where gasoline is used as the secondary fuel. Low-temperature combustion (LTC) research in diesel engines focuses on stringent emission norms and the use of limited fossil fuel reserves. LTC helps in the simultaneous reduction of nitrogen oxides ( $\text{NO}_x$ ) and particulate matter (PM)/soot emissions in a diesel engine. PM is generated by the incomplete combustion of fuel hydrocarbons and oil, with lubricating oil playing a minor role. Soot formation usually occurs at temperatures higher than 1800 K in a diesel combustion environment. The difference between the formation and oxidation of soot is known as net soot release. Soot formation and oxidation and  $\text{NO}_x$  formation are closely correlated with the combustion temperature. PM and PN in soot are critical emission parameters with profound health impacts on the human body, specific to cardiovascular disease. PM emission correlates with human health and the environment, especially a small particle diameter. Hence, PM and PN are included in different engine exhaust emission legislations.

In the first section of the chapter, the various low-temperature combustion strategies are briefly discussed. It is then demonstrated that, in terms of fuel flexibility and combustion controllability, RCCI has some advantages over homogenous charge compression ignition and premixed charge compression ignition combustion techniques. This literature highlights upcoming research directions and the significance of RCCI method as a potential remedy for future car engines.

#### **2.4.1 Steps in LTC Mode**

- EGR is provided to dilute the fuel–air mixture to control combustion and heat release rate.
- The entire charge in cylinder spontaneously ignites at various points simultaneously at the end of compression stroke whenever the test condition of the fuel–air mixture reaches auto-ignition temperature.
- Controlling the heat release rate precisely is key to emission and combustion efficiency.

### **2.4.2 Benefits of LTC**

1. Reduces emission of PM and NO<sub>x</sub> simultaneously
2. Control of heat transfer losses
3. Reduces the cost of major EATS hardware to meet legislative norms
4. Better fuel economy

### **2.4.3 Challenges with LTC**

1. To achieve LTC combustion in the vehicle's entire operating region, across a wide range of speed and torque
2. To decrease HC and CO emissions in low engine load condition and increase combustion efficiency
3. After-treatment catalyst loading and the additional component of secondary fuel system integration
4. To control HC emission with the increase in low reactive fuel, thermal management, and optimization of PGM loading in oxidation catalyst
5. Different ranges across all engine speed zones, as LTC does not provide accurate control over the commencement of combustion (The problem becomes significant during transient engine operation.)
6. Load restrictions on the LTC regime, which can only be used at low-to-medium loads (The engine operation modes must alternate between LTC mode at lower loads and standard CI mode at larger loads for real-world LTC implementation.)

LTC can be a viable technique by addressing these challenges. Fuel reactivity is one key to addressing the LTC challenges. The following sections review the literature on fuel reactivity.

## **2.5 Fuel Reactivity**

Dual fuel is a strategy where two different reactivity fuels are used. Gasoline and natural gas are used as low reactivity fuels (LRFs) while diesel is used as a high reactivity fuel (HRF).

The major advantage of using both gasoline and diesel is that the availability of dual fuel engine makes it reliable for installing in a vehicle, and this can be used in a larger geographic area. Therefore, experimental studies performed on LTC combustion focus on the use of gasoline as a potential fuel along with diesel fuel [138].

Researchers have investigated a variety of fuels with distinct low- and high-reactivity fuel combinations. Fuel reactivity is one of the parameters that can affect the in-cylinder reactivity. By varying the fuel ratio, the reactivity in the cylinder can be varied and subsequently the ignition delay be affected. Fuel reactivity is defined as the tendency of fuel to undergo chemical reaction during combustion. Petroleum and renewable fuels can be classified based on reactivity of fuel. HRFs (such as diesel and biodiesel) show LTHR and HTHR while LRFs (such as gasoline and alcohol) exhibit only HTHR. The HRF shows a two-stage heat release and have a high cetane number (CN) while LRF fuels show a single stage heat release and a high octane number (ON). The oxidation of hydrocarbon (HC) in a low-temperature zone is a complex process that involves various chain branching and chain propagation reactions [139]. When there are more chain branching initiation reactions than chain termination reactions, spontaneous ignition happens [140]. As a result of chain branching, an isomerization reaction occurs in which straight-chain alkanes are heated to form branched isomers. This leads to several radicals kicking off the auto-ignition reaction. The size, structure, and pressure–temperature history of the charge all affect when and how much heat is released during the first stage of ignition [141].

### **2.5.1 Diesel Fuel**

Olefins, branched and straight-chain alkanes, single and multiple-ring aromatics, and other chemical species are all mixed together to form diesel fuel. Diesel has approximately 41% paraffins, 30% cycloparaffins, and 29% aromatics by volumetric composition [142]. Paraffins and naphthalenes are saturated HC molecules. Unsaturated hydrocarbons (HC) such as aromatics and olefins can change a carbon-carbon (C=C) covalent or aromatic bond into a single bond by attaching a hydrogen (H) atom to the nearby carbon (C) atom [143]. High CN and a rapid igniting delay characterize a long chain saturated HC molecule (ID). The chemistry of two-stage ignition in diesel is caused by a significant number of long,

straight-chain alkanes (n-paraffins). Diesel shows low volatility due to strong intermolecular force of attraction and requires high temperature (nearly 453–473 K) for vaporization. The boiling point of liquid is inversely proportional to the intermolecular strength. The long molecular chain shows a high surface area and intermolecular force, thus requiring more energy for boiling [144]. Due to straight and branched chain hydrocarbons ( $C_{10}$ – $C_{19}$ ), the boiling point of diesel ranges from 453 to 643 K [145]. The diesel and biodiesel combustion exhibits two-stage ignition. LTHR, the first step of heat release, is defined as slow kinetic reactions that take place below 850 K with little (7–10% of total) heat release [146]. The rest of the fuel energy is released when the charge temperature is beyond 950 K during the HTHR. The negative temperature coefficient (NTC) regime separates the LTHR and HTHR. Even while the overall charge temperature increases during the NTC area, the reaction rate rapidly drops [147]. A pressure–temperature history of the charge, EGR, and LRF, such as gasoline or ethanol in the event of dual-fuel engine running, can all be used to manage the charge reactivity throughout the NTC period [148].

### **2.5.2 Gasoline Fuel**

Gasoline is a mixture of saturated (42.2%) and unsaturated (57.8%) hydrocarbons [149]. The single sigma bond in branched alkanes (saturated hydrocarbon) shows the maximum number (85%) of small carbon species ranging from  $C_4$  to  $C_9$  hydrocarbons and is very stable and hard to break. The molecular chain branching reduces the molecular surface area and intermolecular force, which results in increased fuel volatility and short combustion duration [150]. A small molecule requires a high energy to break the bonds. Gasoline shows high ON and very low reactivity. Distinct reactions to start the combustion are not present even at high temperatures (close to 700 K). However, during combustion, instantaneous energy is released due to fast oxidation and a low number of reactions [151]. The fuel's auto-ignition depends on chain branching, and it is a function of fuel molecular structure, surrounding the air pressure–temperature and equivalence ratio. For a fuel to start auto-ignition, a large enough radical pool is required. The molecules with a greater number of primary C-H bonds provide more resistance to auto-ignition, while least resistance is offered by tertiary C-H bonds (highly reactive) [152]. A high level of energy is required to dissociate the primary C-H bond at extremities and form the free radicals to propagate the chain branching reactions

in Isooctane [153]. As the LTHR leading alkyl peroxy radical production reaction is reversible and radical formation decreases with increasing temperature, LTHR decreases with an increase in ON and intake air temperature [154]. An optimal combination of fuel reactivity is important to achieve LTC. More studies are required to understand and optimize use of dual reactivity fuel in CI engine [155- 156]. Formation of PM in dual fuel is reviewed in the next section.

## **2.6 Particulate Matter (PM) Formation**

PM is the most significant risk factor for human health, which results in global casualties. Multiple literature reviews have highlighted the impact of effects of PM on health depending on its composition, particle size, and particle nature. Globally, every year an estimated 4.2 million people die from air pollution-related causes such as heart disease, lung cancer, and other respiratory disorders. PM is a most significant risk factor for human health resulting in global casualties. Particle size of diameter 10 microns or less ( $PM_{10}$ ) can cause lung-related problems in human body. Fine PM with a diameter of 2.5 microns or less is defined as  $PM_{2.5}$ . The composition of particulates  $PM_{10}$  and  $PM_{2.5}$  is made up of distinct chemicals that come from diverse sources of pollution. Particle emissions' concentration is very high in diesel engine in comparison with gasoline engines because of high carbon content in exhaust gas. The particle size and number are very sensitive to human body as they are related to issues in the respiratory system. Fine particle pollution can be harmful or include dangerous (including carcinogenic) trace substances, causing immune system disruption. Fine particles irritate lung tissue and cause long-term problems by penetrating deep into the respiratory system. It is important to understand the formation of PM with gasoline and diesel fuel with respect to the PN and size distribution.

Diesel exhaust PM emission is composed of carbon soot with absorbed organic compounds, which grows during gas-to-particle conversion. PM's composition consists of fine particles and liquid droplets, including ash, water SOF, nitrates, oil and fuel content (SOF) from diesel engine. PMs have different characteristics of number, chemical composition, shape, size and origin. The composition of particle size distribution includes three modes of ultra-fine, fine, and coarse particles in their composition. As particle size rings collide, soot coagulates and clusters together like a chain, forming agglomerates with sizes varying from 100 to 1000 nm.

Smoke opacity indicates the amount of soot in exhaust gas. Majority of PM are generated by incomplete combustion of fuel hydrocarbons and oil with lubricating oil playing a minor role. PM formation in a diesel engine is studied extensively in the literature for particle size and number distribution. Particulate formation in diesel engines starts due to the incomplete combustion of fuel in flame. The concentration of PM reaches the maximum during combustion, then rapidly decreases due to the oxidation of soot in the high-temperature environment. PM is classified according to size and density. In nuclei mode particles have diameters ranging from 3 to 30 nm, in aggregation mode from 30 to 500 nm, and in coarse mode it has diameters higher than 500 nm. Diesel exhaust has particles in all three modes. Majority of spherules in the range of 10–50 nm size appear to form clusters of mean diameters of 100–300 nm during the combustion and exhaust process.

### **2.6.1 Particle Matter Formation Mechanisms**

Particles in the sample system may be lost because of particle-to-particle interactions such as thermophoresis, diffusion, coagulation, inertial impaction, electrostatic deposition, and chemical reaction. The movement of a particle caused by unequal forces brought on by a temperature differential is known as thermophoresis. In essence, on the warmer side compared with the cooler side, particles are susceptible to more ferocious gas collisions and more momentum force. The decreasing temperature gradient is followed by a thermal force and a consequent particle motion. For systems with exhaust and sample lines with cool walls that encourage thermophoretic deposition, thermophoresis increases significantly. Particle diffusion can result from both Brownian motion and the movement of particles along with a gradient in particle concentration. Smaller particles diffuse more quickly than larger particles due to the inverse relationship between the particle size and the diffusion coefficient.

The agglomeration process that results from particle-to-particle collisions is known as coagulation. By colliding with each other or with larger particles, particles can grow. Although the size of the particle is altered by coagulation, the mass concentration of all the particles remains constant. This indicates that it has no impact on the outcomes of certification tests that gauge the diesel engines' particle mass output. However, it is crucial

to consider coagulation when trying to comprehend the mechanisms of particle creation. Additionally, because coagulation alters the particle size, size-dependent loss mechanisms are indirectly impacted. The ratio of residence time to characteristic time for coagulation determines how much coagulation occurs. The ratios of the various organic species' saturation, the amount of surface space available for adsorption, the adsorption energy, and the duration of the adsorption process all affect how much organic matter is adsorbed on the particle surface.

## 2.6.2 Particulate Emission Formation in High Reactivity Fuel

High injection pressure and temperature in diesel engines assist in atomisation and spray penetration. Nonuniform dispersion of fuel droplets is responsible for fuel vapor distribution and regions with rich and lean fuel mixture. The local excess air ratio is particularly low near droplets, leading to incomplete combustion due to lack of oxygen. PM is formed mostly due to incomplete combustion. PM consists of insoluble organic fraction (IOF) and soluble organic fraction (SOF), which are explained in Figure 2.1.

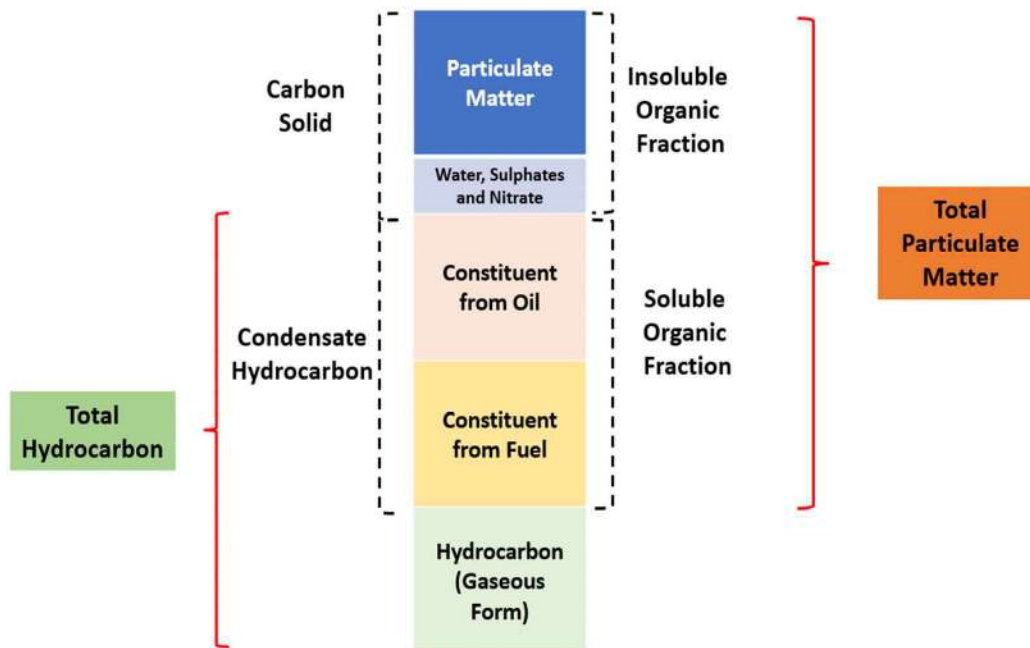


**Figure 2.1. Composition of particulate matter in diesel engine exhaust emission**

The concentration of soot reaches a maximum during the early part of combustion and then rapidly decreases due to oxidation in the later part. A majority of spherules in the size range of 10–50 nm are found in PM. PM formation in diesel engine is shown in Figure 2.2.

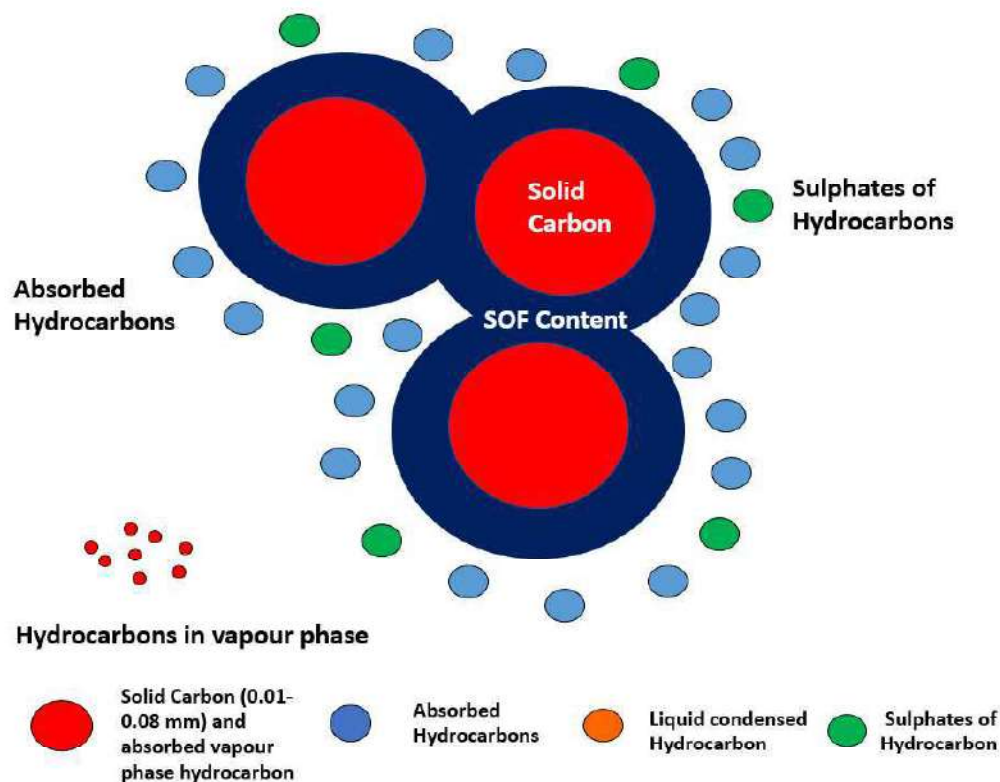


**Figure 2.2. Particulate matter formation in diesel engine**

In diesel engine particulates, carbon soot is present in high percentage jointly with other organic absorbed compounds. The amount of soot is measured by smoke opacity measured during testing. The air–fuel ratio and temperature play major roles in the formation of soot during diesel engine combustion. Unburnt fuel hydrocarbon also contributes to particulate formation of diesel exhaust with a minor percentage of oil content. Formation of soot takes place at a temperature of 1800 K in the diesel engine. The soot formation process in diesel combustion is presented in Figure 2.3.

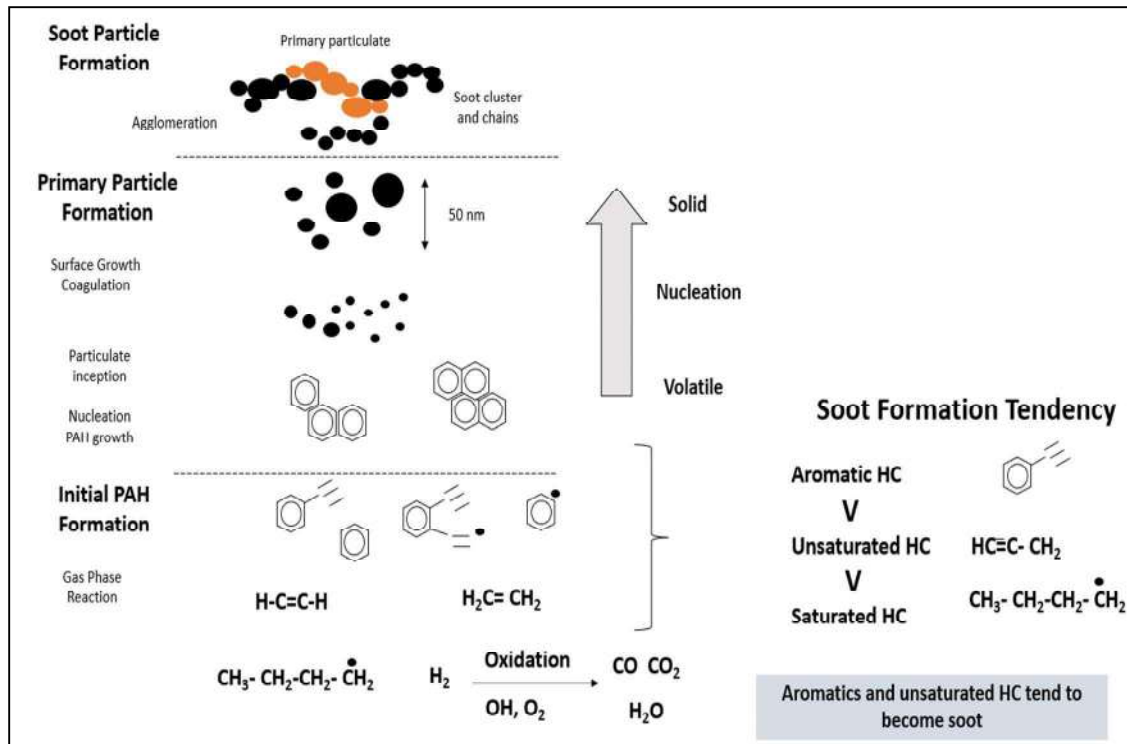


Figure 2.3. Soot formation process

### 2.6.3 Analysis of Diesel Engine Particle Size Distributions

Emission from automotive engines has received attention due to adverse effects on human health. Soot formation begins in the cylinder of CI engines because of incomplete combustion of the hydrocarbons in the fuel and oil. The amount of soot reaches its peak concentration during burning and then rapidly decreases because of oxidation. Most spherules in the 10–50 nm size range are detected in PM morphology data, and they frequently form clusters with a mean diameter of 100–300 nm. Three particle modes can be characterized as mentioned below:

- Nuclei mode:** Nuclei mode particles are typically of sizes 40–50 nm (0.04–0.05  $\mu\text{m}$ ). The nuclei mode covers sizes from 0.003–0.03  $\mu\text{m}$  to 3–30 nm. Nuclei mode particles fall entirely inside the nanoparticle range for all of the aforementioned size ranges. At 10–20 nm, nuclear mode particle concentration is at its peak. Up to 99% of all PM is made up of nuclei mode particles. Hydrocarbons and sulfuric acid make

up most of the volatile condensates that make up nuclei mode particles, which have little solid content.

- b. **Accumulation mode:** The accumulation mode is composed of sub-micron particles with a maximum concentration between approximately 100 and 200 nm (0.1–0.2  $\mu$ m) and a diameter range of 30–500 nm (0.03–0.5  $\mu$ m). The accumulation mode covers the fine, ultrafine, and higher range of nanoparticles. Particles in the accumulation mode are composed of solids (carbon, metallic ash), condensates, and material that has been adsorbed (heavy hydrocarbons, sulphur species).
- c. **Coarse mode:** These particles contribute virtually nothing to PNs and contain 5–20% of the overall PM mass with aerodynamic dimensions over 1  $\mu$ m (1000 nm). The combustion of diesel does not produce coarse particles. Instead, they are created by the deposition and subsequent re-entrainment of PM from the exhaust system, the particle sampling system, or the engine cylinder walls.

Figure 2.4 represents categorization of PM based on its size and density. The dashed line denotes particulate mass distribution with accumulation-mode particles ( $\sim$ 100 nm) and coarse-mode particles. The solid line represents the distribution for nanoparticles and nucleation mode ( $\sim$ 10 nm). Diesel mode particles are divided into particles of diameter size ranging from 3 to 30 nm (nuclei-mode particles), from 30 to 500 nm (aggregation mode particles), and more than 500 nm (coarse mode particles).

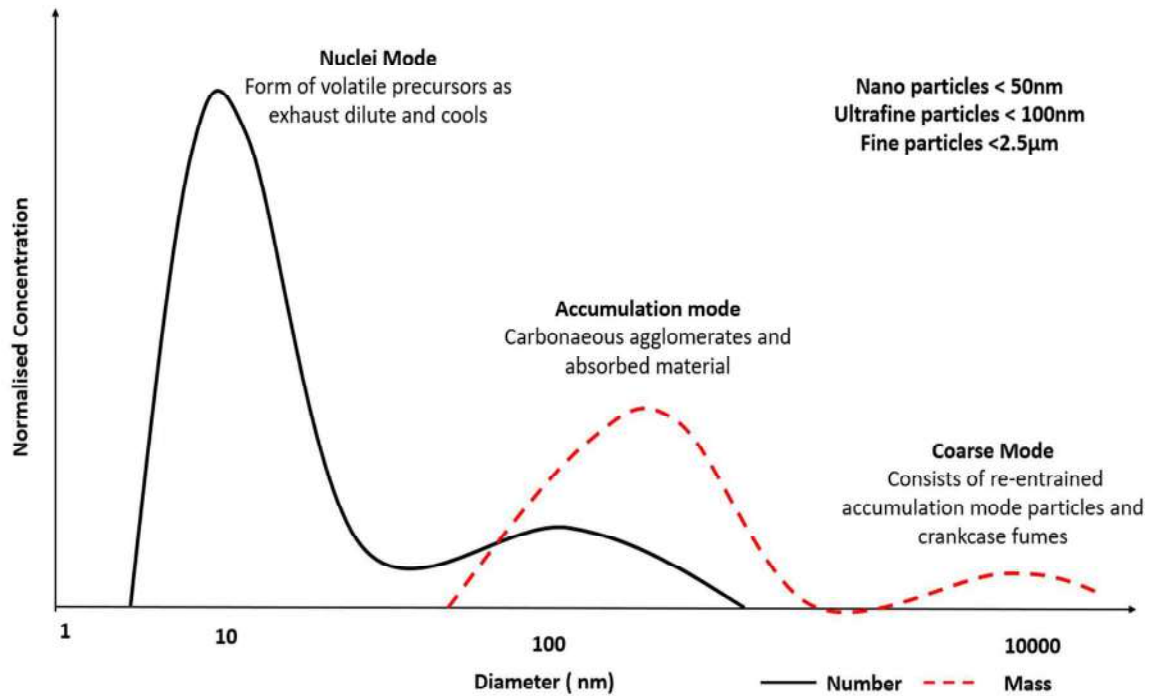


**Figure 2.4. Particle size distribution**

#### **2.6.4 Particulate Emission Formation in Low Temperature Combustion**

Soot production in LTC mode occurs mainly downstream in the jet's head as opposed to upstream soot-producing core found in traditional jets in diesel combustion engine. The charge dilution and mixing between end of injection and second-stage ignition account for this change used in LTC. The relationship between soot reduction and  $\text{NO}_x$  reduction is more complicated in LTC combustion. Figure 5 shows the reaction pathway of diesel combustion in low- and high-temperature combustion and its related emission products.

Dual-fuel combustion results in a significant reduction in  $\text{NO}_x$  and PM emissions. However, it also leads to an increase in HC and CO emissions. A diesel oxidation catalyst (DOC) can play an important role in reducing HC and CO emissions. The selection of DOC and its PGM loading content is very important to meet the stringent emission norms.

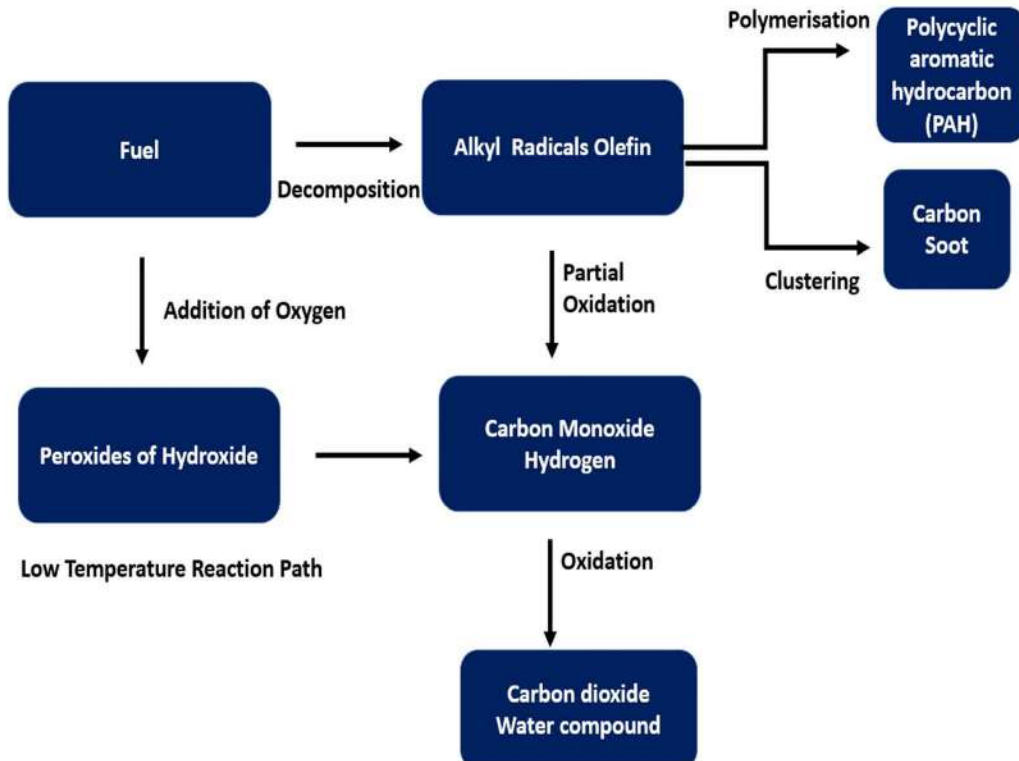


**Figure 2.5. Reactions at low and high temperatures in fuel reaction**

## 2.7 Objectives of the Study

Based on the literature study, it is clear that there is a need to study dual-fuel combustion to study its impact on engine emissions and specifically understand soot formation and its characteristics. Diesel and gasoline are the most widely used fuels globally and are hence taken for experimental trials so that the same can be taken forward in commercial production in future. Diesel engine (high reactive fuel) faces a big challenge in meeting emission standards, where extra cost needs to be incurred for after-treatment solution for tight emission norms of  $\text{NO}_x$  and PM. The major motivation of this study was to investigate the performance and the emissions formed due to diesel and gasoline

The objectives of the experimental study are:

- To evaluate the best technical strategy to control  $\text{NO}_x$  and PM with dual fuel (low- and high reactive fuel) in CI engine

- To understand engine performance characteristic with and without EGR in the dual fuel ratio
- To investigate PM emissions and PM composition for different combinations of high and LRF
- To study impact of injection pressure, EGR content, sulphur content, and engine load on particulate size and mass with dual fuel
- To study physical correlation between particulate mass and PN with dual fuel

## **CHAPTER 3**

### **CFD SIMULATION OF AIR FUEL MIXTURE FORMATION**

#### **3.1 Background**

Intake manifold is a part of intake system, which has an important impact on intake uniformity of the multi-cylinder engine. In dual fuel engine mixing of both fuels in intake manifold are designed to get best mixing homogeneity and uniform velocity for mixing of fuel before entering inside combustion chamber. The flow characteristics of intake manifold are analysed through simulation with single manifold injection and port intake injection. Intake manifold supplies fuel/air mixture to all the cylinders combustion chambers. It ensures a uniform mixture at all cylinder inlets. In this chapter, 3D Computational Fluid Dynamics (CFD) simulations are carried out to investigate the variance of gasoline /air mixture at the inlet port of each cylinder. Commercial CFD software Ansys Fluent is used to study the flow distribution of mixture inside the manifold and runners. Initial estimation of flow pattern is done by performing a steady state simulation to predict the uniformity index of gasoline fuel at cylinder inlet with two different configurations with gasoline entry in single injection and port injection in all cylinders. This investigation was done to compare uniformity index and mixing behaviour of gasoline fuel with air before reaching to combustion chamber.

The main objective of this study is to compare air and fuel distribution within port injection and single injection configuration. Uniformity index is also studied to understand distribution across all intake manifold port. The main function of an intake manifold is to deliver air to the cylinder to aid in combustion. The design is responsible for the swirl ratio or tumble ratio which denotes the mixing of air/fuel mixture inside cylinder. Commercial code ANSYS Fluent is used to simulate the transient phenomenon. Initially, steady state results help predict and improve the uniformity index, and subsequently detailed transient simulations are performed iterations, and validations with the test results have been showcased.

## 3.2 Methodology used in Simulation Work

### 3.2.1 Geometry

Four-cylinder diesel engine inlet manifold has been considered for the study, with dual exit ports from the manifold into each cylinder. The baseline case considered has a side entry manifold design with injector type as shown in Figure 3.1.

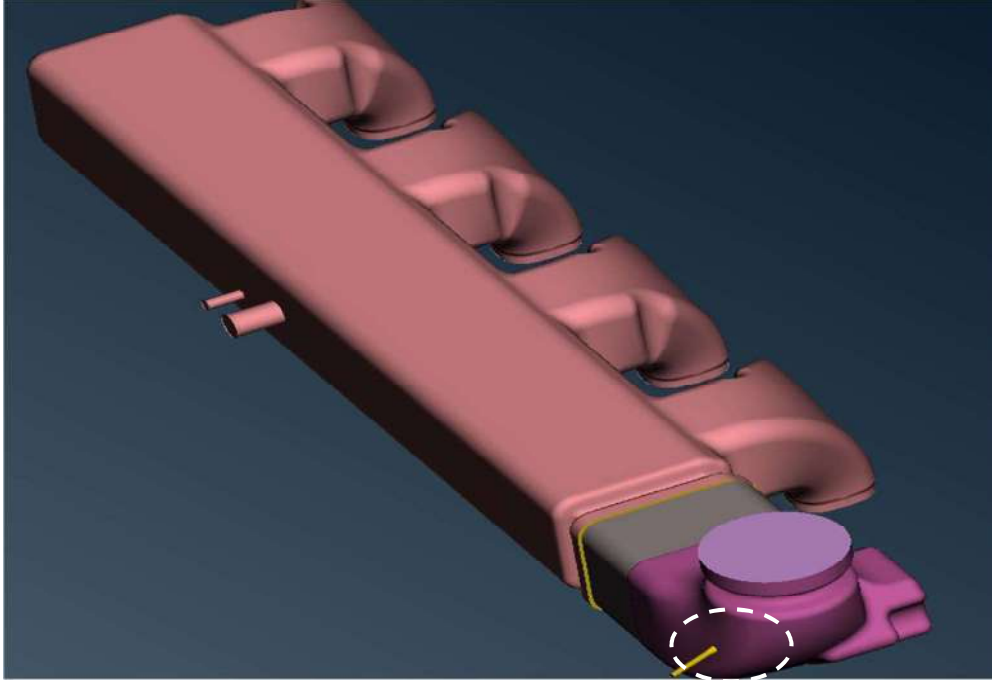


**Figure 3.1: Intake Manifold with single point manifold injection**

Initial pre-processing of CAD clean up and surface meshing has been done in ANSA, while volume meshing has been done in Fluent Meshing. For the current analysis, the fluid domain has been considered from the inlet port of inlet manifold till the inlet of cylinder. All internal thin and intricate fluid passages have been modelled and meshed with sufficient mesh refinement. The scale of the model used is 1:1. In the second configuration (Figure 3.2) simulation was performed with port injection across all intake manifold ports. Further simulation was performed to study mixing and uniformity index with dual fuel entry at both location in intake manifold.

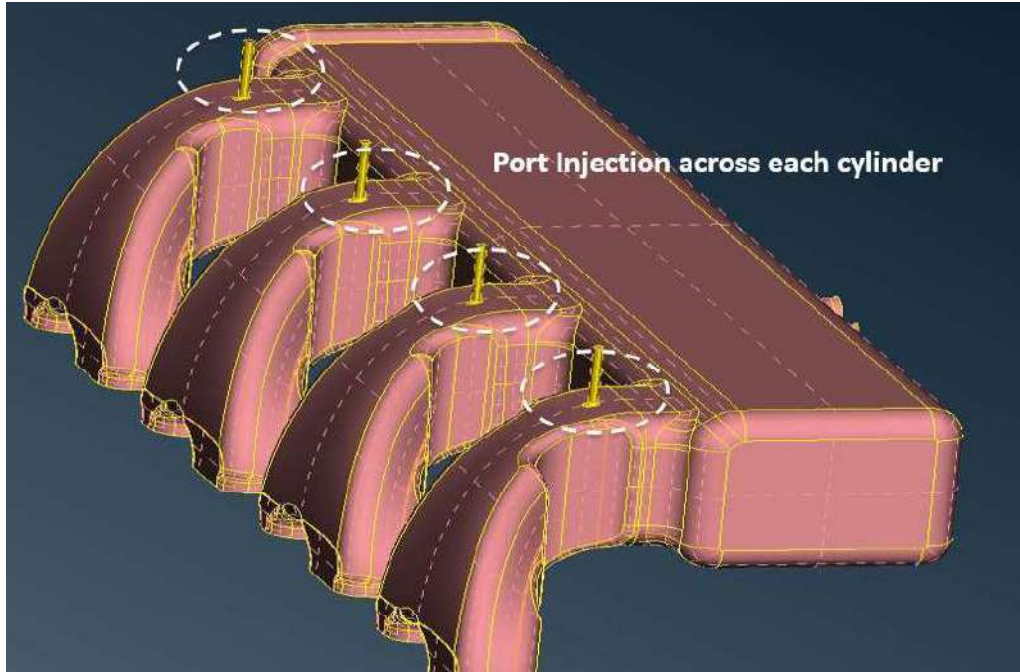


**Figure 3.2: Gasoline Entry across all different Intake Port Area in Intake Manifold**

### 3.2.2 Meshing

There are different meshing techniques available with professional CFD solvers, for example tetrahedral, polyhedral, hexcore, mosaic, etc. Due to the dissipative nature of the fluxes in the current domain and the species mixing involved, tetrahedral mesh was used for all the cases. The surfaces were refined with very small element length of 1mm with growth ratio of 1.35. The baseline case was run with coarser and finer element length and observed that 1-2 mm elements gives consistent accuracy for the results. This final volume mesh count was 8 million cells, with average volumetric skewness of  $< 0.90$ .

### 3.2.3 Solution

CFD simulation is performed in both concepts and approach of dual fuel entry in intake manifold. Firstly, a steady state solution was obtained to get the uniformity indices at the manifold outlets. This is done for all 4 cylinders in firing position one by one, and all other cylinder ports being closed. The gas mass flow rate considered for simulation is at maximum power condition for pressure drop. The continuity, momentum and turbulence equations solved are as shown below:

### 1. Continuity Equation

$$\frac{\partial \rho}{\partial t} + \frac{\partial(\rho u)}{\partial x} + \frac{\partial(\rho v)}{\partial y} + \frac{\partial(\rho w)}{\partial z} = 0 \quad (1)$$

### 2. Navier-Stokes Equation

$$\rho \left( \frac{\partial u}{\partial t} + u \frac{\partial u}{\partial x} + v \frac{\partial u}{\partial y} + w \frac{\partial u}{\partial z} \right) = -\frac{\partial p}{\partial x} + \mu \left( \frac{\partial^2 u}{\partial x^2} + \frac{\partial^2 u}{\partial y^2} + \frac{\partial^2 u}{\partial z^2} \right) + \rho g_x \quad (2)$$

$$\rho \left( \frac{\partial v}{\partial t} + u \frac{\partial v}{\partial x} + v \frac{\partial v}{\partial y} + w \frac{\partial v}{\partial z} \right) = -\frac{\partial p}{\partial y} + \mu \left( \frac{\partial^2 v}{\partial x^2} + \frac{\partial^2 v}{\partial y^2} + \frac{\partial^2 v}{\partial z^2} \right) + \rho g_y \quad (3)$$

$$\rho \left( \frac{\partial w}{\partial t} + u \frac{\partial w}{\partial x} + v \frac{\partial w}{\partial y} + w \frac{\partial w}{\partial z} \right) = -\frac{\partial p}{\partial z} + \mu \left( \frac{\partial^2 w}{\partial x^2} + \frac{\partial^2 w}{\partial y^2} + \frac{\partial^2 w}{\partial z^2} \right) + \rho g_z \quad (4)$$

### 3. Turbulence Equation

$$\frac{\partial(\rho k)}{\partial t} + \frac{\partial(\rho k u_i)}{\partial x_i} = \frac{\partial[(\mu + \mu_t) \frac{\partial k}{\partial x_j}]}{\partial x_j} + G_k + G_b - \rho \varepsilon - Y_M + S_k \quad (5)$$

$$\frac{\partial(\rho \varepsilon)}{\partial t} + \frac{\partial(\rho \varepsilon u_i)}{\partial x_i} = \frac{\partial[(\mu + \mu_t) \frac{\partial \varepsilon}{\partial x_j}]}{\partial x_j} + C_{1\varepsilon} \varepsilon / k (G_k + C_{3\varepsilon} G_b) - \frac{C_{2\varepsilon} \rho \varepsilon^2}{k} + S_\varepsilon \quad (6)$$

### 3.3 Simulation Result

According to the definition given above, the uniformity index can reach 1.0 if the flow inside a substrate is constant on a cross-sectional plane, which means that the local velocities' magnitudes and directions are constant throughout the cross-sectional plane. More consistent flow is indicated by a higher uniformity index.

Results are visualized and analysed to summarize the comparative performance with both design concepts. Uniformity Index (UI) is a parameter defined on a scale of 0 to 1, as the uniformity with which species is distributed or mixed with the main fluid at the given surface cross section – with 0 being least and 1 denoting maximum uniformity. The uniformity index study from steady state shows good mixing between gasoline and air (above 0.85) at all cylinder inlets in both configurations of air mixing in intake manifold. Figure 3.3 and 3.4 show uniformity index in single port injection for dual fuel mixing (gasoline mixing with air) is having proper mixing and distribution with uniform index of value 0.95 across all intake ports is observed.

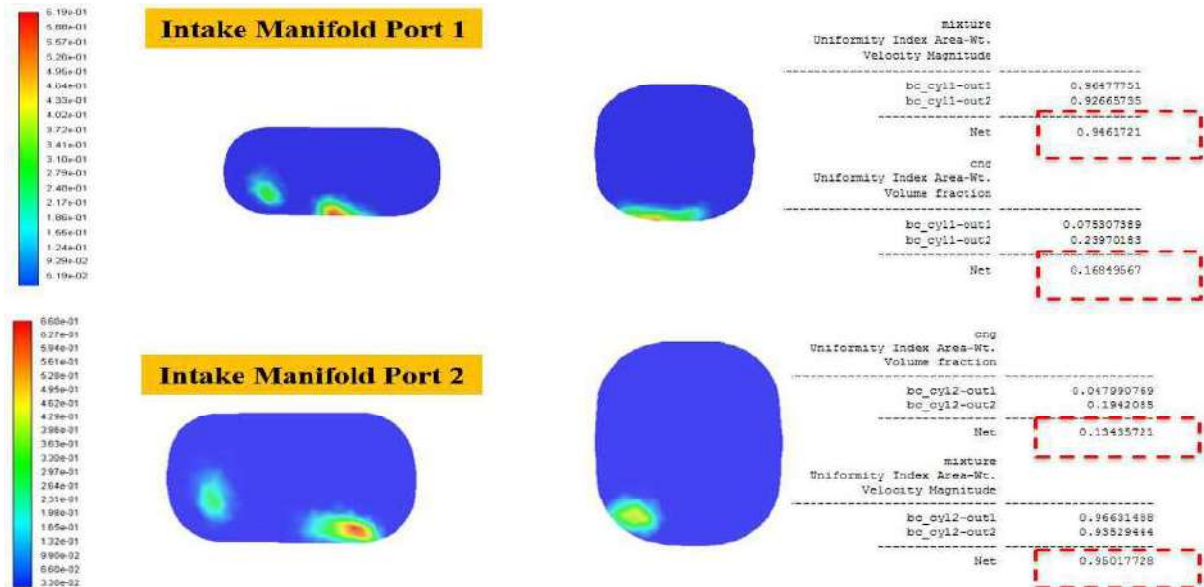


**Figure 3.3: Uniformity Index in Port 1 and 2 with single injection in Intake Manifold**

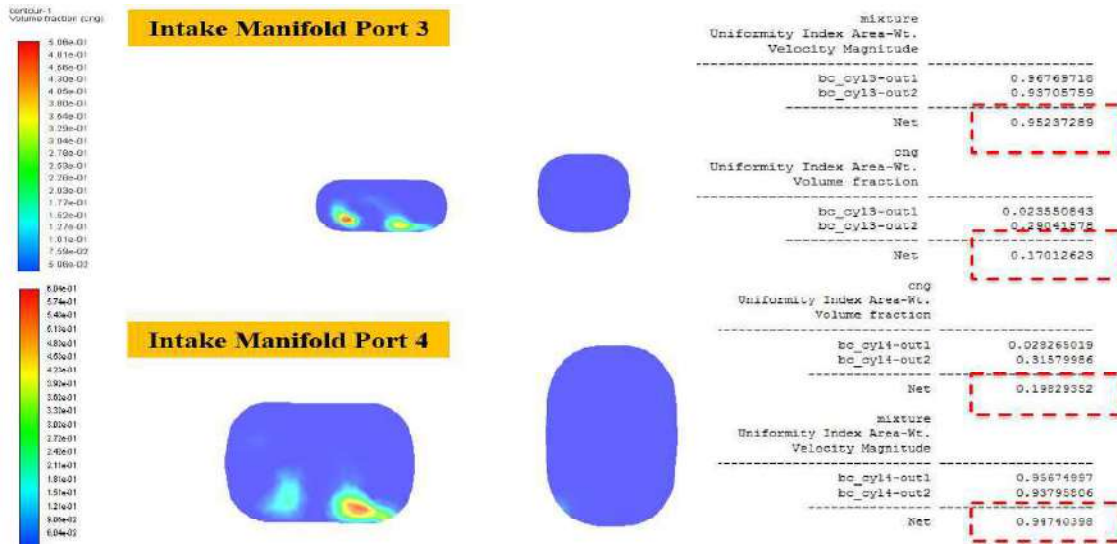


**Figure 3.4: Uniformity Index in Port 3 and 4 with single injection in Intake Manifold**

The uniformity index observed with gasoline injection across all port in intake manifold zone is shown in Figure 3.5 & 3.6. The uniformity index with port injection is area for dual fuel mixing (gasoline mixing with air) is 0.90 (Intake Manifold Port 4) which may lead issue of proper mixing and distribution of dual fuel with concept 2. This may lead to emission and performance related concerns with dual fuel combustion.

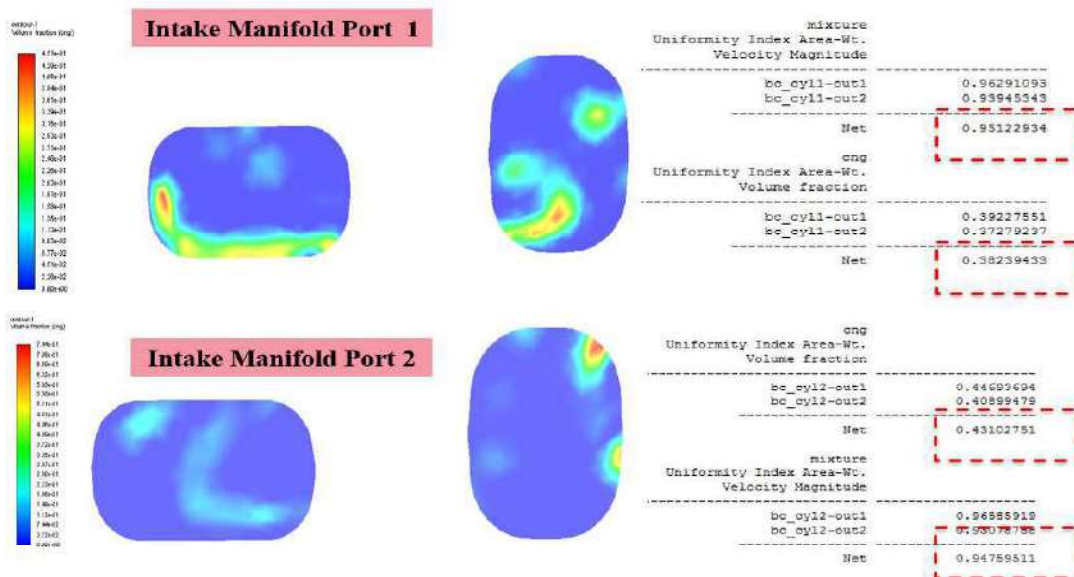


**Figure 3.5: Uniformity Index in Port 1 and 2 with Multiple Injection in Intake Port**

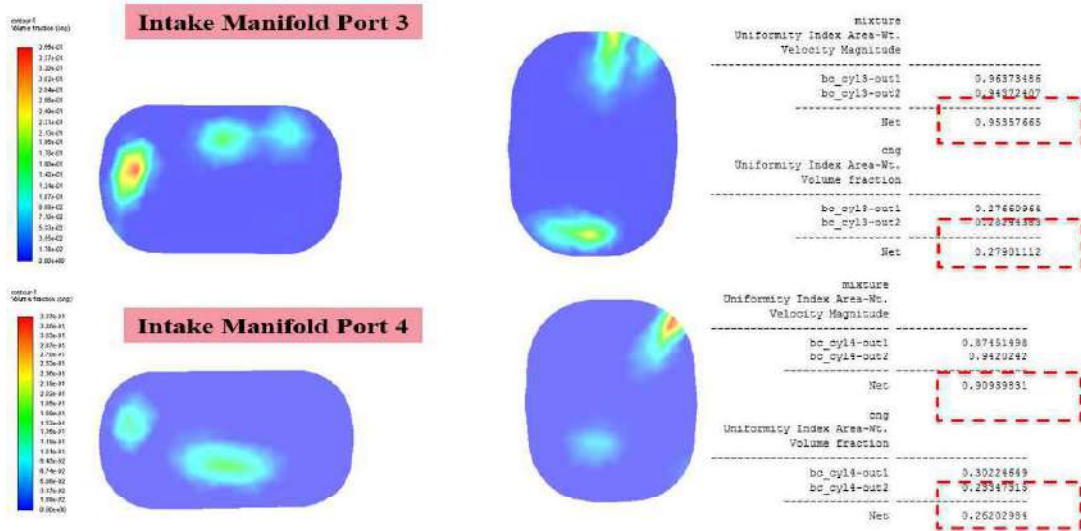


**Figure 3.6: Uniformity Index in Port 3 and 4 with Multiple Injection in Intake Port**

Simulation results highlights poor air fuel mixing with multi single port configuration in comparison to multi-port injection. Based on the simulation results it is observed that design concept 1 yields (single injection in intake manifold) give uniform distribution of gasoline with better uniformity index. Hence similar strategy is taken for experimental trial with dual fuel. Better mixing is observed with single injection compared to port injection due to more length available for mixing in intake manifold.

### 3.4 Summary

The fuel distribution at the inlet port of each cylinder is studied using CFD software. Two configurations (Single Port and Multi Port Injection) for fuel distribution and uniformity index. First configuration with fuel injection in intake manifold and second injection in intake port. More uniform fuel distribution is observed with intake manifold injection due to longer length available and higher residence time. The configuration 2 with intake port injection showed poor distribution of fuel in intake port. Based on the simulation results intake manifold injection was selected for further study due to better uniformity index ratio. Uniformity distribution for velocity index with port injection is low with respect to single injection in intake manifold. The next chapter explains experimental set up used for the study. The methodology used for the experiments and analysis is also explained in detailed.

## **CHAPTER 4**

### **EXPERIMENTAL SETUP AND METHODOLOGY**

This chapter presents details of experimental setup conducted to understand and analysis dual fuel combustion behaviour with gasoline and diesel fuel. The engine test setup for dual fuel combustion is explained in detail with operating conditions for experimentation. Trials were performed with different diesel oxidation to find technical approach to meet BSVI regulation norms. Engine performance and emission trials are performed were performed in transient test bed with dual fuel set up prepared for LTC combustion experimental trials. Engine test bed is discussed along with technical details used in test bed equipment's used in test. The injection setup for diesel and gasoline was described in this chapter. Test bed equipment's technical specification and instrumentation accuracy is explained in detailed. Fuel specification used in experimental test for both gasoline and diesel is provided. Further to understand soot behaviour filter paper analysis was performed with different configuration of dual fuel composition.

The experimental setup consists of below sections:

- Specification of Engine test bed
- Injector Specification – Gasoline and Diesel Injection System
- Engine Test bed Equipment's Technical Specification
- Diesel Oxidation Catalyst Specification
- Emission and performance test rig with dual fuel
- Instrumentation and Accuracy of Test Bed Measurement Units
- Controllers and Data Acquisition System
- Fuel Specification for Dual Fuel

#### **4.1 Engine Specification in Test Bed**

Engine testing is performed on a four-cylinder diesel engine with a common rail diesel injection system. A gasoline injection system is installed in the intake manifold which is controlled by EMS. The specifications of engine hardware are given in Table 4.1.

<b>Engine</b>	<b>3.8 L, 4-cylinder</b>
Diesel fuel injection system	Electronic–Direct Injection System
Compression ratio	17:05
Maximum torque	450 Nm @ 1200-1600 rpm
Maximum power	100 kW @ 2600 rpm
Maximum peak combustion pressure	160 bar
Bore X Stroke (mm)	100 X 120
Swirl Ratio	2.0

**Table 4.1 –Engine Specification**

Engine Control Unit (ECU) is used to control gasoline and diesel injectors. Table 4.2 and 4.3 provides technical specification of diesel and gasoline injectors respectively. Both injectors are precisely controlled in fuel flow demand and actual as physically verified before the engine tests.

<b>Injector Specification</b>	<b>Diesel Fuel Injector</b>
Type of actuation	Solenoid Actuated by EMS
Injectors make	CRIN Bosch Injector
Hydraulic through flow	600 mm <sup>3</sup> /30 sec
Number of holes	9
Diameter of hole	0.18 mm
Injector spray angle	148°
Maximum diesel injection pressure	1800 bar
Injection strategy	Multiple Injection
Total injection numbers	1 Main Injection, 2 Pre–Injection, and 3 Post Injection

**Table 4.2 –Diesel Injector Specification**

<b>Injector Specification</b>	<b>Gasoline Fuel Injector</b>
Type of actuation	Saturated operated by EMS
Hydraulic through flow	7.2 kg/hr
Number of holes	6
Injector spray angle	30°
Maximum gasoline injection pressure	9 bar
Injection strategy	Single injection

**Table 4.3 – Gasoline Injector Specification**

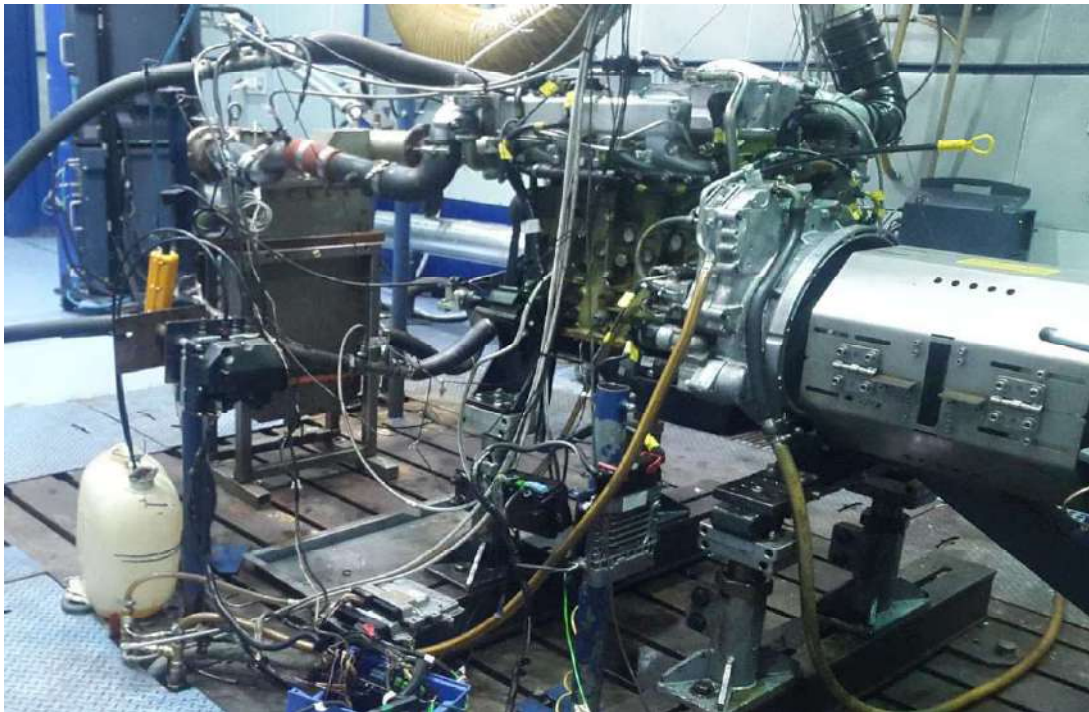


**Figure 4.1 –Engine Test Bed**

Three configurations of DOCs were tested with different PGM content to understand particulate mass and particle number trends. Filter paper analysis was carried out to understand SOF and IOF with different configuration of dual fuel composition. Technical specification of 3 Diesel Oxidation Catalyst is compared in Table 4.4

<b>Specification</b>	<b>DOC Configuration 1</b>	<b>DOC Configuration 2</b>	<b>DOC Configuration 3</b>
Diameter (inch) (mm)	9.5	9.5	9.5
Length (mm)	3"	3"	3"
Volume (lts)	3.48	3.48	3.48
Substrate Material	Cordierite	Cordierite	Cordierite
Nobel Material	Platinum and Palladium	Platinum and Palladium	Platinum and Palladium
PGM loading	10 g/cft <sup>3</sup>	15 g/cft <sup>3</sup>	20 g/cft <sup>3</sup>
Pt: Pd Ratio	4:1	4:1	4:1
CPSI	300	300	300

**Table 4.4 - Technical Specification of Diesel Oxidation Catalyst**

The technical specification of DPF is given in Table 4.5.

<b>Specification</b>	<b>DPF Specification</b>
Diameter	9.5"
Length	6"
Volume (lts)	7.55
Substrate Material	Recrystallized Silicon Carbide (RSiC)
Nobel Material	Platinum and Palladium
PGM loading	4 g/cft <sup>3</sup>
Pt: Pd Ratio	4:1

CPSI	300
------	-----

**Table 4.5 - Technical Specification of Diesel Particulate Filter**

Different configuration of DOCs samples was used to understand particulate matter and particulate number behaviour. Filter paper analysis is done to understand its characteristic of IOF and SOF content with different content of dual fuel composition. Filter paper analysis is done in particulate mass emissions on filter paper. The primary, secondary and blank filter papers holding particulate matter are separately weighted and both filters taken together with Soxhlet solvent extraction in the laboratory. For SOF analysis chromatographic is analysed to determine fuel and oil-derived hydrocarbon fractions in SOF using the method of standard IP 442 testing condition. IOF Contents were analysed by Thermo Gravimetric Analysis (TGA) method. Particulate matter collected on primary, secondary and black filter paper is subjected to TGA test after solvent extraction. The thermo grams are evaluated for weight loss over the defined temperature range 40 - 540 °C and 540 - 700°C to determine (sulphates +nitrates+ water) and (carbon soot and metal oxide + others). EGR rate is calculated based on the below equation for all experimental trials:

$$\text{EGR}(\%) = 100 * \frac{\text{Inlet CO}_2 - \text{Ambient CO}_2}{\text{Exhaust CO}_2}$$

## 4.2 Engine Test Bed Layout

Schematic of the engine and instrument layout is given in Figure 4.2. Single point gasoline injection is used in intake manifold of engine for this experimental test. Two sample line emission analysers are used at pre and post after-treatment system to understand its emission characteristic and behaviour. Engine tests are conducted in AVL transient test bed dynamometer. The temperature of coolant is maintained at 80±2°C and lubricating oil temperature is maintained constant during the testing. Intake air is conditioned at 1000 millibar pressure, 25°C temperature, and 40% humidity during the tests.

EGR is precisely controlled with electronic control EGR valve based on ECU input. EGR rate is expressed as ratio of concentration of CO<sub>2</sub> in intake and exhaust gases. AVL AMAi60 emission analyser is used to measure NO, NO<sub>x</sub>, HC, CO, CO<sub>2</sub> and O<sub>2</sub> concentrations independently. Filter Smoke Number (FSN) and Soot Concentration are measured at engine out using AVL 415S (SM) and AVL Micro Soot Sensor (MSS). The Particle Number (PN) concentration in exhaust gas was measured using an AVL Particle Counter (APC). AVL Micro Soot Sensor uses a photoacoustic technique to measure solely solid components of particulate matter (mainly soot). Smokemeter measures the blackening of filter paper through which exhaust gases flow in the measurement line. A detailed description of test bed instrumentation and its accuracy is given in Table 4.6

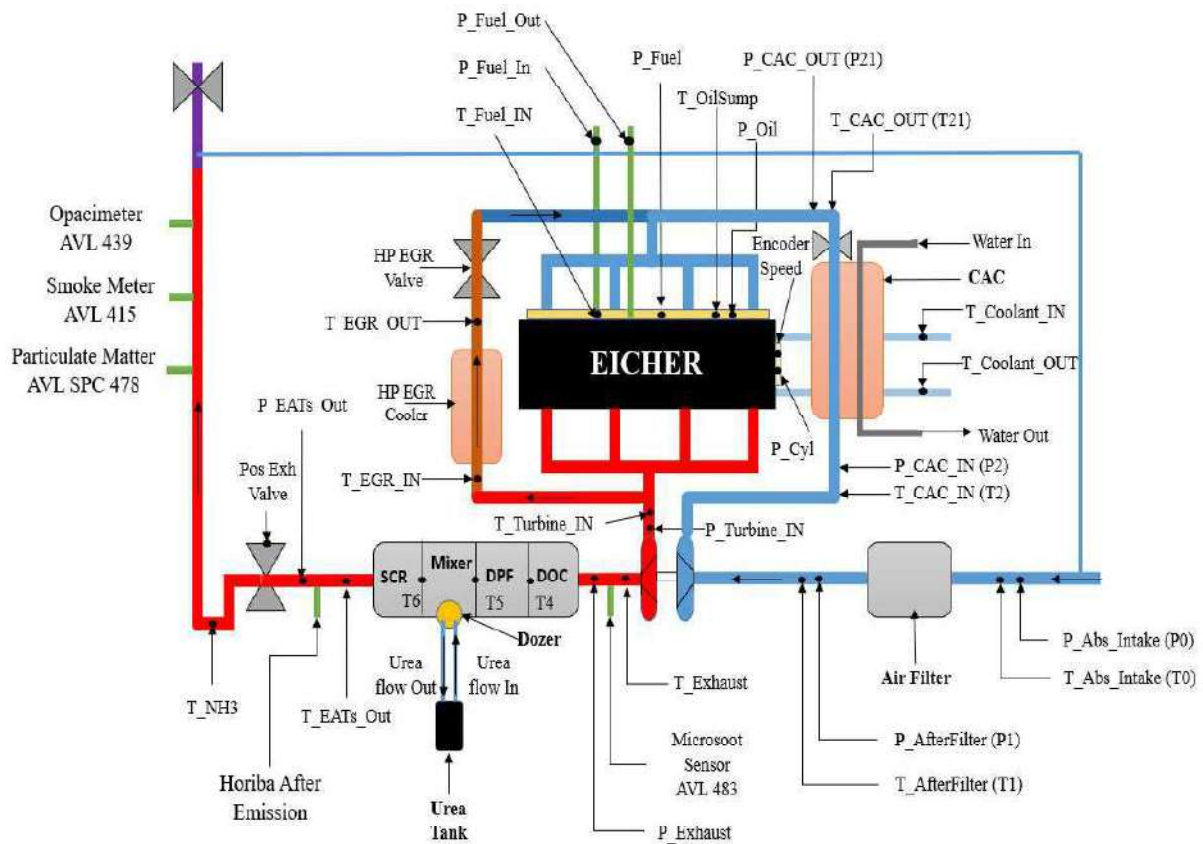


**Figure 4.2 – Engine Test and Measurement Layout**

## **4.3 Engine Test Equipment's**

### **4.3.1 Dynamometer**

The purpose of the dynamometer is to apply different loading circumstances to the engine that is being tested throughout a wide range of engine speeds and durations. This enables precise measurement of the engine's torque and power output. The driveshaft (or prop shaft) is bolted to the engine crankshaft, and the dynamometer shaft is connected to it. The engine crankshaft and the dynamometer shaft will both be rotating at the same speed (revolutions per minute [rpm]). The variable speed generator or alternator that powers the AC or DC transient dynamometer delivers its electrical output to a configurable load bank outside the test cell. The generator cooling air is drawn from the test cell. The transient dynamometer can be used for motoring the engine. Dynamometer AVL DYNOROAD SL was used for experimental trials to test the engine in different operating conditions. This dynamometer is capable to produce 220 kW at 4000 rev/min and absorbing over 950 Nm between 1000 and 4000 rev/min. The temperature of the dynamometer was monitored (type K thermocouple) and kept below 50 °C to extend its life and reduce potential test-cell downtime. A tachometer provided dynamometer speed, which was compared to engine speed to determine driveshaft integrity, while a load cell measured engine torque. This was zeroed and tested on a regular basis by applying a calibrated weight equal to 24 Nm torque to ensure the torque measurement's stability and accuracy.

### **4.3.2 Oil and Coolant System**

The engine coolant is kept separate from the cooling raw water in a host radiator chamber that may also include the heat exchanger. The engine coolant heat is carried away by the cooling raw water to the hot well and cooling towers. On the inflow side of the raw water system, before the water manifold, the Hale-Hamilton coolant damper valve is installed. Its purpose is to reduce pump surges and collect pressured water in a pressure reservoir. This ensures that a constant supply of pressured cooling water is available for supplying to the dynamometer via the test cell's manifold. Engine-in temperatures for coolant and oil were both set to 90 °C, and all flows including the flow through EGR coolers were kept constant.

The temperature of coolant in the engine was also measured (type K thermocouple). The coolant flow was modified early in the engine commissioning phase to achieve a temperature increase of 7 °C across the cylinder head, which was identical to the figure attained on the 4-cylinder engine when operating at 4000 rev/min full load. The thermal tension over the cylinder head was reduced as a result. When compared to a multi-cylinder engine, where the flow is proportionate to engine speed, this strategy provides a constant throughout the study programme, but it may result in excessive cooling at lower engine speeds

### **4.3.3 Air Handling System**

At the rated speed and full load, the charge air temperature must be recorded and must not exceed the manufacturer's maximum charge air temperature within  $\pm 5$  K. The cooling medium's temperature must be at least 293 K (20 °C). If an external blower or test laboratory system is being utilised, the coolant flow rate must be regulated to achieve a charge air temperature that is no more than 5 K over the maximum charge air temperature allowed at rated speed and full load. The charge air cooler's coolant temperature and coolant flow rate must remain constant during the entire test cycle at the fixed point. To verify that the pressure drop across charge-air cooling system under engine conditions is within testing limit, pressure-drop limits across the system were established.

#### **4.3.3.1 Air Temperature**

The engine's performance is dependent on the quality of the air, which will be reflected in the engine test results. There are two primary functions that the air provides for the engine: cooling and breathing air services to the engine test cell. The engine's performance is influenced by the quality of the air in terms of temperature, pressure, humidity, and condition. The temperature of the air entering the inlet manifold has a direct impact on the complete integration of air and fuel as a mixture, especially in terms of evenness and atomization (the dispersal and size of the fuel droplets throughout the air stream and on the mass of the air fuel mixture).

During all experimental trials, ambient temperature is kept 25±2 deg C in test cell for dual fuel and single fuel testing.

#### **4.3.3.2 Air Pressure**

The combustion or induction air pressure has a direct impact on the internal combustion engine's performance. A high or low air pressure can increase or decrease the mass of fuel air mixed charge within the input manifold ready to be pushed into the cylinder. The mass of the fuel-air combination drawn into the cylinder determines the power created by the cylinder of an engine. The present procedure used during testing is to continuously monitor the air pressure within the cell, with the data gathering equipment performing automatic adjustment calculations. Ambient pressure of 1000mBar is kept during the experimental trials in test bed.

#### **4.3.3.3 Air Humidity**

Controlling humidity within the cell becomes increasingly important as legislative emission limits get stricter because humidity impacts NO<sub>x</sub> emissions and the development of particle platelets in the combustion area. Both humidity and air induction temperature are regulated due to same. Air humidity is kept 40% during experiment test data.

#### **4.3.3.4 Air and Fuel Measurement Method**

This involves measurement of the airflow and the fuel flow with suitable flowmeters. The calculation of the instantaneous exhaust gas flow mentioned below:

$$q_{mew,i} = q_{maw,i} + q_{mf,i}$$

where:

$q_{mew,i}$  is the instantaneous exhaust mass flow rate, kg/s

$q_{maw,i}$  is the instantaneous intake air mass flow rate, kg/s

$q_{mf,i}$  is the instantaneous fuel mass flow rate, kg/s

#### **4.3.3.5 Air Cooling and Ventilation**

Air as a cooling medium is ineffective compared to liquid cooling systems, especially when it comes to cooling hot surfaces, such as those found in engines and dynamometers that are operating flat-out under load. The main reasons for this are that air has a lesser density than liquid and is considered invisible to radiant heat, implying that air has poor heat transfer capabilities under typical conditions.

The absolute temperature ( $T_a$ ) of engine intake air expressed in Kelvin, and the dry atmospheric pressure ( $p_s$ ), expressed in kPa is measured during experimental trials.

#### **4.3.4 Fuel System**

There were two distinct sections to the fuel system. The fuel tank, low-pressure pumps, filter, temperature control system, and fuel metre were all parts of the low-pressure side. In order to condition the fuel, it required to reach a temperature of 40 °C after passing through the high-pressure side and before returning to the high-pressure pump. The fuel metre utilised in the test bed was an AVL 735 Dynamic Fuel Meter, which uses a gravimetric balance approach to calculate fuel use. Over the course of a minute, the fuel was weighed; the accuracy was  $\pm 1.0\%$ . Test bed complete equipment list is shown in figure 4.3 containing layout and equipment used during experimental test.

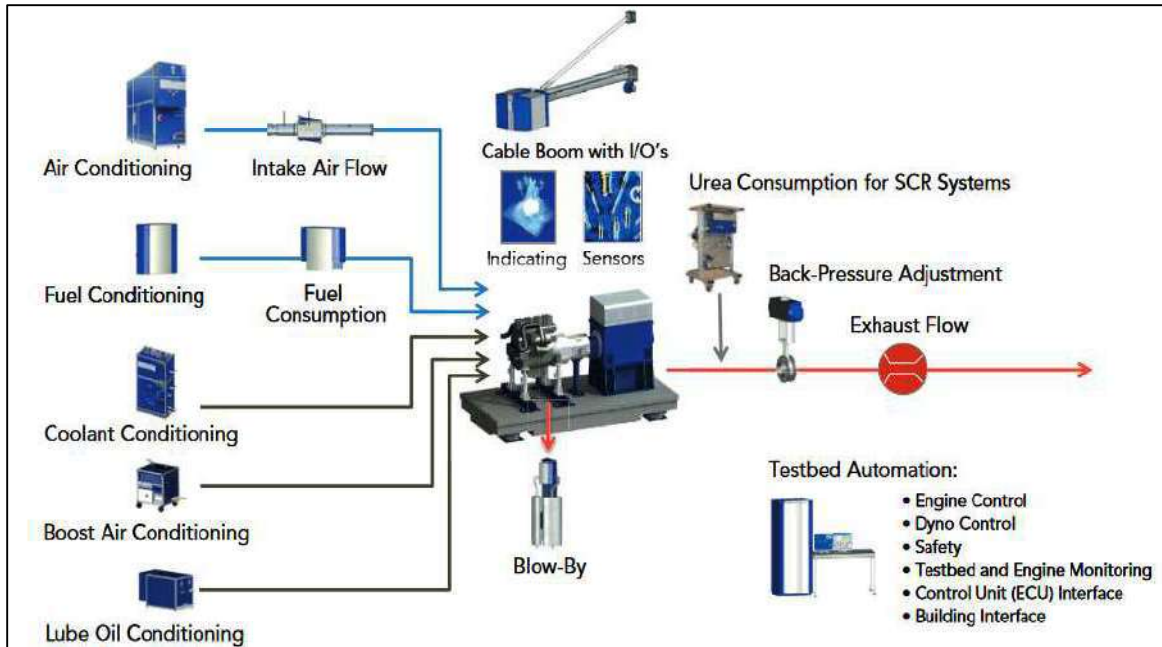


**Figure 4.3 – Test Cell Layout**

Test bed instrument accuracy and model are mentioned in Table 4.6.

<b>Instrumentation Unit</b>	<b>Model Type</b>	<b>Operating principle</b>	<b>Accuracy</b>
Dynamometer	AVL	Transient Dyno	$\pm 2\%$
Speed Measurement	Magnetic Pick Up	Inductive Principle	$\pm 5\text{rpm}$
Torque	Load Cell	Strain gauge type load cell	$\pm 1\%$
Fuel mass flow meter	AVL – 735	Coriolis mass flow meter	$\pm 0.5\%$
Air mass flow meter	KVG G100	Hot film anemometer	$\pm 0.5\%$
Pressure Sensor	Piezo-resistive Transducers	Resistance based Whitestone Type	$\pm 25\text{mbar}$
Temperature Sensor	Thermocouple – Type K	See-back effect	$\pm 2.5 \text{ deg C}$

**Table 4.6 - Instrumentation and Accuracy of Test Bed Measurement Units**

### 4.3.5 Emission System:

For CH<sub>4</sub>, NO/NO<sub>2</sub>/NO<sub>x</sub>, CO, CO<sub>2</sub>, N<sub>2</sub>O, O<sub>2</sub>, and SO<sub>2</sub>, the AVL AMA i60 has analysers with a wide dynamic measurement range that are tailored to the application (diluted/undiluted exhaust gas or gasoline/diesel/hydrogen/etc.). The iGEM AMA bench control software enables touchscreen control of the AMA i60 that is simple and intuitive. The control software includes automatic diagnostic functions and supports troubleshooting all the way down to the sensor and valve level. Different types of analysers can be utilised with the AMA i60 exhaust measurement system, depending on the application. The sample point, which can be up to 20 metres away or up to 60 metres with a heated boost pump, is drawn into the measurement system by integrated pumps.

Near to the sample point, heated lines, pre-filters, or sample point selector devices are used. With the use of modern conventional gas analysers, measurement gas is analysed. Emission analyser equipment layout in test bed in Figure 4.4

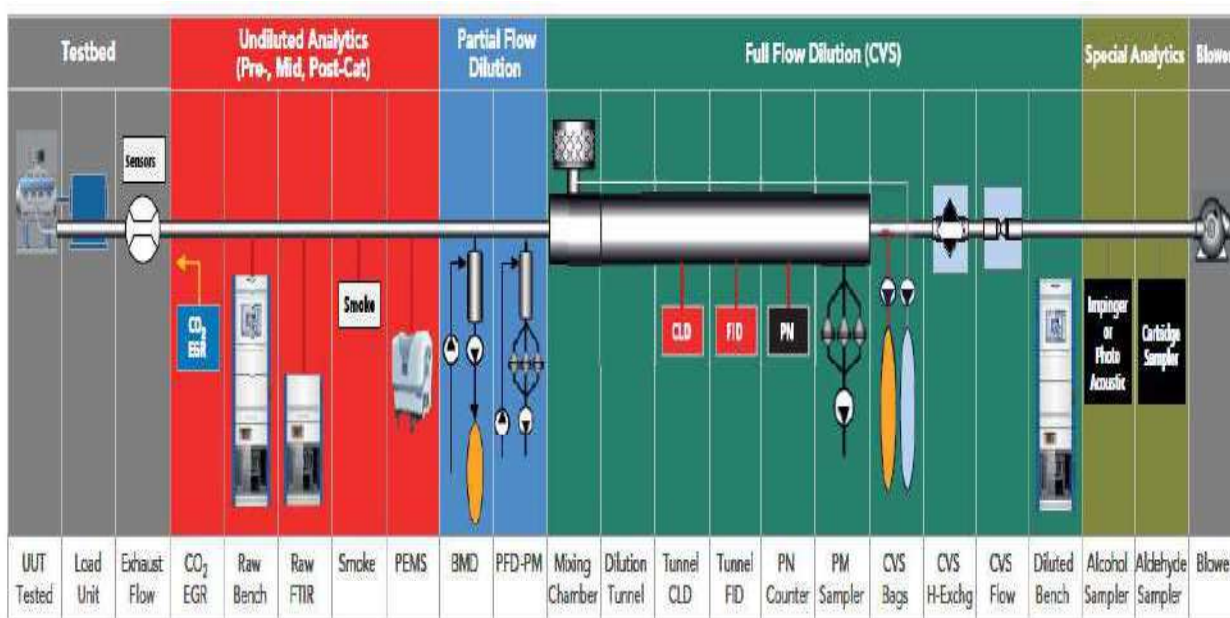


**Figure 4.4 – Emission Analyzer Equipment Layout**

AMA i60 or connected to remote control system to monitor and capture all data's. The smoke metre and exhaust gas analyser that made up the emissions system were placed far enough from the exhaust manifold so that the measurement was indicative of the entire flow. The smoke metre was an AVL 415 Variable Sampling Smoke Meter, which functions through the filtering principle. A reflecting photometer is used to analyse the filter paper's darkness, producing FSN outputs (filter smoke number). This figure is then translated into the amount of created PM or soot emissions. Two measurements on average were obtained for 50 accuracy and dependability. The precision was within  $\pm 0.2$  FSN.

The exhaust gas analyser was initially AVL AMA i60 analyser used for the investigations in test bed trials. With an accuracy of 3% over a maximum of 8 hours and a linearity of the signals of  $\pm 1\%$ , both systems used the same measurement principles. The concentrations of total hydrocarbon, oxygen, carbon dioxide (exhaust and inlet for the EGR), carbon monoxide, and nitrous oxides are five different types of emissions in the exhaust could be measured:

1. The flame ionization detection technique is the foundation of the HC emissions analyzer. A hydrogen flame that is flowing between two electrodes is filled with the gas to be studied. An ion flow that is proportionate to the number of carbon atoms is produced by the constant voltage application.
2. Based on the magneto-pneumatic condenser microphone detection technology, oxygen ( $O_2$ ) emissions analyzers are used. Gases with paramagnetic sensitivity will gravitate toward the strongest section of the magnetic field when an unequal magnetic field is applied to them by excitation of an electromagnet, raising the pressure there. The pressure oscillations can be transformed to electrical signals using a condenser microphone by alternately stimulating two electromagnets. The amount of oxygen has a linear effect on this production.
3. Non-dispersive infrared absorptiometry detection is the foundation of the  $CO_2$  and CO emissions analyzers. An atom-based molecule will absorb infrared light at a certain wavelength and to a degree proportional to its concentration. When an infrared beam passes through a reference gas and the gas being studied, there is a difference in infrared intensities that can be detected. For the measurement, concentration of each gas molecule, two metallic membrane detectors provide

electrical signals. The signals are next translated into the CO<sub>2</sub> and CO concentrations in the gas under study.

<b>Instrumentation Unit</b>	<b>Model Type</b>	<b>Operating principle</b>	<b>Accuracy</b>
FSN	Smoke Meter – AVL415S	Exhaust measurement in Filter Paper	+0.001 FSN
Particulate Size and number	SMPS – AVL Make	Bio Polar Aerosol Charger	+3.5%
NO <sub>x</sub>	AVL AMAi60	Chemiluminescence detector	2%
HC		Flame ionization detector	
CO		Infrared detector	

**Table 4.7 – Emission Analyser Operating Principle and Accuracy**

Emission analyser operating principle and accuracy is mentioned in Table 4.7. Test Bed measurement of instruments uncertainty is mentioned in Table 4.8.

<b>Parameter</b>	<b>Uncertainty (<math>\pm\%</math>)</b>
Speed (rpm)	0.1
Torque (Nm)	0.5
Fuel Consumption	
Diesel (kg/hr)	1
Gasoline (kg/hr)	1
Emissions	
NO <sub>x</sub> (ppm)	2
HC (ppm)	2
CO (ppm)	3

**Table 4.8 - Uncertainty Percentage in Test Lab Equipment**

#### **4.3.6 Controllers and Data Acquisition System**

Several calculations relating to emissions were also monitored by the operations-control computer, along with the various temperatures and pressures stated previously (AFR, EGR rate, mass flows and total emissions). These data made comprised the initial collection of low time resolution data for each test location. The stored value is an average calculated over a 30 s transaction period. The following is a list of the parameters mentioned below:

##### **Temperatures (°C):**

- Engine Coolant (In and Out)
- Engine Oil (In and Out)
- Ambient temperature
- High Fuel Pressure (In and Out)
- Dynamometer Air Out
- Viscous flow air meter (In)
- Intake plenum and manifold
- EGR (In and Out)
- EGR Coolant (In and Out)
- Exhaust manifold

##### **Pressure (mBar):**

- Absolute and relative pressures (mbar)
- Ambient pressure
- Viscous flow air meter in and out
- Inlet manifold
- Throttled inlet manifold (swirl system)
- Exhaust manifold

##### **Emission Emissions (ppm or g/h) and fuel consumption (kg/h):**

- HC, CO, CO<sub>2</sub>, O<sub>2</sub>, NO<sub>x</sub>, Inlet CO<sub>2</sub>, Exhaust CO<sub>2</sub>, Smoke (FSN)
- Fuel Consumption and Lambda
- Emissions analyzer ranges

Diesel (High Reactive) and gasoline (Low Reactive) fuels are considered for this experimental study as this widely used across world. Both these fuels are hydrocarbon derivative fossil fuel used for internal combustion engine. The fuel ignition delay period and self-ignition temperature properties of both fuels differentiate it and impacts in combustion behaviour. Physical and chemical properties of fuels verified in IOCL Lab (NABL Certified) are compared in Table 4.9 & Table 4.10.

Characteristics	Unit	Requirements
Ash, max	% mass	0.01
Carbon Residue (Ramsbottom) on 10 % residue, max	% mass	0.3 without additives
Cetane number (CN), min		51
Cetane Index (CI), min		46
Distillation:		
95% vol. recovery at $^{\circ}\text{C}$ , max	$^{\circ}\text{C}$	360
Flash point:		
a) Abel, min	$^{\circ}\text{C}$	42
Kinematic Viscosity @ 40 $^{\circ}\text{C}$	cst	2.0-4.5
Density @15 $^{\circ}\text{C}$	$\text{kg/m}^3$	820-845
Total Sulphur, max.	$\text{mg/kg}$	10
Water content, max	$\text{mg/kg}$	200
Cold filter Plugging point (CFPP)		
a) Summer, max	$^{\circ}\text{C}$	18
b) Winter, max	$^{\circ}\text{C}$	6
Total contaminations, max	$\text{mg/kg}$	24
Oxidation stability, max	$\text{g/m}^3$	25
Polycyclic Aromatic Hydrocarbon (PAH), max	% mass	11
Lubricity, corrected wear scar diameter @ 60 $^{\circ}\text{C}$ , max	$\mu\text{m}$ (microns)	460
Copper strip corrosion for 3 hrs @ 50 $^{\circ}\text{C}$	rating	Class – 1

**Table 4.9 - Technical specification of BSVI Diesel Fuel**

Parameter	Unit	Limits <sup>1</sup>		Test method
		Minimum	Maximum	
Research octane number, RON		95.0	98.0	EN ISO 5164
Motor octane number, MON		85.0	89.0	EN ISO 5163
Density at 15 °C	kg/m <sup>3</sup>	743.0	756.0	EN ISO 12185
Water content	% m/m	max 0.05 [ Appearance at - 7°C: Clear and Bright]		EN 12937
Distillation:				
– evaporated at 70 °C	% v/v	34.0	46.0	EN ISO 3405
– evaporated at 100 °C	% v/v	54.0	62.0	EN ISO 3405
– evaporated at 150 °C	% v/v	86.0	94.0	EN ISO 3405
– final boiling point	°C	170	195	EN ISO 3405
Residue	% v/v	—	2.0	EN ISO 3405
Hydrocarbon analysis:				
– olefins	% v/v	6.0	13.0	EN 22854
– aromatics	% v/v	25.0	32.0	EN 22854
– benzene	% v/v	-	1.00	EN 22854 EN 238
– saturates	% v/v	report		EN 22854
Oxygen content	% m/m	3.3	3.7	EN 22854
Sulphur content	mg/kg	—	10	EN ISO 20846 EN ISO 20884
Ethanol	% v/v	9.0	10.0	EN 22854

**Table 4.10 - Technical specification of BSVI Gasoline Fuel**

### 4.3.7 Summary

The experiments for performance and emission data are performed with dual fuel in transient test bed with LTC set up with different composition of dual fuel during test bed trials. Two separate injectors are used during the test bed trials with gasoline and diesel. Fuel injection system and engine management system is from Bosch which is controlled by EDC17 ECU controller. Filter paper were analysed to understand behaviour and pattern of soot behaviour with dual fuel combustion. Different diesel oxidation catalyst as after treatment were tested to find out optimum approach to meet emission with dual fuel.

1. The dual fuel combustion was studied to control NO<sub>x</sub> and soot free clean emissions to meet BSVI emission norms. Technical approach and direction were highlighted in test result with low reactive and high reactive fuel to meet emission with low cost after treatment.
2. Filter paper analysis are performed with dual fuel and compared with diesel fuel emission to understand soluble fraction and insoluble fraction from particulate matter
3. Particle number and particle mass is captured with different dual fuel to understand its correlation after engine out, diesel oxidation catalyst out and particulate filter out.
4. Particle mass and diameter behaviour was studied with different configuration of diesel oxidation catalyst by varying Platinum content of wash coat.

The diesel, gasoline and different composition of diesel and gasoline dual fuels are compared to understand its combustion and emission behaviour with compression ignition engine.

## CHAPTER 5

### ENGINE PERFORMANCE WITH DUAL FUEL

Four-cylinder diesel engine is used for this investigation with modification in intake manifold for mounting gasoline injector. A standard ECU is used to control gasoline and diesel injectors. A single-point gasoline injection in the intake manifold of an engine is used to prepare a homogeneous intake charge. Each cylinder gets a uniform homogenized air-gasoline mixture during the intake stroke. The quantity of gasoline and diesel is varied to control combustion phase behavior. The gasoline flow rate is varied from 0 to 120 g/min. The strategies of gasoline–diesel dual-fuel combustion was investigated concerning exhaust emissions and combustion characteristics for the light-duty commercial vehicle engine. Reference diesel fuel was used in to generate test data with dual-fuel combustion. Similar trials were conducted with commercial fuel and the same test result observed with dual fuel. The difference between reference fuel and commercial fuel of BSVI represented the difference in the sulfur and cetane content in both fuels. Sulfur in the reference diesel fuel is 9 ppm and 12 ppm in the commercial fuel. The cetane number is 51 in reference fuel and 49 in commercial diesel fuel. Different combustion-related parameters like injection duration, gasoline ratio, injection timing, and EGR were varied to study their influence on the performance of engine emissions. Engine performance was evaluated in engine speed of 1520 rpm with dyno torque of 200 and 300 Nm with different configuration of dual fuel. Test was performed with and without EGR in this experimental test. Low reactive fuel of gasoline content was added in dual fuel from 0% to 85% during these experimental trials. EGR was added from 20% to 50 % in these trials. Trials are done with dual fuel to understand trend of emission  $\text{NO}_x$  & soot with the variation of EGR content. Emission data of  $\text{NO}_x$ , hydrocarbon, carbon monoxide and soot were studied with dual fuel combustion.

#### 5.1 Effect of Dual Fuel combustion on Soot and $\text{NO}_x$ Emission

The effect of the gasoline ratio on soot and  $\text{NO}_x$  emissions is compared in Fig. 5.1. Engine emissions of soot and  $\text{NO}_x$  decrease markedly with increasing gasoline ratio. Consequently, there is a reduction in the emission of  $\text{NO}_x$ .

Further, due to the homogeneous mixture, the quantity of soot decreases. In the composition of dual fuel with 85% gasoline, smoke is 0.042 g/kWhr and  $\text{NO}_x$  is 3 g/kWhr, which is significantly lower compared to conventional diesel engine operation. This shows that dual-fuel operation can avoid  $\text{NO}_x$  smoke trade-off simultaneously and reduce emissions significantly at an engine speed of 1520 with a torque of 200 Nm.

Addition of low reactive fuel in dual fuel with high reactive fuel leads to significant drop of both  $\text{NO}_x$  and soot emission from exhaust. Increase of gasoline content in dual fuel leads to increase the homogeneity of premixed homogenous mixture. Low reactive fuel was injected into the intake manifold so this can get longest interval between injection, mixing and ignition forming most homogeneous mixture before entering inside combustion chamber. This leads to longer ignition delay period compared to conventional diesel engines. The long ignition delay allows for mixing and homogenizing the air and fuel. Addition of EGR further leads to lower oxygen concentration, overall equivalence ratio is more fuel rich than diesel combustion engine. This combustion phenomena leads to lower both  $\text{NO}_x$  and soot simultaneously together in same time with dual fuel combustion.

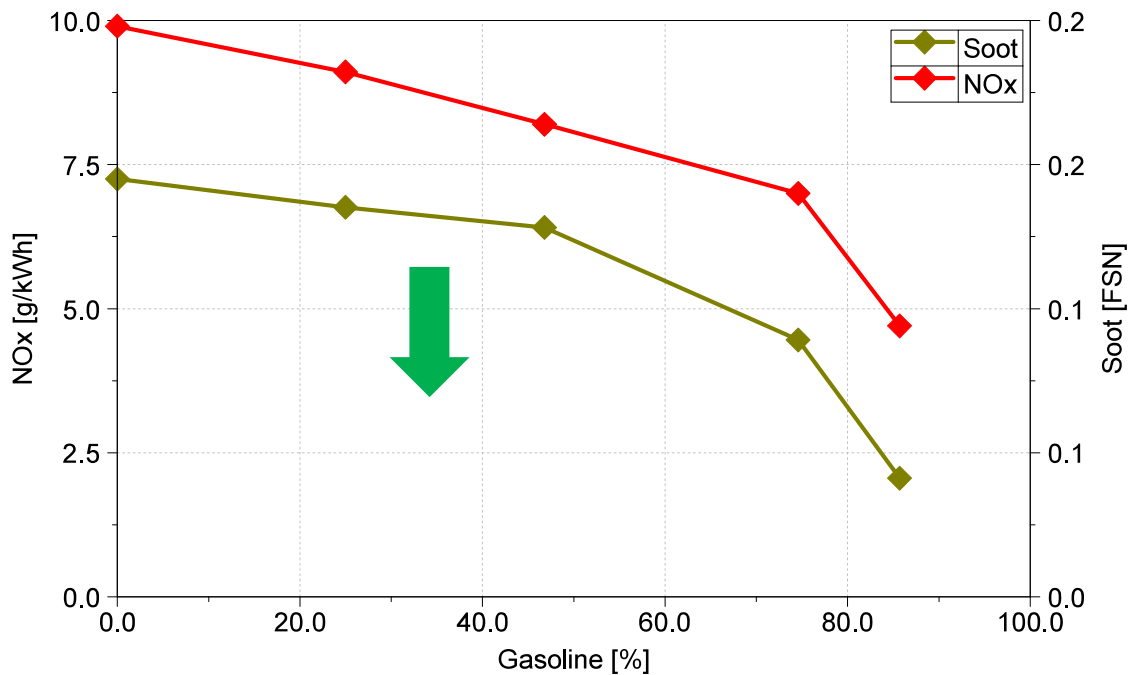


**Figure 5.1 Effect of Gasoline Ratio on  $\text{NO}_x$  and Soot Emission with Dual Fuel**

## 5.2 Impact of EGR on Dual Fuel Combustion

The impact of EGR on engine emission and performance is studied at an engine speed of 1520 rpm with dyno torque of 300 Nm. Trials are done in the composition of D35G65 having a content of 65% gasoline in dual fuel to understand the trend of emission  $\text{NO}_x$  & soot with the variation of EGR content. In Fig. 5.2, there is a considerable reduction in  $\text{NO}_x$  and soot observed with an increase of EGR content. This simultaneous reduction may be due to homogenous combustion and reduction in local temperature inside the cylinder and dilution and thermal effects of EGR. This also indicates the combustion in the LTC regime. The introduction of EGR helps in the complete combustion of dual-fuel and increased the peak value of pressure and MPRR. The mixture of gasoline and air must be ignited by diesel injected directly into the cylinder, whereas the mixture of diesel and air in the cylinder can be ignited once it reaches the desired temperature and equivalence ratio. As the in-cylinder temperature is lower when diesel was injected early, the mixing period of diesel and air increased longer, thus lowering the local equivalency ratio increasing the ignition temperature demanded by the combination. The same early diesel injection results in the ignition delay.

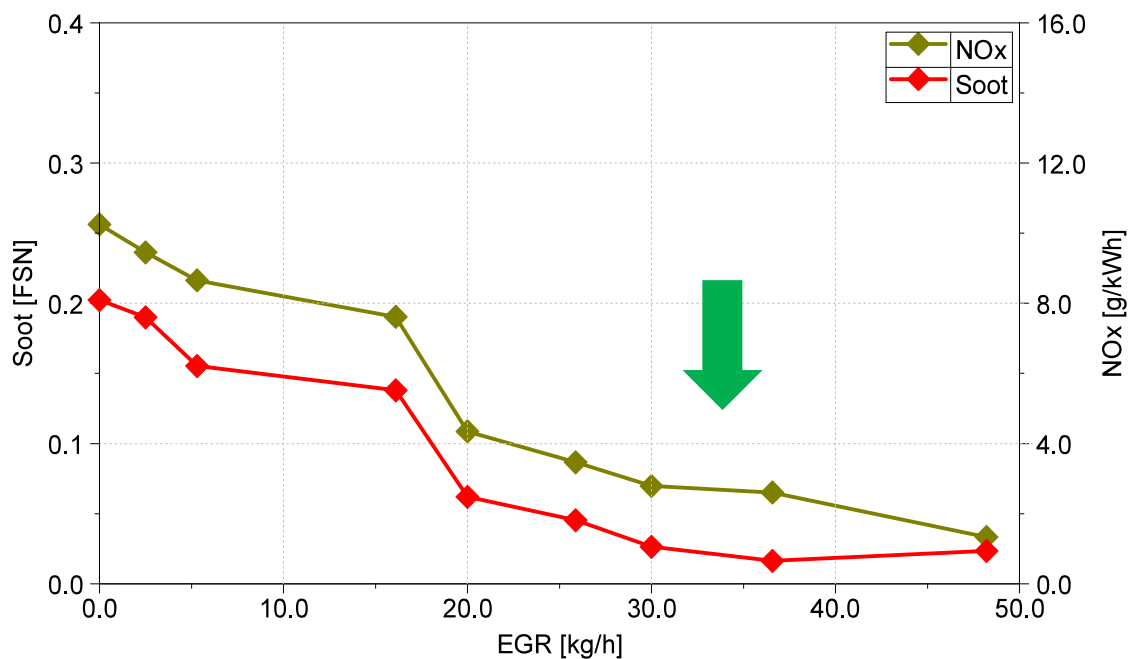


**Figure 5.2.  $\text{NO}_x$  and Soot reduction with different EGR Flow Rate in Dual Fuel**

### 5.3 Impact of HC and CO on Dual Fuel Combustion

Figure 5.3 highlights the influence of HC and CO emissions in increasing the gasoline percentage. The EGR rate is kept fixed at 20% in this experiment test to reduce NO<sub>x</sub> and soot and further to study the impact of HC and CO with the increase of gasoline content. The emissions of HC and CO increase with an increase in gasoline quantity. The addition of gasoline decreases the intake charge temperature, leading to an increase in ignition delay for diesel fuel and hence an overall increase of HC and CO emissions. These emissions are regulated by fuel-air mixing, injector nozzle dribble, local reaction temperature, and residence time at high temperatures. The increase of gasoline makes the mixture homogenous in the intake but its high mass content leads to unburnt hydrocarbon and carbon monoxide found in test data. The increase in gasoline content makes the local mixture lean for hydrocarbon slip in dual-fuel combustion. Overmixing of fuel and air beyond the lean limit of combustion in low-temperature combustion. To reduce simultaneously the emission of both NO<sub>x</sub> and soot, the gasoline content needs to be increased in dual fuel, which leads to a penalty of HC & CO.

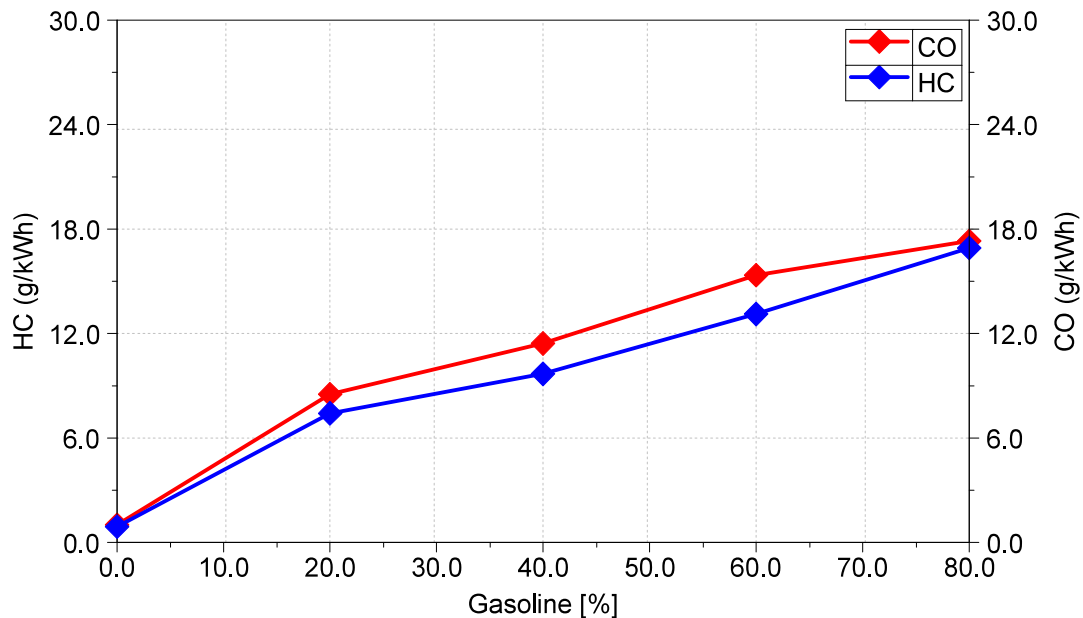


**Figure 5.3. HC and CO emissions with increasing gasoline percentage (EGR 20%)**

## 5.4 Effect of gasoline content on Brake-specific Fuel Consumption

The effect of the gasoline percentage on NO<sub>x</sub> emission and BSFC is shown in Fig. 5.4. The diesel percentage is varied along with gasoline fuel to achieve a torque of 200 Nm to study combustion behavior. Rail pressure of 1300 bar and AFR of 29 is maintained during the test. Injection timing is kept at -3 deg BTDC. No pilot and post-injection are given in this test. BMEP is kept at 9.5 bar during this test. BSFC increases with an increase in the percentage of gasoline. The increase of BSFC is high for gasoline beyond 75%, which might be due to the knocking type of combustion in the diesel engine. There is a decrease in NO<sub>x</sub> with an increase in gasoline percentage from 25% to 60%, possibly due to the formation of homogeneous lean gasoline-air combination, resulting in low-temperature combustion. The production of NO<sub>x</sub> is related to the temperature rise in the cylinder, reaction time, and concentration of oxygen. Lean air-fuel mixture and drop in local temperature in the air can lead to lower NO<sub>x</sub> formation.

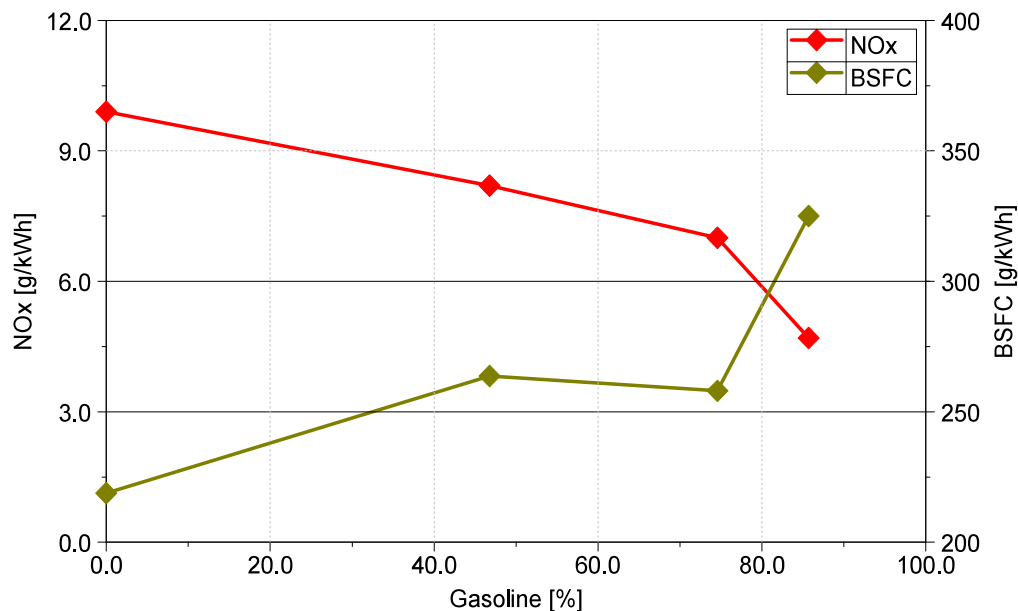
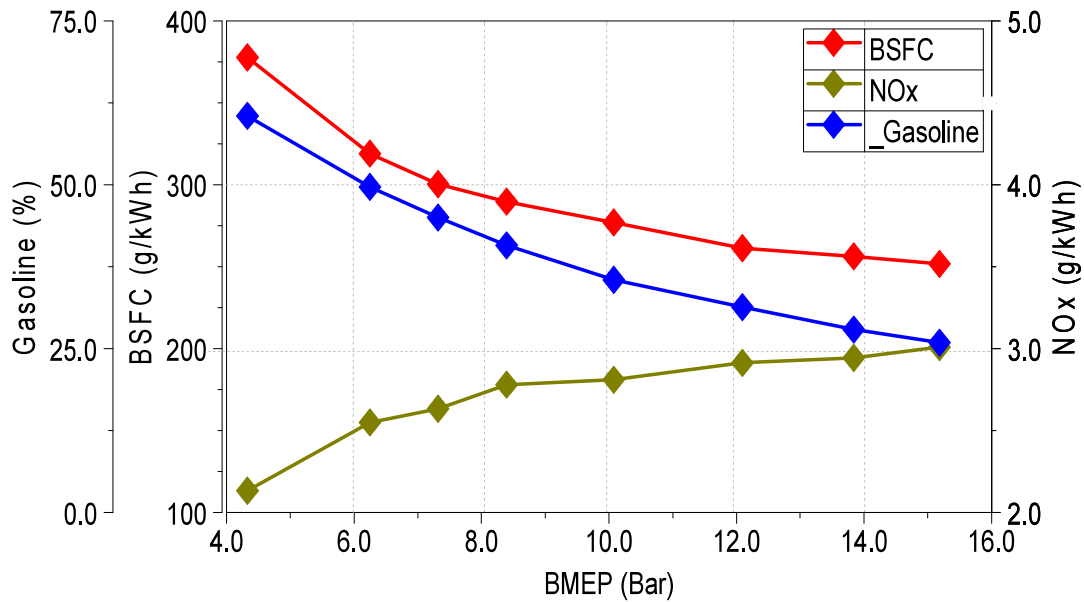


Figure 5.4 – NO<sub>x</sub> and BSFC comparison with different compositions of dual-fuel

## 5.5 Effect on NO<sub>x</sub> and Brake-specific Fuel Consumption with Dual Fuel

Emission and performance testing is done at various load conditions and compared in Fig. 5.5. The BSFC increases from 250 g/kWhr to 373 g/kWhr for an increase in gasoline

content from 10% to 50%. However,  $\text{NO}_x$  emissions are significantly reduced up to BMEP of 14 bar. The trend of BSFC and  $\text{NO}_x$  is not uniform with respect to the variation of load and dual-fuel composition. The best-optimized point for both BSFC and  $\text{NO}_x$  is observed at 40% gasoline in terms of fuel economy and emission. The  $\text{NO}_x$  emission trend is low across both loads of the engine operating zone.



**Figure 5.5 Comparison of  $\text{NO}_x$  and BSFC for different load points (1520rpm)**

## 5.6 Effect of EGR on Emissions with Dual Fuel

Improved combustion of premixed air-fuel mixtures at lean and low-temperature situations is possible at a higher mixing ratio.  $\text{NO}_x$  emissions and emissions of smoke decrease simultaneously due to locally lean conditions. Emissions of smoke are significantly lower, because of the long duration for mixing, leading to a homogeneous air-gasoline mixture, as observed from Fig. 5.6. The addition of EGR, along with gasoline, shows a further reduction in  $\text{NO}_x$  emission. Test data highlights that with EGR and 77% of gasoline,  $\text{NO}_x$  levels are very low, which is one of the promising aspects of elimination of after-treatments for  $\text{NO}_x$  emission. However, HC and CO emissions are higher because of more homogeneous combustion characteristics

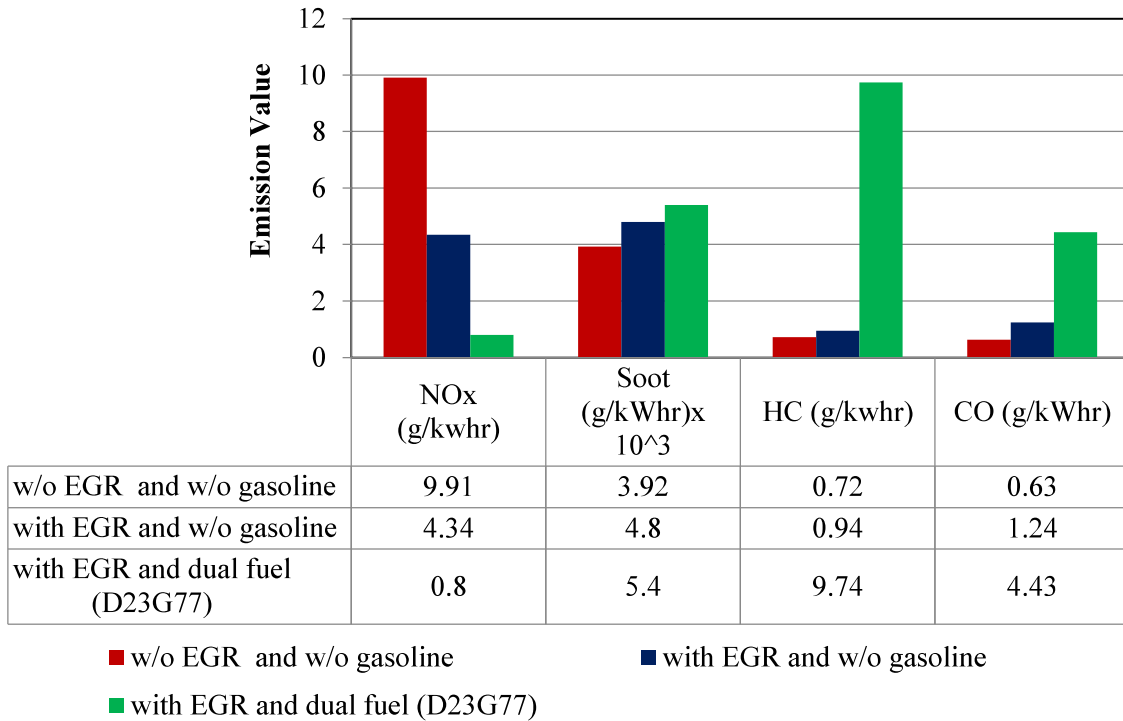
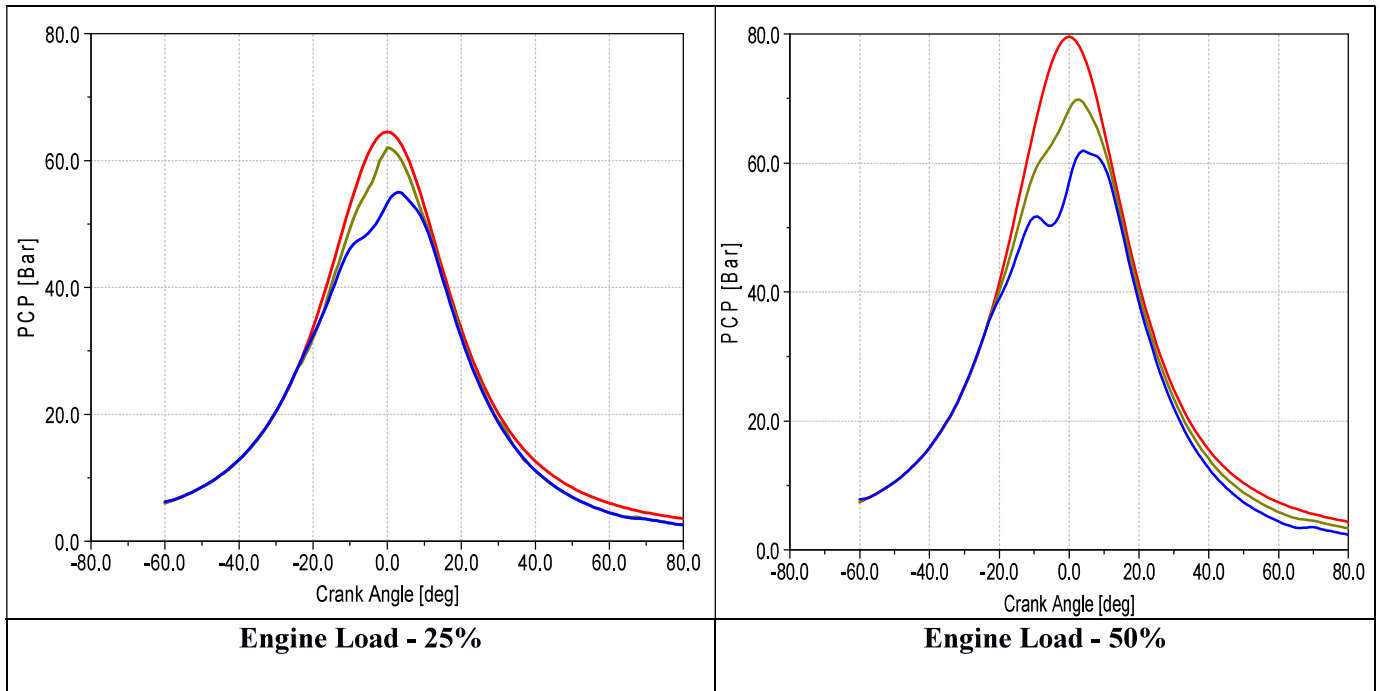


**Figure 5.6 – Comparison of Emission Parameters (with and without EGR)**

In the LTC strategy, by premixing a substantial amount of fuel and increasing ignition delay, high-temperature flame fronts can be circumvented, which curbs NO<sub>x</sub> formation and decreases heat transfer losses. The efficiency increases further due to a higher ratio of specific heats. Elongated ignition delay ensures proper mixing, resulting in reduced fuel-rich regions and lower PM formation. Ignition delay is longer when gasoline is mixed in the intake charge due to the lower temperatures of the intake charge. This provides sufficient time for the mixing of air and fuel before the start of combustion. Consequently, the rich region is reduced and the formation of soot inhibited while maintaining high fuel efficiency. Compared to the conventional fuel mixing or diffusion-controlled strategies, premixed low-temperature combustion is advantageous for fuel efficiency when combustion phasing is appropriately controlled. It can be summarized that increase in the gasoline ratio and optimized compression ratio leads to the homogeneous mixing of fuel-air and produces higher thermal efficiency, ultra-low NO<sub>x</sub>, and PM.

## 5.7 Effect on Cylinder Pressure with dual fuel

In-cylinder pressure is measured at 1520 rpm engine speed with load conditions varying from 100 Nm to 400 Nm. The mass flow rate of gasoline is kept constant at 7 kg/hr, while that of diesel is varied depending on the load requirement. In-cylinder pressure curves are compared in Fig. 7 at different load conditions and for different percentages of gasoline. The experiment results were focused to show the trends of PCP with different compositions of dual fuel. The increase in the gasoline content leads to an increase in combustion duration and reduced peak combustion pressure (PCP) in part-load conditions. The mixture of air and gasoline is ignited by direct injection of diesel inside the cylinder, while ignition of diesel-air mixture commences when it reaches the auto-ignition condition. If diesel is introduced early into the combustion chamber, the time taken for the mixing of diesel and air rises due to the lower temperature inside the cylinder. The combustion duration increases with a higher engine load. In general, the peak cylinder pressure decreases with an increase in gasoline from 45 % to 90% at all load conditions, except for the 100% load condition. The possible reason for the presence of a dual peak with dual fuel may be the mixing duration of diesel and gasoline and ignition delay due to the dual fuel before the combustion phase.



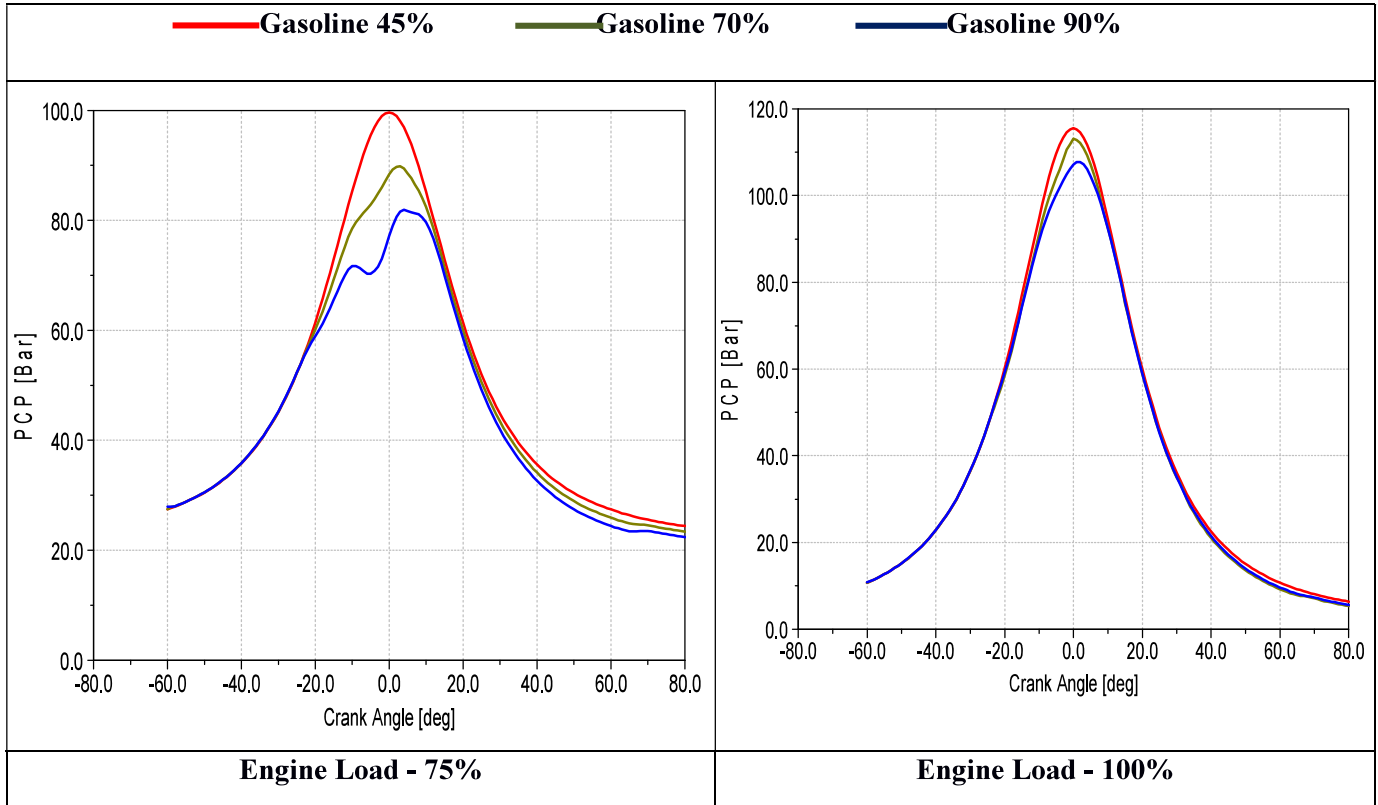


**Figure 5.7- Impact of Gasoline percentage on cylinder pressure at different load point**

### **5.8 Effect of injection timing on BSFC with Dual Fuel**

Injection timing plays a very important role in emission and BSFC. Injection timing refers to the time between the piston position and crankshaft angular velocity when ignition occurs in the combustion chamber (during the compression stroke). The selection of the right injection timing is a very important parameter to meet the performance and exhaust emission of an engine. The goal of the experimental investigation is to determine the effects and trend of ignition timing on BSFC with dual fuel. Rail pressure of 1200 bar and AFR of 30 is maintained during the test. No pilot and post-injection quantities are given in this test. Injection timing variation is from 0 to -10 deg BTDC. No injection timing swing is considered in advance timing above 0 deg, as this leads to an increase of  $\text{NO}_x$  with advance timing. Further, the effect of injection time on BSFC is studied at an engine speed of 1520 rpm, 50% load (200 Nm) conditions, and gasoline at 65%.

The emission and fuel consumption study above shows that 65% of gasoline can yield the best engine performance and minimum emissions. Hence, a test injection timing swing is performed for the optimization of injection timing with 65% gasoline. The effect of injection timing on BSFC is compared in Figure 10. It is observed with the advance of ignition timing, BSFC decreases following a trend like the diesel engine observed with dual fuel. Advanced ignition timing leads to an increase in the mean effective pressure combustion chamber, increasing torque, as observed during the experimental test. A further advance in ignition timing also leads to a reduction of the specific fuel consumption, as observed in the test result data.

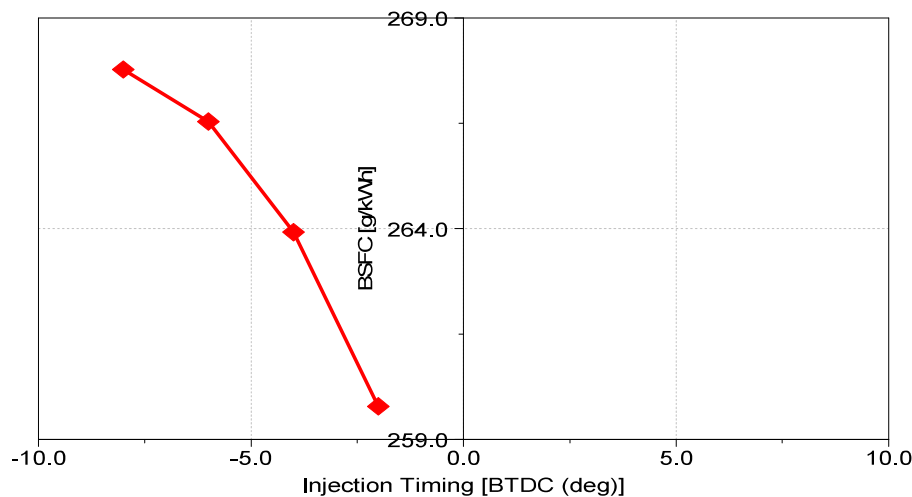


**Figure 5.8 - Impact of Injection Timing on Dual-fuel Combustion**

## 5.9 Summary

The decrease in  $\text{NO}_x$  and soot emission with gasoline is due to homogeneous lean mixture leading to low-temperature combustion. A premixed charge entering the combustion chamber avoids the rich fuel-air mixture pockets inside the combustion chamber at the time of combustion. Premixed charge avoids fuel-rich combustion, thus reducing soot formation. The local air-fuel ratio is lean and hence low combustion temperature, thus reducing the  $\text{NO}_x$  emissions. This indicates that the use of gasoline to prepare a premixed mixture and diesel as high reactivity fuel to initiate combustion helps in simultaneous reduction of soot and  $\text{NO}_x$  with minimal modification in the engine setup.

A balanced combination of EGR rate and injection timing in dual-fuel combustion behavior is the most effective method to reduce combustion temperature significantly, leading to a significant drop of  $\text{NO}_x$  and soot emission.  $\text{NO}_x$  and soot emissions were reduced with an increase in the gasoline content ratio when the engine was tested at a constant speed of 1520 rpm with EGR during combustion. Dual Fuel test results highlight that with the fuel composition D30G70, fuel consumption improved by 1.9% in comparison with diesel fuel combustion with simultaneous reduction of  $\text{NO}_x$  and soot emissions. Compared to D100 fuel, it was observed that the introduction of gasoline fuel in dual fuel comparison reduces  $\text{NO}_x$  emission with dual fuel combustion, as per the experiment test results. Hydrocarbon and carbon monoxide emissions increased more than 10- 15 times with an increase in gasoline content. This is one of the key challenges in dual-fuel combustion with an increase of low reactive fuel. Oxidation Catalyst will be required in after-treatment, only to control this emission to meet legislative regulation. LTC combustion will eliminate costly after-treatments like Selective Catalytic Reduction (SCR) and Diesel Particulate Filter (DPF) from the exhaust layout to meet emission from a diesel engine.

Premixed auto-ignition of the lean mixture increased gasoline content. This helps to maintain the combustion temperature low, resulting in the reduction of heat transfer loss and more moderate PCP. Thermal efficiency can be significantly improved with a compromise of the high level of HC and Carbon monoxide to get ultra-low  $\text{NO}_x$ . The technical approach to control HC & CO can be pilot injection introduction during combustion, along with advanced injection timing, with the introduction of EGR leading to LTC combustion was found to vary from 10- 40 bar with the increase of gasoline content in dual-fuel across different load conditions. The increase in gasoline content leads to an increase in combustion time and a reduction in peak combustion pressure (PCP). Direct injection of diesel into the cylinder ignites the mixture of air and gasoline, whereas ignition of the diesel-air mixture begins when it reaches the auto-ignition condition. A challenge relating to the dual-fuel combustion mode is the high MPRR at high loads; so, fuel properties should change for different operating conditions. Early oxidation reactions were reduced as the gasoline ratio was increased, MPRR tends to decrease with higher gasoline percentages. As a result of a too-rich fuel-air combination, the combustion duration was

prolonged and MPRR reduced. The increase of the EGR rate reduced MPRR and simultaneously,  $\text{NO}_x$  and soot emission also decreased. A high equivalence ratio in dual-fuel ignition mode was observed, with both peak heat release rate and exhaust gas temperature increasing due to the shorter combustion duration. The extent of a gradient in fuel reactivity and local equivalence ratio inside the cylinder is key for the PCP trend. The increasing gasoline percentage shows an increase in combustion duration, leading to a reduction of combustion pressure.

## CHAPTER 6

### PARTICULATE MASS & NUMBER CHARACTERIZATION

A dual-fuel combustion with a homogeneous mixture like a gasoline engine and compression ignition like diesel engine has a potential to reduce particulate, nitrogen oxides ( $\text{NO}_x$ ) and other emissions from engines. The study presents an experimental investigation in a four-cylinder compression ignition engine with high and low reactivity fuel to understand soot formation in terms of particulate matter, particulate number, and composition. The effect of dual-fuel, injection pressure, exhaust gas recirculation (EGR), and sulphur content on soot emission is presented. The soot and  $\text{NO}_x$  emission decreased with increasing the gasoline percentage in the dual fuel. The reduction in soot up to 30% is observed for 75% gasoline content.  $\text{NO}_x$  emission is reduced by 15% for 50% gasoline content and reduced further 10% with increasing gasoline to 75%. The dual fuel with 85% gasoline has smoke 0.08 FSN and  $\text{NO}_x$  4.74 g/kWhr, which is significantly lower compared to conventional diesel engine operation. An increase in gasoline reduces both particle diameter and particle concentration. The particulate number and size move from accumulation mode to nuclei mode with increase of gasoline content. The filter paper analysis shows that hydrocarbon fraction in soot increases for higher gasoline percentage. Use of dual fuel has a potential for simultaneous reduction in soot and  $\text{NO}_x$  emission and reduce after treatment cost for a diesel engine.

#### 6.1 Particulate size distribution with different Gasoline Ratio

The load on the engine was varied from 500 Nm to 200 Nm at a constant engine speed of 1500rpm, while injection pressure was maintained at 1200 bar. Gasoline content is changed as 0, 50, and 85% during trials. The particulate size distribution and average particulate size is compared at different test conditions. The particulate size decreased with increasing gasoline content in dual fuel (Fig.6.1).

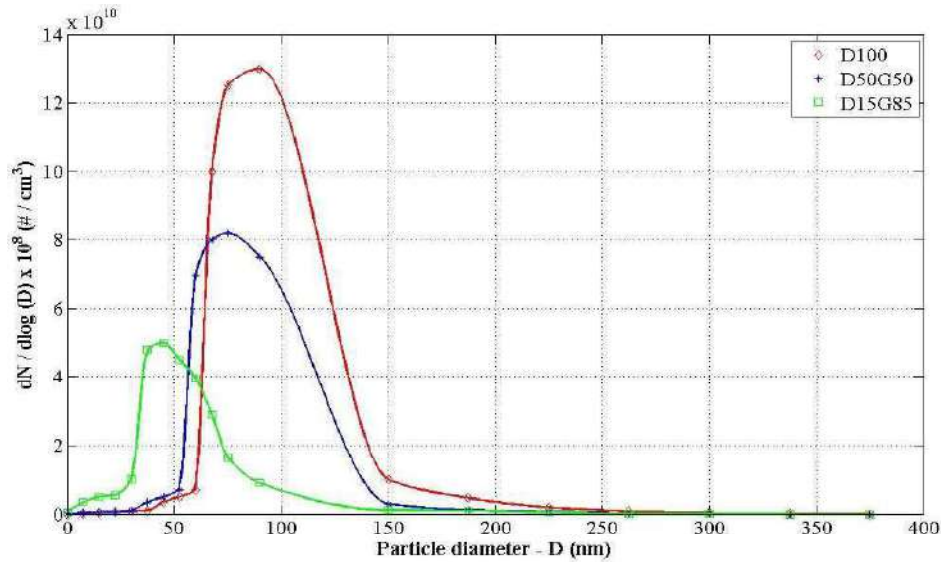


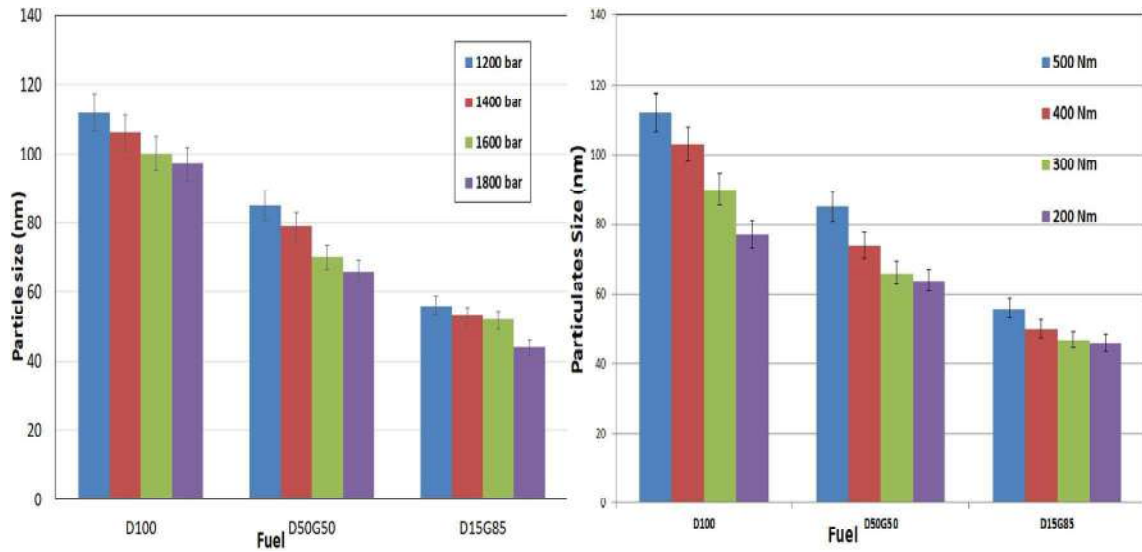
**Figure 6.1- Particulate size distribution for different gasoline ratio**

The increase in gasoline content indicates combustion moving towards homogeneous combustion mode, and a higher amount of heat is released from premixed fuel. A decrease in diffusion combustion reflects in reduced particulate formation. Increasing gasoline content also shows a reduction in average particulate diameter and reduction in the spread of particulate diameter in emission.

## 6.2 Effect of fuel, injection pressure, and engine load on particulate size

Figure 6.2 compares average particulate size for different injection pressures. The particulate size decreases with an increase in the injection pressure for all fuels. The average particle size for diesel is around 100 nm, while for D50G50 average particle size is reduced to 70 nm. An increase in diesel injection pressure leads to fine atomization, increased air-fuel mixing, thus leading to better combustion. Improvement in fuel atomization accelerates combustion rate and raises in-cylinder combustion temperature hence higher particulate oxidation in the late combustion process. An increase in engine load shows an increase in the average particulate diameter in Fig 6.2. The increase in particle diameter is significant for diesel, 31% for increasing torque from 200 to 500 Nm. This is due to an increased quantity of diesel injected at a higher load that primarily promotes diffusion combustion leading to high soot formation.

The particle size increased 24% and 17% for D50G50 and D15G85, respectively. For D15G85 fuel, with increasing load, most of the fuel is in the form of gasoline, thus forming a homogeneous mixture and hence increase in the soot particle is small. With a change in engine load from 500 Nm to 200 Nm, the particle size distributions changed towards more nuclei mode particles and less accumulation mode.



(a) Injection pressure (Load 500 Nm) (b) Engine load (Injection pressure 1200 bar)

**Figure 6.2- Particulate size diameter at different injection pressure and load points**

### 6.3 Effect of EGR on particulate size distribution

The particle size distributions changed towards more nuclei mode particles and less accumulation mode. The EGR is a main parameter in LTC combustion for soot and NO<sub>x</sub> control emissions. Experiments are carried out with varying EGR content in dual-fuel D50G50 at an engine speed of 1500 rpm and load of 250 Nm. EGR is varied from 0% to 60% EGR ratio. With the addition of EGR, average particle diameter is higher, including a higher spread in the particle diameter distribution. The particle number density is low for 10% and 20% EGR. With the addition of EGR, average particle diameter is higher, including a higher spread in the particle diameter distribution (Fig. 6.3).

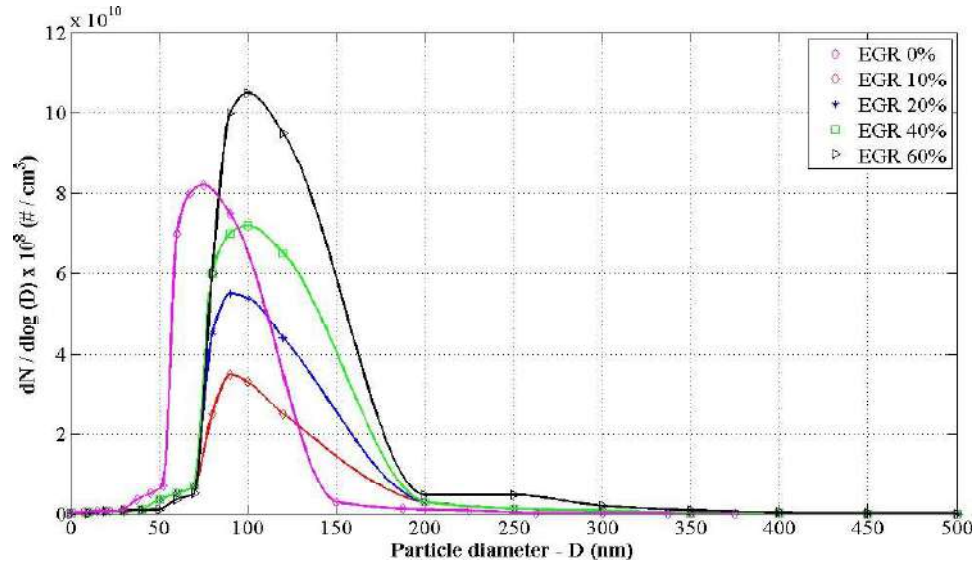


**Figure 6.3- Effect of EGR on particulate size distribution**

Figure 6.3 highlight an increase in particulate number density and particle diameter with an increase of EGR content from 10 to 60% in dual-fuel combustion. Low in-cylinder temperature and extremely low activity prevent complete oxidation of boundary layer and crevice-bound hydrocarbons. This results in higher HC precursor concentrations and higher nucleation soot with EGR. An increase of EGR content leads to a reduction in local temperature, hence controlling  $\text{NO}_x$ . However, EGR also lowers the combustion temperature, and oxidation rate subsequently increasing soot emission. The results indicate that only higher EGR is not good for a reduction in soot and  $\text{NO}_x$  emissions.

#### 6.4 Effect of sulphur content on particulate size distribution

The impact of sulphur content in diesel on particulate size in engine-out emission is compared for D50G50 dual fuel without EGR. Diesel fuel with sulphur content of 10 ppm and 350 ppm is used for the study. The particulate size distribution for two fuels is shown in Fig. 6.4.

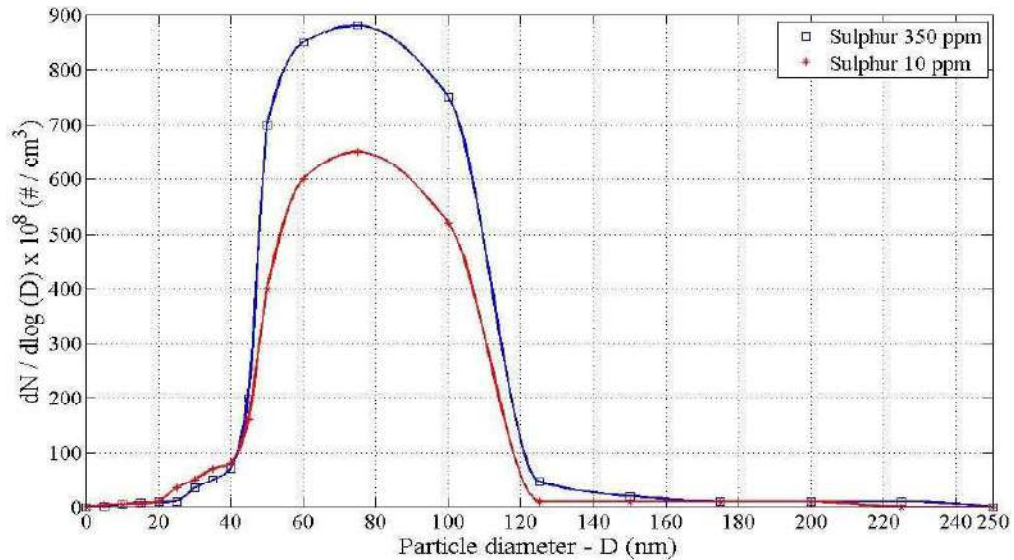





**Figure 6.4- Effect of sulphur content in diesel on particulate size distribution**

The diesel with 350 ppm sulphur shows higher particulate size concentration than 10 ppm sulphur diesel. Total particulate matter mass emissions are more with high sulphur fuel. With increase in sulphur content of fuel, engine out emission is having high soluble organic content leading to higher number of nuclei mode with 350 ppm sulphur fuel.

## 6.5 Composition of PM and PN with filter paper measurement in dual fuel

Filter paper analysis is conducted for engine-out emission to investigate the composition of soot, particulate matter and particulate number. The filter paper measurements are conducted with and without EGR for D50G50 fuel and compared with D100 fuel. The results of filter paper analysis are compared in Table 6.1. Particulate matter and the particulate number reduced with D50G50 fuel compared to D100 fuel. The use of EGR in D50G50 fuel further reduced particulate mass and number in engine-out emission. The difference in particle size gives a difference in particle number and mass concentration as observed with respect to D100 fuel to D50G50 fuel.

<b>Index</b>	<b>D100</b>	<b>D50G50</b>	<b>D50G50 (20% EGR)</b>
<b>Filter Paper</b>			
<b>Particulate Mass(mg/kWhr)</b>	31	19	11
<b>Particulate Number</b>	2x 1E+12	1.7x 1E+11	1.5x 1E+10

**Table 6.1- Filter paper sample with dual fuel (with and without EGR)**

Filter paper analysis is conducted on particulate mass emitted from the engine. Primary, secondary, and blank filter papers holding particulate matter are separately weighted. Filter papers are taken together with Soxhlet solvent extraction in the laboratory for a minimum hour duration with 80:20 benzene methanol mix as solvent. Extracted filter papers are dried at 70 deg C for 30 mins. The weights of filter papers are taken to determine soluble organic fraction (SOF) and insoluble organic fraction (IOF) in particulate matter composition. Chromatographic Analysis is used for SOF analysis, and SOF content analysis is done in Perkin Elmer Auto system XL gas chromatograph. This is analyzed to determine fuel and oil-derived hydrocarbon fractions in SOF using the method of standard IP 442 testing condition. IOF Contents are analyzed by the thermo-gravimetric analysis method. Particulate matter collected on primary, secondary, and black filter paper are subjected to TGA test after solvent extraction. The thermograms are evaluated for weight loss over a defined temperature range 40-540° C and 540-700° C to determine sulphates, nitrates, water, along with carbon soot and metal oxides. Filter paper analysis of soot composition is presented in Fig.6.5 for D100, D50G50, and D15G85 fuels. An increase of gasoline content in dual fuel reduces soot content but adversely increases soluble organic fraction in particulate matter.

This reduces particulate number and mass but indicates an increase in unburnt hydrocarbon in the exhaust. Other contents such as sulphates, nitrates are the same in all fuels. With the use of EGR, both NO<sub>x</sub> and soot can be controlled in low-temperature combustion, but there will be a requirement of the after-treatment device to control hydrocarbon emissions.

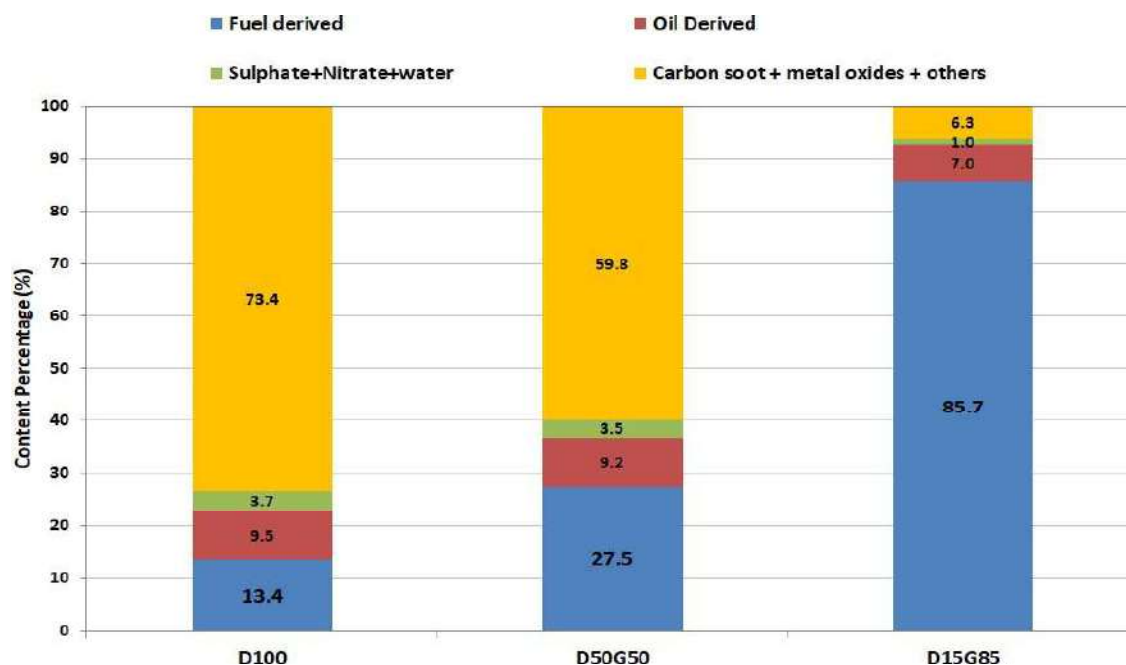


**Figure 6.5- Filter paper composition with D100, D50G50 and D15G85 Fuel**

This experimental investigation aims to understand the characteristics of particulate mass and particulate size distribution in engine emission with Low and High Reactivity dual fuel. The particulate numbers and their correlation for engine out, DOC Out, and DPF out emission are investigated in a 3.8-liter diesel common-rail engine with gasoline port injection and 20% EGR. A particulate emission correlation with dual fuel combination of D50G50, D25G75, and D15G85 are compared with diesel fuel. Three DOCs with different PGM content are tested with dual fuel to understand particulate matter composition. The chemical composition of exhaust particulate from engine Out and DOC out are compared. An increase in low reactive fuel (D15G85) and an increase of PGM content (DOC3) show a significant reduction in PM from 31 mg/kWhr to 2 mg/kWhr.

A major reduction in particulate size distribution at 40 nm is observed. The selection of DOC with PGM content is critical for low-temperature combustion (dual fuel) to control HC and CO emissions. Three configurations of DOCs were tested with different PGM content to understand particulate mass and particle number trend. Filter paper analysis carried out to understand SOF and IOF with different configuration of dual fuel composition.

## **6.6 Effect of composition with Dual Fuel on Particulate Mass Emission**

Experiment was conducted for different composition of dual fuel (Diesel and Gasoline) from D50G50, D25G75 and D15G85. The results were compared with emissions for pure diesel fuel. Engine was tested at engine speed of 1500 rpm and torque of 250 Nm. The EGR content of 20% was constant in all tests. Dual fuel composition was varied maintaining same torque to understand its particulate matter behavior. Particulate mass decreased with increase of low reactive fuel (gasoline) as highlighted in Figure 6.6. Increase of low reactive fuel in dual fuel reduced particulate mass from 31 mg/kWhr for (D100) to 7 mg/kWhr for (D15G85). The presence of homogeneously mixed gasoline elongates ignition delay due to lower temperatures of intake charge which also leads to lower combustion temperature. The strategy to increase low reactivity fuel (gasoline) in diesel engine combustion is one methodology to reduce particulate mass from exhaust emission.

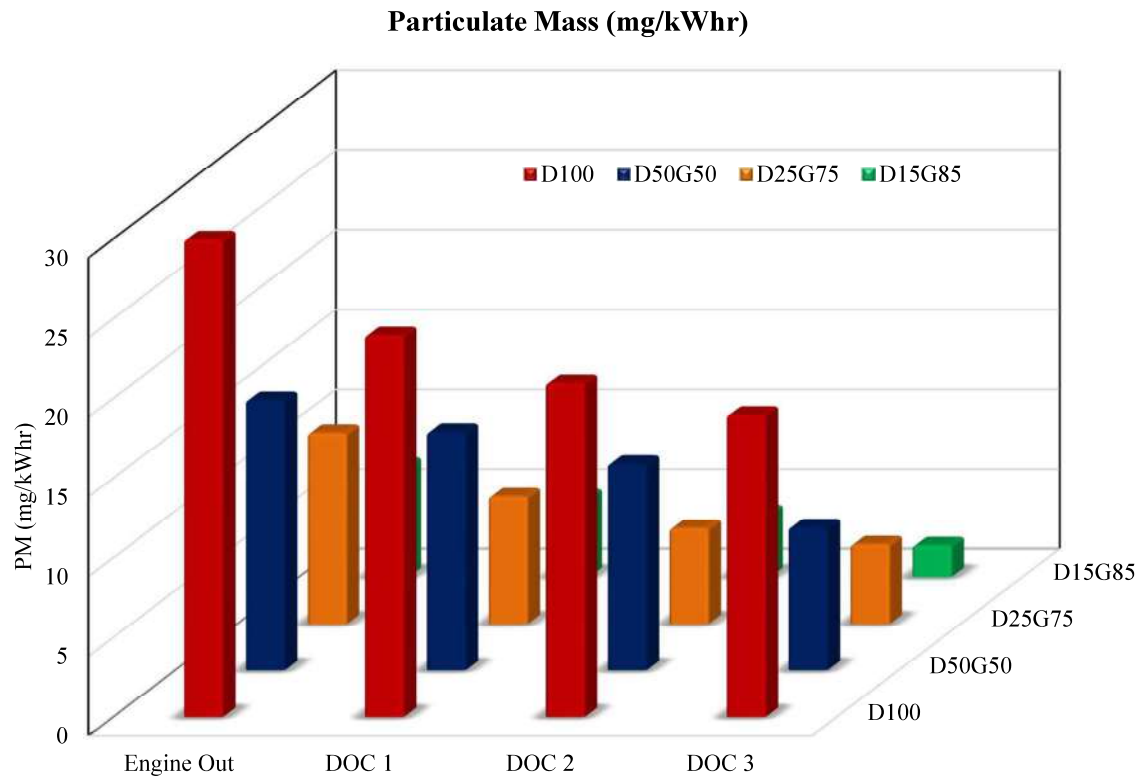


**Figure 6.6- Particulate Mass with different dual fuel ratio and DOC configuration**

Particulate mass emission is reduced compared to base engine out emission with use of DOC system. Diesel oxidation catalyst reduces hydrocarbon and carbon monoxide from exhaust along with reduction of soluble organic fraction. Conversion efficiency majorly depends upon exhaust mass and temperature along with PGM loading of catalyst. Increase of noble metal content (Platinum) in DOC wash coat leads to improve light off property in lower temperature required for conversion of HC& CO along with better efficiency to reduce SOF content from particulate matter. Engine out particulate mass reduced from 31 mg/kWhr to 19 mg/kWhr with different DOC configuration. DOC3 showed high reduction in particulate mass due to high content of noble material (Platinum) that helps in better oxidation of HC, CO and SOF. Increase of low reactive fuel (D15G85) along with increase of PGM (Platinum) in DOC3 is giving best result which lead reduce significantly from 31 mg/kWhr to 2 mg/kWhr. Selection of DOC and PGM content is very critical and important for low temperature combustion (dual fuel) to control HC and CO.

This will lead the possibility to meet BSVI equivalent to Euro VI norms in diesel engine combustion without DPF. Catalyst Temperature is key challenge for conversion efficiency with increase of low reactive fuel which need to be studied at different operating engine condition.

### **6.7 Effect of composition with Dual Fuel on Particulate Size distribution**

Particulate size distribution in different dual fuel from D50G50, D25G75 and D15G85 is compared with diesel fuel (D100). Test condition was kept at 1500 rpm engine speed and torque of 250 Nm with fixed EGR content of 20%. In test data, particle size distribution reduced from 71 nm to 46 nm with increase of gasoline content from 0% to 85% in dual fuel. No major particulate size distribution impact observed with DOC out with all three DOC's tested during experiment test. Increase of PGM content in DOC plays is having minor impact of particle size distribution between engine out and DOC out. The behavior of particle size distribution with different ratio of dual fuel and DOC's are highlighted in Figure 6.7. Major reduction in particulate size distribution observed with DOC3 is 40 nm with dual fuel configuration of D15G85. The possible cause of this minor reduction in particulate size distribution is due to very less soot oxidation takes place inside DOC with dual fuel combustion.

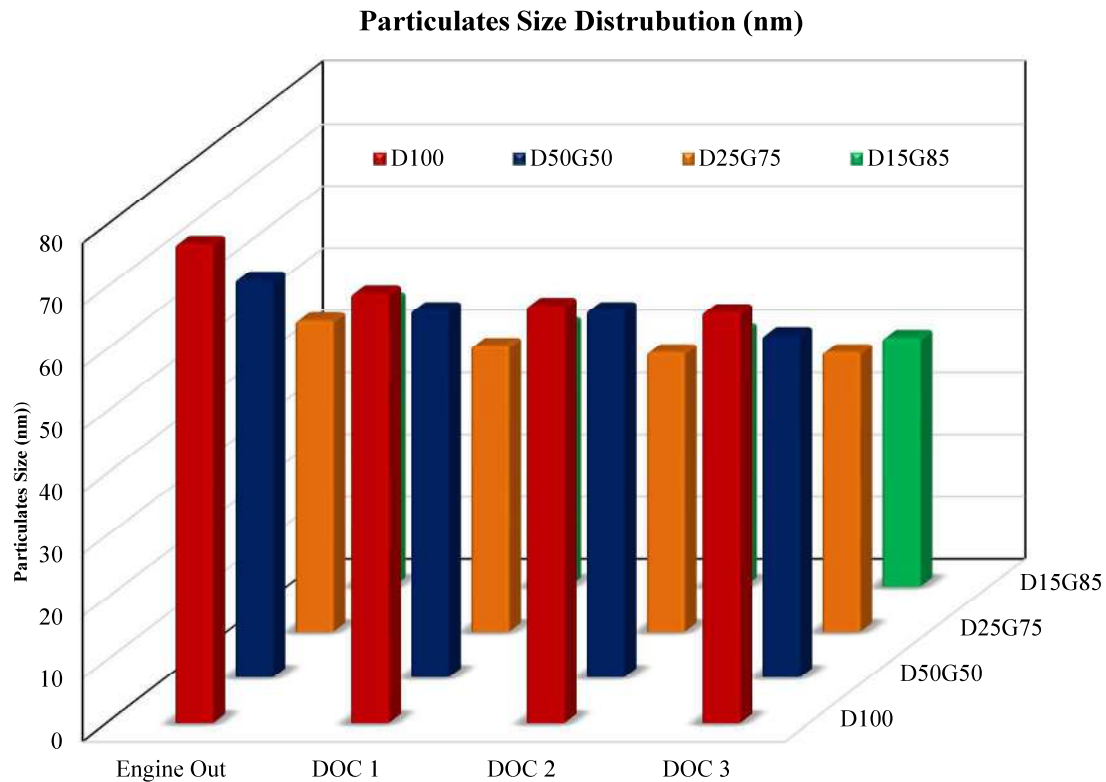


**Figure 6.7 – Particulate Size distribution with different dual fuel ratio and DOC**

### **6.8 SOF and IOF distribution from Engine and DOC Out with Dual Fuel**

Filter paper analysis conducted on particulate mass emissions emitted from engine. IOF and SOF analysis are performed from engine out emission and all three DOC's out to investigate SOF and IOF content from exhaust emission with dual fuel composition of D50G50 and compared with D100 engine. SOF is formed with hydrocarbon derived from lube oil and diesel fuel. Figure 6.8 highlights that DOC is useful to reduce SOF content in particulate matter from D50G50 fuel and D100 fuel. Increase of Platinum content in DOC from DOC1 (10 g/cft<sup>3</sup>) to DOC3 (20 g/cft<sup>3</sup>) helps in reduction of SOF content from 17% to 5% in D100 fuel. Similar pattern is also observed with D50G50 composition where SOF content is reduced from 31% to 23% with increase of PGM content. Amount of SOF content is high with D50G50 fuel due to increase of unburnt hydrocarbon observed in this combustion. However, the total particulate mass and particle number is less with D50G50 fuel. Selection of DOC configuration and its precious material content is very important with low temperature combustion as this reduce both high content of hydrocarbon and

passive soot oxidation in SOF. It can be observed that BSVI emission can be achieved only from DOC with this low temperature combustion technology.

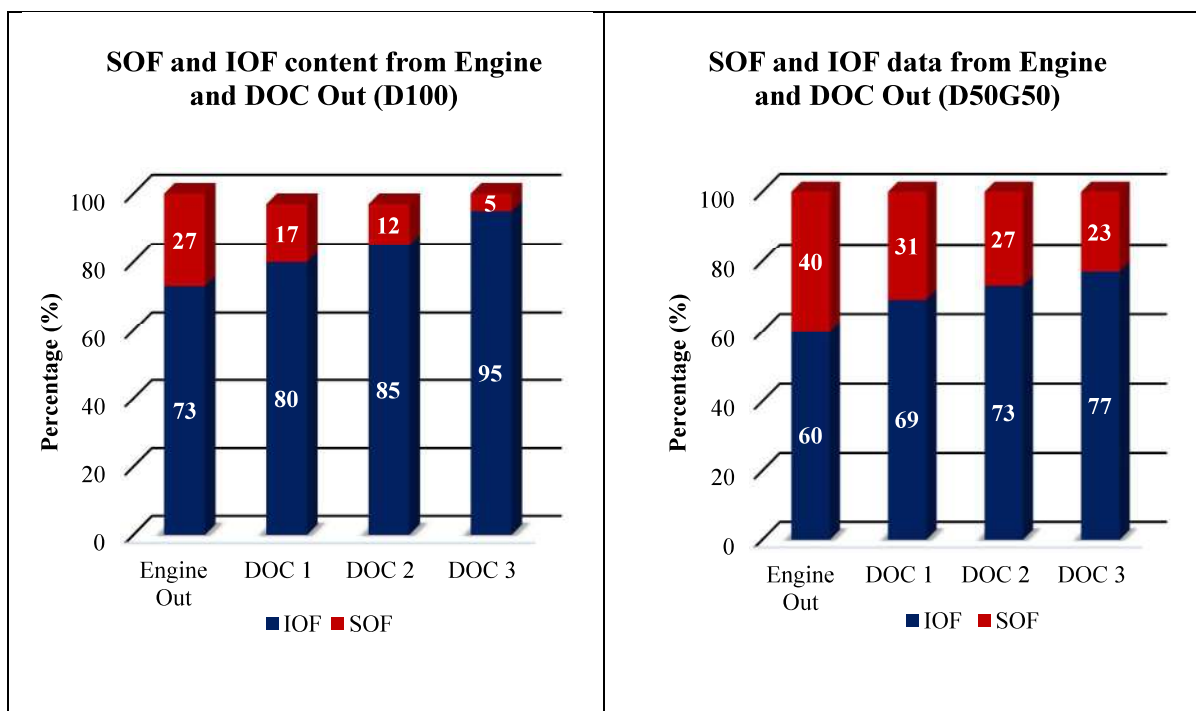


**Figure 6.8– SOF and IOF ratio from Engine and DOC Out with Dual Fuel and Diesel**

## 6.9 Correlation of Particulate Mass and Particle Number with Dual Fuel

Experiment study was performed to understand behavior and correlation of particulate number size distribution, particulate mass and particle number emissions trend after engine out, DOC out and DPF out with D50G50, D25G75 and D15G85 dual fuel in comparison to conventional diesel fuel. In experiment test, it was observed that particulate number and particulate mass follow almost linear correlation in engine out found with diesel and different dual fuel ratio. This leads to PM to PN correlation is only stable when agglomeration rate is low as per results shown in Figure 6.9. This relationship between particle number and particle mass emissions pattern gets changed after DPF out in comparison with engine out. This characteristic and pattern of behavior between particle number and particle mass emission characteristics could be useful to work in areas of after treatment solution. No correlation is observed for PN with PM emissions in DPF out both

for diesel and dual fuel also. Increase of low reactivity fuel in diesel fuel leads to very small particle number size due to homogeneous mixture inside combustion.

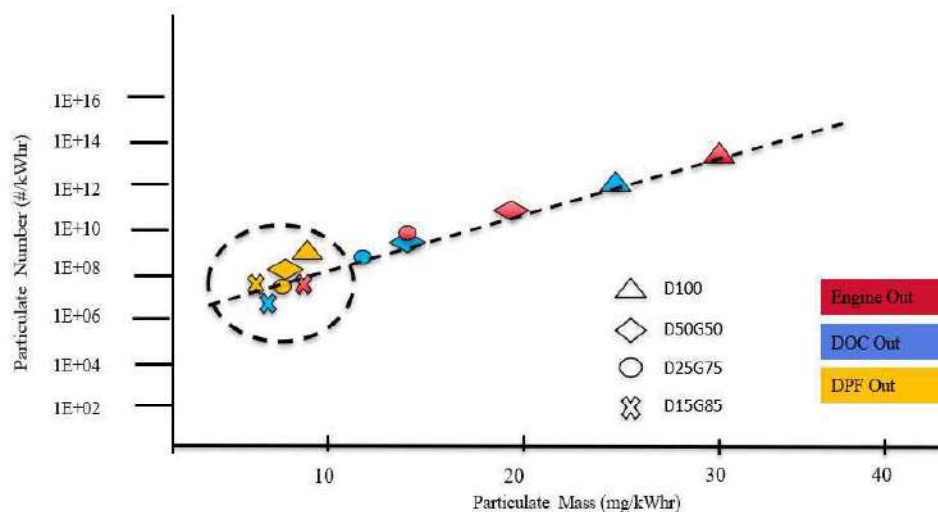


**Figure 6.9 – Correlation of Particulate Mass and Particle Number with Dual Fuel Ratio**

Diesel engine out emission contains large mass concentration from exhaust as found during test data. From DOC out, due to reduction of SOF part the PN number is reduced from engine out test data as shown in Table 6.2. Best approach to control PM and PN is to increase low reactive fuel in dual fuel combustion.

Engine Speed	Torque	Fuel Ratio	PM	PN	PM	PN	PM	PN
			Engine Out		DOC Out		DPF Out	
rpm	Nm	%	mg/kWh	#/kWh	mg/kWh	#/kWh	mg/kWh	#/kWh
1500	250	D100	31	8.0E+13	24	5.0E+12	6	6.0E+09
		D50G50	17	6.0E+11	15	7.0E+10	5	7.0E+08
		D25G75	12	6.0E+10	8	8.0E+09	3	5.0E+07
		D15G85	7	7.0E+08	5	4.0E+08	1	5.0E+07

**Table 6.2 - Particulate Mass and Particle Number test data with dual fuel**

## 6.10 Summary

The experimental investigation on engine emission was performed to understand particle mass and particle size distribution with different compositions of dual fuel. Particle emissions from the engine out, DOC out, and DPF out are compared to understand their correlation. The PM emission and PN characteristics are studied with dual-fuel combustion. High reactive diesel fuel is combined with low reactive gasoline port injection. Experimental results show that the dual-fuel concept can escape from NO<sub>x</sub>-smoke trade-off, reducing both to near zero values but leading to the challenge of increasing HC and CO. Particulate matter emissions from a dual-fuel engine are investigated for a different combination of high reactivity and low reactivity fuel. Effect of injection pressure, engine load, EGR, and sulphur content is compared for various dual-fuel combinations. Filter paper analysis is conducted to understand particulate matter composition. Particle number and particle mass emissions from engine out, DOC out and DPF out are compared to understand their correlation. The particulate matter (PM) emission and particle number (PN) characteristics is studied with dual fuel combustion. High reactive diesel fuel is used in combination with low reactive gasoline port injection. High octane fuel (gasoline) is supplied in intake port in base compression ignition diesel engine to investigate primarily effects of balance between low reactivity and high reactivity fuels.

- An increase in the low reactivity fuel content in dual-fuel shifts diffusion combustion towards homogeneous low-temperature combustion, which leads to a reduction in both NO<sub>x</sub> and particulate matter emission simultaneously. Soot particles in the exhaust of dual-fuel combustion are mostly from nucleation mode particles. An increase in gasoline content leads to soot particle formation mode shift from accumulation to nuclei mode. The accumulation mode particles are composed of carbon soot particles and adsorbed volatile content leading to high PM mass and PN numbers. The particle diameter and particle concentration reduced with increasing gasoline content due to the homogeneous mixture. The average particle size decreased with an increase in injection pressure, while particle diameter increased with an increase in engine load.

- The sulphur content is found to increase in soot emission due to high soluble content. The SOF increase with increasing gasoline as combustion becomes lean leading to increase in HC emissions. Unburnt hydrocarbon inhibits liquid fuel vaporization, thus increasing amount of liquid fuel in combustion chamber, which cannot burn completely before being emitted to exhaust emission. Use of Gasoline and Diesel as dual fuel does not require any special design changes or infrastructure for delivery. The study highlights no additional SCR and DPF after treatment required in diesel engine to meet stringent legislative norms equivalent to Euro VI with dual fuel.
- Experimental results showed dual-fuel concept can escape from  $\text{NO}_x$ - smoke trade-off, reducing both to near zero values but leading to challenge of increase of HC and CO. Increase in amount of gasoline in dual fuel combustion experiment, it was observed reduction of PM and PN as mixture becomes more homogeneous, fully vaporized fuel-air mixture will give low levels of PN emissions in comparison with D100 fuel combustion.
- Selection of Diesel oxidation catalyst and its PGM content is very important parameter to meet emission with dual fuel combustion. Particulate mass can be reduced to 99% without DPF. This was achieved with dual fuel combustion approach with increase of gasoline content (D15G85) and DOC3 with PGM loading of 20 g/cft<sup>3</sup>. Nobel material content (PGM) in DOC helps in reduction of HC and CO along with SOF content from emission. This helps in reduction of particulate mass due to SOF reduction and soot oxidation. No major impact observed in particle number size distribution found with DOCs with increase of Platinum content. High hydrocarbon is observed reflecting similar trend followed in SOF content with increase of gasoline content as result of extremely low air/fuel ratios. Increase of amount of gasoline fuel in combustion chamber leading to unburnt hydrocarbon in form of liquid fuel which cannot fully burn before being discharged into the exhaust.
- Diesel oxidation catalyst and its PGM content is critical to meet emission with dual fuel combustion. Particulate mass can be reduced to 99% without DPF with dual-fuel (D15G85) and DOC3 with PGM loading of 20 g/cft<sup>3</sup>. Nobel material content

(PGM) in DOC helps in reduction of HC and CO along with SOF content from emission. No significant impact was observed in particle number size distribution found with DOCs with an increase of Platinum content. High hydrocarbon is observed reflecting similar trend followed in SOF content with increase of gasoline content as result of extremely low air/fuel ratios. Increase of amount of gasoline fuel in combustion chamber leading to unburnt hydrocarbon in form of liquid fuel which cannot fully burn before being discharged into the exhaust.

- Particulate mass and Particulate Number show a liner correlation for engine out and DOC out condition emission with diesel and dual-fuel due to high particulate mass emission from engine out from the engine. This is due to agglomeration rate is low and high content of non-volatile fractions (soot) emissions from engine out. From DPF out, correlation between PM and PN is nonlinear due to significantly low PM and PN due to high filtration efficiency from DPF. This is due to presence of semi volatile particles from DPF out. The trend and correlation of particle number and particle mass will behave with other alternative fuels due to possible reason of chemical composition difference between particles mass as well as different size distributions.
- An increase in the amount of gasoline in dual-fuel leads to reduction of PM and PN as mixture becomes more homogeneous fuel-air mixture resulting in low levels of PN emissions compared to D100 fuel. To meet BSVI emission norms limit of  $\text{NO}_x$  and PM both SCR and DPF are not required in after treatment system with dual fuel combustion. DOC is only required to meet emission for BSVI emission with this low temperature combustion technology using low and high reactive fuel.

## **CHAPTER 7**

### **CONCLUSION AND WAY FORWARD**

Low-temperature combustion is investigated to study engine emissions and soot characteristics using diesel-gasoline dual fuel. A four-cylinder diesel engine is used for the study. A single-point gasoline injection in the intake manifold of an engine is used to prepare a homogeneous intake charge. A standard ECU is used to control gasoline and diesel injectors. Each cylinder gets a uniform, homogenized air-gasoline mixture during the intake stroke. The quantity of gasoline and diesel is varied to control combustion phase behavior. Different combustion-related parameters like injection duration, gasoline ratio, injection timing, and EGR were varied to study their influence on the performance of engine emissions.

High-octane fuel (Gasoline) is injected intake manifold of diesel engine (high reactive fuel) to investigate combustion performance primarily. The novelty of the experiment is the study of emission and performance behavior with dual fuel (Low and high reactive fuel) and to assess best strategy to control  $\text{NO}_x$  and PM. Engine tests are conducted with and without EGR in dual fuel to understand its behavior in emission and BSFC. Investigations are conducted with high and low reactivity fuel to understand soot formation in terms of particulate matter, particulate number, and composition. The effect of dual-fuel, injection pressure, exhaust gas recirculation (EGR), and sulphur content on soot emission is presented.

#### **Conclusions**

The addition of gasoline in the intake charge helps to reduce the combustion temperature and help for simultaneous reduction in soot and  $\text{NO}_x$ . The use of gasoline had small effect on engine performance and fuel consumption. An increase in gasoline reduces both particle diameter and particle concentration. The particulate number and size move from accumulation mode to nuclei mode with increase of gasoline content. The filter paper analysis shows that hydrocarbon fraction in soot increases for higher gasoline percentage.

The study also highlights that no additional SCR & DPF after-treatment will be required in the diesel engine to meet the stringent legislative norms of BSVI. The particulate numbers and their correlation for engine out, DOC Out, and DPF out emission are investigated with gasoline port injection and 20% EGR.

A particulate emission correlation with dual fuel combination of D50G50, D25G75, and D15G85 are compared with diesel fuel. Three DOCs with different PGM content are tested with dual fuel to understand particulate matter composition. The chemical composition of exhaust particulate from engine out and DOC out are compared. The selection of DOC with PGM content is critical for low-temperature combustion (dual fuel) to control HC and CO emissions. The important conclusion from the study is summarized below:

1. A balanced combination of EGR rate and injection timing in dual-fuel combustion behavior is the most effective method to reduce combustion temperature significantly, leading to a significant drop of  $\text{NO}_x$  and soot emission.  $\text{NO}_x$  and soot emissions reduced with increase in the gasoline content ratio when the engine was tested at a constant speed of 1520 rpm with EGR. Dual Fuel test results highlight that with the fuel composition D30G7, fuel consumption improved by 1.9% in comparison with diesel fuel combustion with simultaneous reduction of  $\text{NO}_x$  and soot emissions.
2. Hydrocarbon and carbon monoxide emissions increased more than 10- 15 times with an increase in gasoline content. This is one of the key challenges in dual-fuel combustion with an increase of low reactive fuel. Oxidation Catalyst will be required in after-treatment, only to control this emission to meet legislative regulation. LTC combustion will eliminate costly after-treatments like Selective Catalytic Reduction (SCR) and Diesel Particulate Filter (DPF) from the exhaust layout to meet emission from a diesel engine.
3. An increase in the low reactivity fuel content in dual-fuel shifts the diffusion combustion towards homogeneous low-temperature combustion, which leads to a reduction in both  $\text{NO}_x$  and particulate matter emission simultaneously.

4. Soot particles in the exhaust of dual-fuel combustion are mostly from the nucleation mode particles. An increase in the gasoline content leads to soot particle formation mode shift from accumulation to nuclei mode. The accumulation mode particles are composed of carbon soot particles and adsorbed volatile content, leading to high PM mass and PN numbers.
5. The particle diameter and particle concentration decrease with increasing gasoline content due to the homogeneous mixture. The average particle size decreases with an increase in the injection pressure, while particle diameter increases with an increase in engine load. The sulfur content is found to increase in soot emission due to high soluble content. The SOF increases with increasing gasoline as combustion becomes lean, leading to an increase in HC emissions.
6. Diesel oxidation catalyst and its PGM content is critical to meet emission with dual fuel combustion. Particulate mass can be reduced to 99% without DPF with dual-fuel (D15G85) and DOC3 with PGM loading of 20 g/cft<sup>3</sup>. Nobel material content (PGM) in DOC helps in reduction of HC and CO along with SOF content from emission. No significant impact was observed in particle number size distribution found with DOCs with an increase of Platinum content.
7. High hydrocarbon is observed reflecting similar trend followed in SOF content with increase of gasoline content as result of extremely low air/fuel ratios. Increase of amount of gasoline fuel in combustion chamber leading to unburnt hydrocarbon in form of liquid fuel which cannot fully burn before being discharged into the exhaust.
8. Particulate mass and Particulate Number show a linear correlation for engine out and DOC out condition emission with diesel and dual-fuel due to high particulate mass emission from engine out from the engine. This is due to low agglomeration rate and high content of non-volatile fractions (soot) emissions from engine out.
9. From DPF out, correlation between PM and PN is nonlinear due to significantly low PM and PN due to high filtration efficiency from DPF. This is due to presence of semi volatile particles from DPF out. The trend and correlation of particle number and particle mass will behave with other alternative fuels due to possible reason of chemical composition difference between particles mass as well as different size distributions.

## **Way Forward**

The study provides significant directions and results for use of dual fuel to reduce diesel engine emission. The future research direction for the work are as follows:

1. The technical approach with dual fuel can be investigated in complete engine load points with ultra low NO<sub>x</sub> and soot emission.
2. Different chemical composition of fuels tests can be performed to understand combustion behavior during LRF and HRF fuel for emission and heat release behavior.
3. A detailed investigation is required on after treatment devices to meet emission in legislative regulation mode points to conclude this final approach in transient mode.

## BIBLIOGRAPHY

1. M. Noguchi, Y. Tanaka, T. Tanaka, and Y. Takeuchi, "A study on gasoline engine combustion by observation of intermediate reactive products during combustion," SAE Paper 790840, 1979.
2. Wang H, Vescovo D, Yao M, Reitz R. "Numerical Study of RCCI Combustion Processes Using Gasoline, Diesel, iso-Butanol and DTBP Cetane Improver", SAE Technical Paper; 2015
3. Dec JE. "A conceptual model of DI diesel combustion based on laser-sheet imaging." SAE Technical paper 970873; 1997.
4. Singh S, Reitz RD, Musculus MPB "2-Color thermometry experiments and high-speed imaging of multi-mode diesel engine combustion", SAE technical paper 2005-01-3842; 2005.
5. N. P. Komninou and C. D. Rakopoulos, "Modeling HCCI combustion of biofuels: a review," Renewable & Sustainable Energy Reviews, vol. 16, no. 3, pp. 1588–1610, 2012.
6. M. Richter, J. Engström, A. Franke, M. Aldén, A. Hultqvist, and B. Johansson, "The influence of charge inhomogeneity on the HCCI combustion process," SAE Paper 2000-01-2868, 2000.
7. M. P. B. Musculus, P. C. Miles, and L. M. Pickett, "Conceptual models for partially premixed low-temperature diesel combustion," Progress in Energy and Combustion Science, vol. 39, no. 2-3, pp. 246–283, 2013.
8. Heywood, J.B. "Internal Combustion Engine Fundamentals", McGraw-Hill Book Co., U.S.A. 1988.
9. Bosch. "Bosch Automotive Handbook", 7th Edition. Robert Bosch GmbH, Placing, Germany, 2007
10. J. T. Kashdan, N. Docquier, and G. Bruneaux, "Mixture preparation and combustion via LIEF and LIF of combustion radicals in a direct-injection HCCI diesel engine," SAE Paper 2004-01-2945, 2004.

11. T. Fang, R. E. Coverdill, C.-F. F. Lee, and R. A. White, "Low-temperature combustion within a HSDI diesel engine using multiple-injection strategies," *Transactions of the Asme—Journal of Engineering for Gas Turbines and Power*, vol. 131, no. 6, Article ID 062803, 2009.
12. T. Fang, Y.-C. Lin, M. F. Tien, and C.-F. Lee, "Reducing NO<sub>x</sub> emissions from a biodiesel-fueled engine by use of low-temperature combustion," *Environmental Science & Technology*, vol. 42, no. 23, pp. 8865–8870, 2008.
13. H. Liu, J. Xu, Z. Zheng, S. Li, and M. Yao, "Effects of fuel properties on combustion and emissions under both conventional and low temperature combustion mode fueling 2,5-dimethylfuran/diesel blends," *Energy*, vol. 62, pp. 215–223, 2013.
14. R. R. Steeper and S. de Zilwa, "Improving the NO<sub>x</sub>-CO<sub>2</sub> trade-off of an HCCI engine using a multi-hole injector," *SAE Technical Paper 2007-01-0180*, 2007.
15. H. Liu, S. Li, Z. Zheng, J. Xu, and M. Yao, "Effects of n-butanol, 2-butanol, and methyl octynoate addition to diesel fuel on combustion and emissions over a wide range of exhaust gas recirculation (EGR) rates," *Applied Energy*, vol. 112, pp. 246–256, 2013.
16. W. Berntsson and I. Denbratt, "HCCI combustion using charge stratification for combustion control," *SAE Technical Paper 2007-01-0210*, 2007.
17. S. Kook and C. Bae, "Combustion control using two-stage diesel fuel injection in a single-cylinder PCCI engine," *SAE Paper 2004-01-0938*, 2004.
18. H. Liu, C.-F. F. Lee, M. Huo, and M. Yao, "Combustion characteristics and soot distributions of neat butanol and neat soybean biodiesel," *Energy & Fuels*, vol. 25, no. 7, pp. 3192–3203, 2011.
19. Z. Zheng, L. Yue, H. Liu, Y. Zhu, X. Zhong, and M. Yao, "Effect of two-stage injection on combustion and emissions under high EGR rate on a diesel engine by fueling blends of diesel/gasoline, diesel/n-butanol, diesel/gasoline/n-butanol and pure diesel," *Energy Conversion and Management*, vol. 90, pp. 1–11, 2015.
20. Z. Zheng, C. Li, H. Liu, Y. Zhang, X. Zhong, and M. Yao, "Experimental study on diesel conventional and low temperature combustion by fueling four isomers of butanol," *Fuel*, vol. 141, pp. 109–119, 2015.

21. Upatnieks and C. J. Mueller, "Controlled DI diesel combustion using dilute, cool charge gas and a short-ignition-delay, oxygenated fuel," SAE Technical Paper 2005-01-0363, 2005.
22. J. Mueller and A. Upatnieks, "Dilute clean diesel combustion achieves low emissions and high efficiency while avoiding control problems of HCCI," in Proceedings of the 11th Annual Diesel Engine Emissions Reduction Conference (DEER '05), Chicago, USA, August 2005.
23. H. Liu, X. Bi, M. Huo, C.-F. F. Lee, and M. Yao, "Soot emissions of various oxygenated biofuels in conventional diesel combustion and low temperature combustion conditions," *Energy & Fuels*, vol. 26, no. 3, pp. 1900–1911, 2012.
24. H. Liu, C.-F. Lee, M. Huo, and M. Yao, "Comparison of ethanol and butanol as additives in soybean biodiesel using a constant volume combustion chamber," *Energy & Fuels*, vol. 25, no. 4, pp. 1837–1846, 2011.
25. X. Bi, H. Liu, M. Huo, C. Shen, X. Qiao, and C.-F. F. Lee, "Experimental and numerical study on soot formation and oxidation by using diesel fuel in constant volume chamber with various ambient oxygen concentrations," *Energy Conversion and Management*, vol. 84, pp. 152–163, 2014.
26. R. Collin, J. Nygren, M. Richter, M. Aldén, L. Hildingsson, and B. Johansson, "Simultaneous OH- and formaldehyde-LIF measurements in an HCCI engine," SAE Technical Paper 2003-01-3218, 2003.
27. G. Särner, M. Richter, M. Aldén, L. Hildingsson, A. Hultqvist, and B. Johansson, "Simultaneous PLIF measurements for visualization of formaldehyde- and fuel-distributions in a DI HCCI engine," SAE Paper 2005-01-3869, 2005.
28. H. Zhao, Z. Peng, and T. Ma, "Investigation of the HCCI/CAI combustion process by 2-D PLIF imaging of formaldehyde," SAE Paper 2004-01-1901, 2004.
29. Hildingsson, H. Persson, B. Johansson et al., "Optical diagnostics of HCCI and UNIBUS using 2-D PLIF of OH and formaldehyde," SAE Paper 2005-01-0175, 2005.
30. W. Berntsson and I. Denbratt, "Optical study of HCCI combustion using NVO and an SI stratified charge," SAE Paper 2007-24-0012, SAE International, 2007.

31. W. Berntsson, M. Andersson, D. Dahl, and I. Denbratt, "A LIF-study of OH in the negative valve overlap of a spark-assisted HCCI combustion engine," SAE Paper 2008-01-0037, 2008.
32. Schulz, J. B. Jeffries, D. F. Davidson, J. D. Koch, J. Wolfrum, and R. K. Hanson, "Impact of UV absorption by CO<sub>2</sub> and H<sub>2</sub>O on NO LIF in high-pressure combustion applications," *Proceedings of the Combustion Institute*, vol. 29, no. 2, pp. 2735–2742, 2002.
33. Schulz, J. D. Koch, D. F. Davidson, J. B. Jeffries, and R. K. Hanson, "Ultraviolet absorption spectra of shock-heated carbon dioxide and water between 900 and 3050 K," *Chemical Physics Letters*, vol. 355, no. 1-2, pp. 82–88, 2002.
34. W. G. Bessler, C. Schulz, T. Lee, J. B. Jeffries, and R. K. Hanson, "Strategies for laser-induced fluorescence detection of nitric oxide in high pressure flames. I. A–X<sub>0,0</sub> excitation," *Applied Optics*, vol. 41, no. 18, pp. 3547–3557, 2002.
35. W. G. Bessler, C. Schulz, T. Lee, J. B. Jeffries, and R. K. Hanson, "Strategies for laser-induced fluorescence detection of nitric oxide in high pressure flames. II. A–X<sub>0,1</sub> excitation," *Applied Optics*, vol. 42, no. 12, pp. 2031–2042, 2003.
36. W. G. Bessler, C. Schulz, T. Lee, J. B. Jeffries, and R. K. Hanson, "Strategies for laser-induced fluorescence detection of nitric oxide in high-pressure flames. III. Comparison of A–X excitation schemes," *Applied Optics*, vol. 42, no. 24, pp. 4922–4936, 2003.
37. R. Augusta, D. E. Foster, J. B. Ghandhi, J. Eng, and P. M. Najt, "Chemiluminescence measurements of homogeneous charge compression ignition (HCCI) combustion," SAE Paper 2006-01-1520, 2006.
38. E. Murase, K. Hanada, T. Miyaura, and J. Ikeda, "Photographic observation and emission spectral analysis of homogeneous charge compression ignition combustion," *Combustion Science and Technology*, vol. 177, no. 9, pp. 1699–1723, 2005.
39. Man E. Mancaruso and B. M. Vaglieco, "Optical investigation of the combustion behaviour inside the engine operating in HCCI mode and using alternative diesel fuel," *Experimental Thermal & Fluid Science*, vol. 34, no. 3, pp. 346–351, 2010.
40. Dec, W. Hwang, and M. Sjöberg, "An investigation of thermal stratification in HCCI engines using chemiluminescence imaging," SAE Technical Paper 2006-01-1518, 2006.

41. Vressner, A. Hultqvist, and B. Johansson, "Study on the combustion chamber geometry effects in an HCCI engine using high-speed cycle-resolved chemiluminescence imaging," SAE Paper 2007-01-0217, 2007. View at Google Scholar. WHO (2018). Ambient (outdoor) air pollution report.
42. J. E. Dec and R. E. Canaan, "PLIF imaging of NO formation in a DI diesel engine," SAE Technical Paper 980147, 1998.
43. S. D. Zilwa and R. Steeper, "Predicting NO<sub>x</sub> emissions from HCCI engines using LIF imaging," SAE Paper 2006-01-0025, 2006.
44. J. E. Dec and E. B. Coy, "OH radical imaging in a DI diesel engine and the structure of the early diffusion flame," SAE Transactions, vol. 105, no. 3, pp. 1127–1148, 1996.
45. J. E. Dec and D. R. Tree, "Diffusion-flame/wall interactions in a heavy-duty DI diesel engine," SAE Transactions, vol. 110, no. 3, pp. 1618–1634, 2001.
46. P. G. Aleiferis, A. G. Charalambides, Y. Hardalupas, A. M. K. P. Taylor, and Y. Urata, "Modelling and experiments of HCCI engine combustion with charge stratification and internal EGR," SAE Paper 2005-01-3725, 2005.
47. Alriksson M, Denbratt I. Low temperature combustion in a heavy-duty diesel engine using high levels of EGR. SAE technical paper 2006–01-0075;2006.
48. S. Ma, Z. Zheng, H. Liu, Q. Zhang, and M. Yao, "Experimental investigation of the effects of diesel injection strategy on gasoline/diesel dual-fuel combustion," Applied Energy, vol. 109, no. 2, pp. 202–212, 2013.
49. H. Liu, X. Wang, Z. Zheng, J. Gu, H. Wang, and M. Yao, "Experimental and simulation investigation of the combustion characteristics and emissions using n-butanol/biodiesel dual-fuel injection on a diesel engine," Energy, vol. 74, pp. 741–752, 2014.
50. S. L. Kokjohn, R. M. Hanson, D. A. Splitter, and R. D. Reitz, "Fuel reactivity-controlled compression ignition (RCCI): a pathway to controlled high-efficiency clean combustion," International Journal of Engine Research, vol. 12, no. 3, pp. 209–226, 2011.
51. X. Lu, J. Ma, L. Ji, and Z. Huang, "Simultaneous reduction of NO<sub>x</sub> emission and smoke opacity of biodiesel-fueled engines by port injection of ethanol," Fuel, vol. 87, no. 7, pp. 1289–1296, 2008.

52. Y. J. Kim, K. B. Kim, and K. H. Lee, "Effect of a 2-stage injection strategy on the combustion and flame characteristics in a PCCI engine," *International Journal of Automotive Technology*, vol. 12, no. 5, pp. 639–644, 2011.
53. W. H. Su and W. B. Yu, "Effects of mixing and chemical parameters on thermal efficiency in a partly premixed combustion diesel engine with near-zero emissions," *International Journal of Engine Research*, vol. 13, no. 3, pp. 188–198, 2012.
54. X. G. Wang, Z. H. Huang, O. A. Kuti, W. Zhang, and K. Nishida, "An experimental investigation on spray, ignition and combustion characteristics of biodiesels," *Proceedings of the Combustion Institute*, vol. 33, no. 2, pp. 2071–2077, 2011.
55. X. G. Wang, Z. H. Huang, W. Zhang, O. A. Kuti, and K. Nishida, "Effects of ultra-high injection pressure and micro-hole nozzle on flame structure and soot formation of impinging diesel spray," *Applied Energy*, vol. 88, no. 5, pp. 1620–1628, 2011.
56. Glassman, *Combustion*, Academic Press, New York, NY, USA, 3rd edition, 1996.
57. K. Kumano, Y. Yamasaki, and N. Iida, "An investigation of the effect of charge inhomogeneity on the ignition and combustion processes in a HCCI engine using chemiluminescence imaging," *Journal of Thermal Science & Technology*, vol. 2, no. 2, pp. 200–211, 2007.
58. M. P. B. Musculus, "Multiple simultaneous optical diagnostic imaging of early-injection low-temperature combustion in a heavy-duty diesel engine," *SAE Paper* 2006-01-0079, 2006.
59. T. Lachaux and M. P. B. Musculus, "In-cylinder unburned hydrocarbon visualization during low-temperature compression-ignition engine combustion using formaldehyde PLIF," *Proceedings of the Combustion Institute*, vol. 31, no. 2, pp. 2921–2929, 2007.
60. A.S. Cheng, B. T. Fisher, G. C. Martin, and C. J. Mueller, "Effects of fuel volatility on early direct-injection, low-temperature combustion in an optical diesel engine," *Energy & Fuels*, vol. 24, no. 3, pp. 1538–1551, 2010.
61. J. E. Dec, "A conceptual model of D.I. diesel combustion based on laser-sheet imaging," *SAE Transactions*, vol. 106, no. 3, pp. 1319–1348, 1997.

62. C. Espey, J. E. Dec, and T. A. Litzinger, "Quantitative 2-D fuel vapor concentration imaging in a firing D.I. diesel engine using planar laser-induced Rayleigh scattering," SAE Transactions, vol. 103, no. 3, pp. 1145–1160, 1994.
63. T.-G. Fang, R. E. Coverdill, C.-F. F. Lee, and R. A. White, "Effect of the injection angle on liquid spray development in a high-speed direct-injection optical diesel engine," Proceedings of the Institution of Mechanical Engineers, Part D: Journal of Automobile Engineering, vol. 223, no. 8, pp. 1077–1092, 2009.
64. T. Fang, R. E. Coverdill, C.-F. F. Lee, and R. A. White, "Effects of injection angles on combustion processes using multiple injection strategies in an HSDI diesel engine," Fuel, vol. 87, no. 15-16, pp. 3232–3239, 2008.
65. T. Fang and C.-F. F. Lee, "Low sooting combustion of narrow-angle wall-guided sprays in an HSDI diesel engine with retarded injection timings," Fuel, vol. 90, no. 4, pp. 1449–1456, 2011.
66. H. Liu, S. Ma, Z. Zhang, Z. Zheng, and M. Yao, "Study of the control strategies on soot reduction under early-injection conditions on a diesel engine," Fuel, vol. 139, pp. 472–481, 2015.
67. R. Kiplimo, E. Tomita, N. Kawahara, and S. Yokobe, "Effects of spray impingement, injection parameters, and EGR on the combustion and emission characteristics of a PCCI diesel engine," Applied Thermal Engineering, vol. 37, pp. 165–175, 2012.
68. J. T. Kashdan and J. F. Papagni, "LIF imaging of auto-ignition and combustion in a direct-injection, diesel-fuelled HCCI engine," SAE Technical Paper 2005-01-3739, 2005.
69. H. Liu, M. Huo, Y. Liu et al., "Time-resolved spray, flame, soot quantitative measurement fueling n-butanol and soybean biodiesel in a constant volume chamber under various ambient temperatures," Fuel, vol. 133, pp. 317–325, 2014.
70. Shibata, G, Oyama, K, Urushihara, T, & Nakano, T. (2004). The effect of Fuel Properties on Low and High Temperature Heat Release and Resulting Performance of an HCCI Engine", SAE Paper 2004-01-0553.
71. Peng, Z, Zhao, H, & Ladommatos, N. (2003). Visualization of the homogeneous charge compression ignition/controlled autoignition combustion process using two-

- dimensional planar laser-induced fluorescence image of formaldehyde.”, *Proc Instn Mech Engrs, Part D*, 217, 1125-1134.
72. Ishibashi, Y, & Sakuyama, H. (2004). An Application Study of the Pneumatic Direct Injection Activated Radical Combustion Two-Stroke Engine to Scooter”, 2004-01-1870.
  73. Zheng, J, Yang, W, Miller, D. L, & Cernansky, N. P. (2002). A skeletal Chemical Kinetic Model for the HCCI Combustion Process”, *SAE Paper* 2002-01-0423.
  74. Jun, D, Ishii, K, & Iida, K. (2003). Autoignition and Combustion of Natural Gas in 4 Stroke HCCI Engine”, *JSME International Journal, Series B*, , 46(1).
  75. Tanaka, S, Ayala, F, Keck, J. C, & Heywood, J. B. (2003). Two-stage ignition in HCCI combustion and HCCI control by fuels and additives”, *Combustion and Flame*, 132, 219-239.
  76. Dec, J. E, & Sjöberg, M. (2004). Isolating the Effects of Fuel Chemistry on Combustion Phasing in an HCCI Engine and the Potential of Fuel Stratification for Ignition Control”, *SAE Paper* 2004-01-0557.
  77. Shibata, G, Oyama, K, Urushihara, T, & Nakano, T. (2004). The effect of Fuel Properties on Low and High Temperature Heat Release and Resulting Performance of an HCCI Engine”, *SAE Paper* 2004-01-0553.
  78. Shuji Kimura, Hiroshi Ogawa, Yoichi Matsui, and Yoshiteru Enomoto. An experimental analysis of low-temperature and premixed combustion for simultaneous reduction of NO<sub>x</sub> and particulate emissions in direct injection diesel engines. *International Journal of Engine Research*, 3(4):249–259, 2002.
  79. Yoshinaka Takeda, Nakagome Keiichi, and Niimura Keiichi. “Emission characteristics of premixed lean diesel combustion with extremely early staged fuel injection.” Technical report, *SAE Technical Paper*, 1996.
  80. Keiichi Nakagome, Naoki Shimazaki, Keiichi Niimura, and Shinji Kobayashi. “Combustion and emission characteristics of premixed lean diesel combustion engine” Technical report, *SAE Technical Paper*, 1997.
  81. Sage Kokjohn, Reed Hanson, Derek Splitter, John Kaddatz, and Rolf Reitz. “Fuel reactivity controlled compression ignition (RCCI) combustion in light-and heavy-duty engines. *SAE International Journal of Engines*, 4(1):360–374,2011.

82. Hiromichi Yanagihara, Yasuo Sato, and Jun'ichi Mizuta. "A study of di diesel combustion under uniform higher-dispersed mixture formation" JSAE review, 18(4):361–367, 1997.
83. Kazuhiro Akihama, Yoshiki Takatori, Kazuhisa Inagaki, Shizuo Sasaki, and Anthony M Dean. "Mechanism of the smokeless rich diesel combustion by reducing temperature." Technical report, SAE technical paper, 2001.
84. Tie Li, Yukihiro Okabe, Hiroyuki Izumi, Toshio Shudo, and Hideyuki Ogawa. "Dependence of ultra-high egr low temperature diesel combustion on fuel properties." Technical report, SAE Technical Paper, 2006.
85. Robert H Thring. "Homogeneous-charge compression-ignition (HCCI) engines." Technical report, SAE Technical paper, 1989.
86. Magnus Christensen, Bengt Johansson, and Patrik Einewall. "Homogeneous charge compression ignition (HCCI) using isooctane, ethanol and natural gas-a comparison with spark ignition operation." Technical report, SAE Technical Paper, 1997.
87. Rudolf H Stanglmaier and Charles E Roberts. "Homogeneous charge compression ignition (HCCI): benefits, compromises, and future engine applications." Technical report, SAE Technical Paper, 1999.
88. Salvador M Aceves, Daniel L Flowers, Charles K Westbrook, J Ray Smith, "A multi-zone model for prediction of HCCI combustion and emissions." Technical report, SAE Technical paper, 2000.
89. Thomas W Ryan and Timothy J Callahan. "Homogeneous charge compression ignition of diesel fuel." Technical report, SAE Technical Paper, 1996.
90. Andreas Vressner, Andreas Lundin, Magnus Christensen, "Pressure oscillations during rapid HCCI combustion." SAE transactions, 112(4):2469–2478, 2003.
91. Jan-Ola Olsson, Per Tunestal, and Bengt Johansson. "Boosting for high load (HCCI) SAE Transactions, Journal of Engines," 113(3):579–588, 2004.
92. Michael Boot, Erik Rijk, Carlo Luijten, Bart Somers, and Bogdan Albrecht. "Spray impingement in the early direct injection premixed charge compression ignition regime." SAE technical paper, pages 01–1501, 2010.

93. Krisman, E. R. Hawkes, S. Kook, M. Sjöberg, and J. E. Dec, "On the potential of ethanol fuel stratification to extend the high load limit in stratified-charge compression-ignition engines," *Fuel*, vol. 99, no. 9, pp. 45–54, 2012.
94. J. E. Dec and P. L. Kelly-Zion, "The effects of injection timing and diluent addition on late-combustion soot burnout in a DI diesel engine based on simultaneous 2-D imaging of OH and soot," *SAE Technical Paper 2000-01-0238*, 2000.
95. Q.-L. Tang, P. Zhang, H.-F. Liu, and M.-F. Yao, "Quantitative measurements of soot volume fractions in diesel engine using laser-induced incandescence method," *Acta Physicochemical Sinica*, vol. 31, no. 5, pp. 980–988, 2015.
96. Xiao, H. Liu, X. Bi, H. Wang, and C.-F. F. Lee, "Experimental and numerical investigation on soot behavior of soybean biodiesel under ambient oxygen dilution in conventional and low-temperature flames," *Energy and Fuels*, vol. 28, no. 4, pp. 2663–2676, 2014.
97. J. Zhang, W. Jing, W. L. Roberts, and T. Fang, "Effects of ambient oxygen concentration on biodiesel and diesel spray combustion under simulated engine conditions," *Energy*, vol. 57, pp. 722–732, 2013.
98. J. Zhang, W. Jing, W. L. Roberts, and T. Fang, "Soot temperature and KL factor for biodiesel and diesel spray combustion in a constant volume combustion chamber," *Applied Energy*, vol. 107, pp. 52–65, 2013.
99. Li, M. Jonsson, M. Algotsson et al., "Quantitative detection of hydrogen peroxide in an HCCI engine using photofragmentation laser-induced fluorescence," *Proceedings of the Combustion Institute*, vol. 34, no. 2, pp. 3573–3581, 2013.
100. P. Zhang, H.-F. Liu, B.-L. Chen, Q.-L. Tang, and M.-F. Yao, "Fluorescence spectra of polycyclic aromatic hydrocarbons and soot concentration in partially premixed flames of diesel surrogate containing oxygenated additives," *Acta Physico-Chimica Sinica*, vol. 31, no. 1, pp. 32–40, 2015.
101. L. Wang, C. W. Lee, R. D. Reitz, P. C. Miles, and Z. Han, "A generalized renormalization group turbulence model and its application to a light-duty diesel engine operating in a lower temperature combustion regime," *International Journal of Engine Research*, vol. 14, no. 3, pp. 279–292, 2013.

102. Perini, P. C. Miles, and R. D. Reitz, "A comprehensive modeling study of in-cylinder fluid flows in a high-swirl, light-duty optical diesel engine," *Computers & Fluids*, vol. 105, pp. 113–124, 2014.
103. J. Kodavasal, D. N. Assanis, G. A. Lavoie, and J. B. Martz, "The effects of thermal and compositional stratification on the ignition and duration of homogeneous charge compression ignition combustion," *Combustion & Flame*, vol. 162, no. 2, pp. 451–461, 2015.
104. D. Dahl, M. Andersson, and I. Denbratt, "The role of charge stratification for reducing ringing in gasoline engine homogeneous charge compression ignition combustion investigated by optical imaging," *International Journal of Engine Research*, vol. 14, no. 5, pp. 525–536, 2013.
105. H. Lee and K. H. Lee, "An experimental study of the combustion characteristics in SCCI and CAI based on direct-injection gasoline engine," *Experimental Thermal and Fluid Science*, vol. 31, no. 8, pp. 1121–1132, 2007.
106. S. Lee, K. H. Lee, and D. S. Kim, "Experimental and numerical study on the combustion characteristics of partially premixed charge compression ignition engine with dual fuel," *Fuel*, vol. 82, no. 5, pp. 553–560, 2003.
107. M. Y. Kim, J. H. Lee, and C. S. Lee, "Combustion characteristics and NO<sub>x</sub> emissions of a dimethyl-ether-fueled premixed charge compression ignition engine," *Energy and Fuels*, vol. 22, no. 6, pp. 4206–4212, 2008.
108. M. Jia, M. Xie, H. Liu, W.-H. Lam, and T. Wang, "Numerical simulation of cavitation in the conical-spray nozzle for diesel premixed charge compression ignition engines," *Fuel*, vol. 90, no. 8, pp. 2652–2661, 2011.
109. S. Choi and K. Min, "Analysis of the combustion and emissions of a diesel engine in early-injection, partially-premixed charge compression ignition regimes," *Proceedings of the Institution of Mechanical Engineers, Part D: Journal of Automobile Engineering*, vol. 227, no. 7, pp. 939–950, 2013.
110. H. Kim, K. Kim, and K. Lee, "Reduction in harmful emissions using a two-stage injection-type premixed charge compression ignition engine," *Environmental Engineering Science*, vol. 26, no. 11, pp. 1567–1576, 2009.

111. H. Kim, J. Lee, K. Kim, and K. Lee, "Effect of the atkinson cycle combined with calibration factors on a two-stage injection-type premixed charge compression ignition engine," *Energy and Fuels*, vol. 23, no. 10, pp. 4908–4916, 2009.
112. K. Akihama, Y. Takatori, K. Inagaki, S. Sasaki, and A. M. Dean, "Mechanism of the smokeless rich diesel combustion by reducing temperature," *SAE Transactions*, vol. 110, no. 3, pp. 648–662, 2001.
113. N. Peters, *Turbulent Combustion*, Cambridge Monographs on Mechanics, Cambridge University Press, Cambridge, UK, 2000.
114. F. Hildenbrand, C. Schulz, J. Wolfrum, F. Keller, and E. Wagner, "Laser diagnostic analysis of NO formation in a direct injection diesel engine with pump-line-nozzle and common rail injection systems," *Proceedings of the Combustion Institute*, vol. 28, no. 1, pp. 1137–1144, 2000.
115. W. G. Bessler, M. Hofmann, F. Zimmermann et al., "Quantitative in-cylinder NO-LIF imaging in a realistic gasoline engine with spray-guided direct injection," *Proceedings of the Combustion Institute*, vol. 30, no. 2, pp. 2667–2674, 2005.
116. S. D. Zilwa and R. Steeper, "Predicting emissions from HCCI engines using LIF imaging," *SAE Paper 2005-01-3747*, SAE International, 2005.
117. , C. J. Mueller, and G. C. Martin, "The influence of charge-gas dilution and temperature on DI diesel combustion processes using a short-ignition-delay, oxygenated fuel," *SAE 2005-01-2088*, 2005.
118. H. Liu, P. Zhang, Z. Li, J. Luo, Z. Zheng, and M. Yao, "Effects of temperature inhomogeneities on the HCCI combustion in an optical engine," *Applied Thermal Engineering*, vol. 31, no. 14-15, pp. 2549–2555, 2011.
119. K. Akihama, T. Fujikawa, and Y. Hattori, "Laser-induced fluorescence imaging of no in a port-fuel-injected, stratified-charge SI engine—correlations between N formation region and stratified fuel distribution," *SAE Paper 981430*, 1998.
120. K. Akihama, Y. Takatori, K. Inagaki, S. Sasaki, and A. M. Dean, "Mechanism of the smokeless rich diesel combustion by reducing temperature," *SAE Transactions*, vol. 110, no. 3, pp. 648–662, 2001.

121. W. Hwang, J. Dec, and M. Sjöberg, "Spectroscopic and chemical-kinetic analysis of the phases of HCCI autoignition and combustion for single- and two-stage ignition fuels," *Combustion & Flame*, vol. 154, no. 3, pp. 387–409, 2008.
122. H. Liu, Z. Zheng, M. Yao, P. Zhang, B. He, and Y. Qi, "Influence of temperature and mixture stratification on HCCI combustion using chemiluminescence images and CFD analysis," *Applied Thermal Engineering*, vol. 33-34, no. 1, pp. 135–143, 2012.
123. S. Singh, R. D. Reitz, and P. B. M. Mark, "2-color thermometry experiments and high-speed imaging of multi-mode diesel engine combustion," *SAE Technical Paper* 2005-01-3842, 2005.
124. Huestis, P. A. Erichkson, and M. P. B. Musculus, "In-cylinder and exhaust soot in low-temperature combustion using a wide-range of EGR in a heavy-duty diesel engine," *SAE Paper* 2007-01-4017, 2007.
125. Kim, M. Kaneko, Y. Ikeda, and T. Nakajima, "Detailed spectral analysis of the process of HCCI combustion," *Proceedings of the Combustion Institute*, vol. 29, no. 1, pp. 671–677, 2002.
126. H.-F. Liu, M.-F. Yao, C. Jin, P. Zhang, Z.-M. Li, and Z.-Q. Zheng, "Chemiluminescence spectroscopic analysis of homogeneous charge compression ignition combustion processes," *Spectroscopy and Spectral Analysis*, vol. 30, no. 10, pp. 2611–2615, 2010.
127. Wu, Y., Zhang, S., Hao, J., Liu, H., Wu, X., Hu and Stevanovic, S. (2017). On-road vehicle emissions and their control in China: A review and outlook. *Science of the Total Environment*, 574, 332-349.
128. G. Gaydon, *The Spectroscopy of Flames*, Chapman & Sons, 2nd edition, 1974.
129. Hultqvist, M. Christensen, B. Johansson, A. Franke, M. Richter, and M. Aldén, "A study of the homogeneous charge compression ignition combustion process by chemiluminescence imaging," *SAE Paper* 1999-01-3680, 1999.
130. M. Yao, Z. Zheng, and H. Liu, "Progress and recent trends in homogeneous charge compression ignition (HCCI) engines," *Progress in Energy and Combustion Science*, vol. 35, no. 5, pp. 398–437, 2009.

131. Abd Alla GH, Soliman HA, Badr OA, Abd Rabbo MF. Effect of injection timing on the performance of a dual fuel engine. *Energy Convers Manag* 2002;43:269–77.
132. S. Kokjohn, R. Reitz, D. Splitter, and M. Musculus, “Investigation of fuel reactivity stratification for controlling PCI heat-release rates using high-speed chemiluminescence imaging and fuel tracer fluorescence,” *SAE Technical Papers*, vol. 5, no. 2, pp. 248–269, 2012.
133. Z. Chen, M. Yao, Z. Zheng, and Q. Zhang, “Experimental and numerical study of methanol/dimethyl ether dual-fuel compound combustion,” *Energy and Fuels*, vol. 23, no. 5, pp. 2719–2730, 2009.
134. Dec and C. Espey, “Chemiluminescence imaging of autoignition in a DI diesel engine,” *SAE Technical Paper* 982685, 1998.
135. Ekoto, W. Colban, P. Miles, S. Park, and D. E. Foster, “Sources of UHC emissions from a light-duty diesel engine operating in a partially premixed combustion regime,” *SAE International Journal of Engines*, vol. 2, no. 1, pp. 1265–1289, 2009.
136. W. Ekoto, W. F. Colban, P. C. Miles et al., “UHC and CO emissions sources from a light-duty diesel engine undergoing late-injection low-temperature combustion,” in *Proceedings of the ASME Internal Combustion Engine Division Fall Technical Conference (ICEF '09)*, Paper no. ICEF2009-14030, pp. 163–172, Lucerne, Switzerland, September 2009.
137. Petersen, P. Miles, and D. Sahoo, “Equivalence ratio distributions in a light-duty diesel engine operating under partially premixed conditions,” *SAE International Journal of Engines*, vol. 5, no. 2, pp. 526–537, 2012.
138. Karim GA. A review of combustion processes in the dual fuel engine – gas diesel engine. *Prog Energy Combust* 1980;6:277–85.
139. Jiang H-F, Wang J-X, Shuai S-J. Visualization and performance analysis of gasoline homogeneous charge induced ignition by diesel. *SAE Technical Paper* 2005-01-0136; 2005.
140. Inagaki K, Fuyuto T, Nishikawa K, Nakakita K. Dual-fuel PCI combustion controlled by in-cylinder stratification of ignitability. *SAE Technical Paper* 2006- 01-0028; 2006.

141. Hanson, R., Kokjohn, S., Splitter, D., and Reitz, R., "An Experimental Investigation of Fuel Reactivity Controlled PCCI Combustion in a Heavy-Duty Engine," SAE Int. J. Engines 3(1):700-716, 2010, 2010-01-0864.
142. Curran, S., Prikhodko, V., Cho, K., Sluder, C. et al., "In-Cylinder Fuel Blending of Gasoline/Diesel for Improved Efficiency and Lowest Possible Emissions on a Multi-Cylinder Light-Duty Diesel Engine," SAE Technical Paper 2010-01-2206, 2010, 2010-01-2206.
143. Hanson, R., Kokjohn, S., Splitter, D., and Reitz, R., "An Experimental Investigation of Fuel Reactivity Controlled PCCI Combustion in a Heavy-Duty Engine," SAE Int. J. Engines 3(1):700-716, 2010, doi:10.4271/2010-01-0864.
144. Chaitanya Kavuri, , Jordan Paz , Sage L. Kokjohn , A comparison of Reactivity Controlled Compression Ignition (RCCI) and Gasoline Compression Ignition (GCI) strategies at high load, low speed conditions. Energy Conversion and Management, Volume 127, 1 November 2016, Pages 324–341
145. Sun, J., Bittle, J., and Jacobs, T., "Influencing Parameters of Brake Fuel Conversion Efficiency with Diesel / Gasoline Operation in a Medium-Duty Diesel Engine," SAE Technical Paper 2013-01-0273, 2013, doi:10.4271/2013-01-0273.
146. Derek Splitter, Reed hanson, Sage Kokjhon and Rolf Reitz ; “Reactivity controlled compression ignition (RCCI) heavy-Duty engine operation at Mid and high loads with conventional and alternatives fuels”, SAE International 2011-01-0363
147. Gürbüz, Habib, et al. "Effect of port injection of ethanol on engine performance, exhaust emissions and environmental factors in a dual-fuel diesel engine." Energy & Environment (2020): 0958305X20960701.
148. Gürbüz, Habib, et al. "The effect of euro diesel-hydrogen dual fuel combustion on performance and environmental-economic indicators in a small UAV turbojet engine." Fuel 306 (2021): 121735.
149. Amin Paykani , Amir-Hasan Kakaee , Pourya Rahn timer and Rolf D Reitz; “Progress and recent trends in reactivity-controlled compression ignition engines”, International Journal of Engine Research 1–44 IMechE 2015

150. Reed hanson, sage Kokjhon, Derek spliter and Rolf reitz; "Effects on Reactivity controlled compression ignition (RCCI) combustion at low load", SAE international 2011-01-0361.
151. Jeongwoo Lee, Sanghyun Chu, Kyoungdoug Min, Minjae, Hyunsung Jing, Hyounghyoun Kim, Yohan Chi; "Classification of diesel and gasoline dual-fuel combustion modes by the analysis of heat release rate shapes in compression ignition engine" Elsevier 2017
152. Yang DB, Wang Z, Wang JX, Shuai SJ. Experimental study of fuel stratification for HCCI high load extension. Appl Energy 2011;88(9):2949–54.
153. Kokjohn SL, Hanson RM, Splitter DA, Reitz RD. Fuel reactivity controlled compression ignition (RCCI): a pathway to controlled high-efficiency clean combustion. Int J Engine Res 2011;12(3):209–26.
154. Hanson RM, Kokjohn SL, Splitter DA, Reitz RD. An experimental investigation of fuel reactivity controlled PCCI combustion in a heavy-duty engine. SAE paper no. 2010-01-0864.
155. Nieman DE, Dempsey AB, Reitz RD. Heavy-duty RCCI operation using natural gas and diesel. SAE paper 2012-01-0379; 2012.
156. Gürbüz, Habib, and Selim Demirtürk. "Investigation of dual-fuel combustion by different port injection fuels (neat ethanol and E85) in a DE95 diesel/ethanol blend fueled compression ignition engine." Journal of Energy Resources Technology 142.12 (2020): 122306.

## APPENDIX

Appendix covers the uncertainty estimation during experimentation. The measured values are subjected to uncertainties due to various parameters. An experimental uncertainty proves the confidence level and accuracy of experiments. The exhaust gas analyzer (AVL AMA i60 analyzer) used for the investigations in test bed trials with an accuracy of 3 % over a maximum of 8 hours and a linearity of the signals of  $\pm 1$  %. Emission analyzer operating principle and accuracy is within range of legislative limits. The uncertainty estimation in detail is explained for various computed parameters of steady state operating CI engine. The engine performance parameters such as brake fuel consumption, brake thermal efficiency and brake mean effective pressure (BMEP) are estimated. Similarly, uncertainties in emission measuring instruments are also estimated.

## LIST OF PUBLICATION

1. Barman, J. and Deshmukh, D., “Effect of Fuel Reactivity on Engine Performance and Exhaust Gas Emissions in a Diesel Engine”, SAE International Journal of Fuels and Lubricants, Volume 16- Issue 2, 2023, doi:10.4271/04-16-02-0012.
2. Barman, J. and Deshmukh, D., “Behavior of Particulate Matter Emissions in a Dual Fuel Engine”, SAE International Journal of Fuels and Lubricants, Volume 16- Issue 2, 2023, doi:10.4271/04-16-02-0011.
3. Jyotirmoy Barman, D. Deshmukh, “After Treatment Control Strategy and Particle Emission Correlation with different ratio of dual fuel”, SAE International Journal of Engines, 2023 – Final Review.
4. Jyotirmoy Barman, D. Deshmukh, "Emission and performance behavior study of LTC with Diesel and Gasoline dual fuel", 5th National Conference on Internal Combustion Engines and Combustion (NCICEC 2017), NITK Surathkal.